

Insights into the molecular adaptation of *Staphylococcus aureus* to copper Schiff's base at proteome level

Dissertation
zur
Erlangung des Doktorgrades (Dr. rer. nat.)
der
Mathematisch-Naturwissenschaftlichen Fakultät
der
Rheinischen Friedrich-Wilhelms-Universität Bonn

Vorgelegt von

Vishwas Kaveeshwar

aus

Bijapur, Indien

Bonn, 2016

Angefertigt mit Genehmigung der Mathematisch-Naturwissenschaftlichen Fakultät
der Rheinischen Friedrich-Wilhelms-Universität Bonn.

1. Gutachter: Prof. Dr. Markus Rothschild

2. Gutachter: Prof. Dr. Erwin A. Galinski

Tag Der Promotion: 02.05.2017

Erscheinungsjahr: 2017

**I dedicate this thesis to
my parents and my wife.**

I Eidesstattliche Erklärung

Hiermit versichere ich, dass diese Dissertation von mir selbst und ohne unerlaubte Hilfe

angefertigt wurde. Es wurden keine anderen als die angegebenen Hilfsmittel benutzt. Ferner erkläre ich, dass die vorliegende Arbeit an keiner anderen Universität als Dissertation eingereicht wurde.

Bonn, 2016

Vishwas Kaveeshwar

II Acknowledgement

While my name might be the only one that appears on the cover of this dissertation, a great many people have contributed to its production. This is a small way of thanking them for their contribution and support.

I express my thanks to my advisor Prof. Dr. Markus Rothschild for giving me the opportunity to work in his institute and providing me with all the necessary facilities and help.

I would like to extend my gratitude to the project leader Dr. Katja Mercer-Chalmers-Bender for enlightening me with the first glance of research in proteomics. I would also like to thank her for making me a part of EMBEK1 project, and for helping me to gain valuable skills and experience in my chosen field. I deeply acknowledge her support in exploring new avenues to reach my desired research goals.

This project was funded by the European Commission's 7th Framework programme *via* the consortium *EMBEK1-FP7 project # 211436*.

A special mention and heartfelt gratitude goes to my co-advisor Prof. Dr. Erwin A. Galinski for guiding me through every aspect of my PhD journey. His valuable guidance not only helped me to sort out the technical details of my work, but also kept me motivated during the difficult times of this journey. I cannot thank him enough for his patience and for the support, which were nothing short of extraordinary. I consider myself extremely fortunate to find a great mentor in him.

I am grateful to Prof. Dr. D. Bartels and Prof. Dr. Thomas H. Reiprich for their kind willingness to be a part of the committee for the examination of my dissertation. Thank also goes to Dr. Stephan Mueller for helping with nano LC-MALDI proteomic

analysis, Dr. Toby Jenkins for providing anti-microbial CSB compound, and Dr. Alexander Lotz for helping me with the ICP-MS analysis. I would also like to thank Prof. Dr. Bjoern Schumacher for his help in establishing *C.elegan* culture, Prof. Dr. Peter M. Schneider and Dr. Eva Gomez for the support and help with gene expression analysis. I would also like to appreciate the help and support provided by all the collaborators involved in the EMBEK1 project.

I want to thank all the former and present members of our lab at Institute of Rechtsmedizin, Cologne, for their support, friendship and encouragement. I thank Dr. Martin Juebner, Dr. Peter Cierniak for their constant support and for sharing their scientific knowledge with me throughout my thesis.

I will forever be thankful to all my friends from 'TLH', 'Roemerstrasse11' and to my fellow 'Bullahh' members who made Bonn/Germany my "home away from home". My special affection goes to Dr. Neha Sharma for her friendship, for her numerous acts of kindness and care, which helped me overcome setbacks and stay focused during my PhD study.

I deeply appreciate Dr. Bharadwaj Vijaysarathy and Dr. Naveen Hegde for the encouragement they provided throughout this arduous journey. Picking their awe-inspiring intellect has not only enlightened my knowledge about various scientific topics which I was completely oblivious about, but also helped shape my overall thought process which benefited my work both directly and indirectly. The time I spent with them discussing everything from movies, to the environment, space research, world politics, religion etc account to some of the most intellectually fulfilling moments of the past few years.

I would like to thank Dr. Pavan Deshpande, Pramod Wadappi, Pavan Chinchankar and Madhu Bidarahalli, my childhood friends from India for their unconditional support and help to pursue my PhD in Germany. I would like to acknowledge their concern and help that they provided me and my family back home in India all while I was pursuing my PhD here in Germany.

My special thanks to my relatives and family friends from India in particular my extended Kaveeshwar family, Kanvikar family, Gudur family, Kulkarni family, Patil family and Kallapur family for lending a hand of support whenever required and being there with my parents and taking care of them.

Thanks go to my in-laws Hasyagar family for the best wishes and support they provided.

Words cannot express my profound gratefulness to the Almighty for His guidance, love and immense blessings.

Finally, I must express my very profound gratitude to my parents Sudhir Kaveeshwar and Sangeeta Kaveeshwar and to my wife Pavana Kaveeshwar for their love, support and belief in me throughout my years of study and through the process of researching and writing this thesis. This accomplishment would not have been possible without them. I am thankful to my family for helping me to pursue my dreams and providing me with the best in everything.

III Abbreviations

2DE	2 Dimensional Electrophoresis
Agr	Accessorry gene regulatory
AIP	Auto inducing peptide
<i>C.elegan</i>	<i>Caenorhabditis elegans</i>
cDNA	Complimentary DNA
CHAPS	3-((3-cholamidopropyl) dimethylammonio)-1-propanesulfonate
CSB	Copper-Schiff's base
Ct	Cycle threshold
DIGE	Differential in gel electrophoresis
DMSO	Dimethylsuphoxide
DTT	Dithiothreitol
EB	Ethidiumbromide
ErCu	Evolutionarily resistant to copper <i>MSSA476</i>
FASP	Filter assisted sample preparation
H ₂ O ₂	Hydrogen peroxide
HE	Hydroethidine
ICP	Inductively coupled plasma
IEF	Isoelectric focusing
IPG	Immobilised pH gradient
L1	Larva stage 1
L4	Larva stage 4
LB	Luria-Bertani
LC	Liquid chromatography

Abbreviation

MALDI	Matrix associated
MIC	Minimal inhibition concentration
MS	Mass spectrometry
<i>MSSA476</i>	Methicilin sensitive <i>Staphylococcus aureus</i> 476
NGM	Nematode growth media
OD	Optical density
PAGE	Poly acrylamide gel electrophoresis
ROS	Reactive oxygen spicies
RT-PCR	Real time polymer chain reaction
SCX	Strong cation Exchange
SDS	Sodium dodecyl sulphate
SOD	Superoxide dismutase
TEABC	Triethylammoniumbicarbonate
TFA	Trifluoroacetic acid

IV Table of contents

Contents		Page Nr.
I	Eidesstattliche Erklärung	i
II	Acknowledgement	ii
III	Abbreviations	v
IV	Table of contents	vii
V	List of figures	x
VI	List of tables	xi
VII	Summary	xii
1	Introduction	1
1.1	Background	1
1.2	Methodology	5
1.3	Motivation	7
2	Materials	9
2.1	Chemicals	9
2.2	Kits and special reagents	11
2.3	Special solutions and buffers	12
2.4	Organisms used	13
3	Methods	14
3.1	Evolution of CSB resistance in <i>MSSA476</i>	14
3.1.1	Microevolved <i>S.aureus</i> strain confirmation	14

3.2	Characterisation of ErCu strain	15
3.2.1	Intracellular superoxide anion measurement	15
3.2.2	Cellular copper concentration measurement	16
3.2.3	Phenotypic expression of virulence factors in <i>MSSA476</i> and in ErCu	17
3.2.3.1	Slide coagulase test	17
3.2.3.2	Blood agar test	18
3.2.3.3	Virulence test of ErCu in comparison with <i>MSSA476</i> strain on <i>C.elegans</i>	18
3.3	Comparative proteomics and gene expression analysis between ErCu and <i>MSSA476</i>	19
3.3.1	Two-Dimensional Differential In Gel Electrophoresis analysis	19
3.3.2	Nano LC- MALDI analysis	22
3.3.2.1	Bacterial growth conditions and sample preparations	22
3.3.2.2	Filter assisted sample preparation	22
3.3.2.3	Isobaric tags for relative and absolute quantitation	23
3.3.2.4	Strong Cation Exchange HPLC	24
3.3.2.5	MALDI Spotting	24
3.3.2.6	LC-MALDI MS/MS analysis	25
3.3.2.7	Database Searches	26
3.3.3	Gene expression analysis	27
3.3.3.1	Isolation of RNA	28
3.3.3.2	c-DNA preparation	28
3.3.3.3	Primers	28

3.3.3.4	Real time PCR assay	29
3.4	Biofilm assay in <i>MSSA476</i> and ErCu strain	30
4	Results	32
4.1	Evolution of CSB resistance in <i>MSSA476</i>	32
4.1.1	Confirmation of microevolved <i>S.aureus</i> strain	34
4.2	Characterisation of ErCu strain	36
4.2.1	Intracellular superoxide anion measurement	36
4.2.2	Cellular copper concentration measurement	37
4.2.3	Phenotypic expression of virulence factors	38
4.3	Comparative studies between ErCu and <i>MSSA476</i> with respect to protein and gene expression	40
4.3.1	Two- Dimensional Differential In Gel Electrophoresis (2D-DIGE) analysis	40
4.3.2	Nano LC- MALDI mass spectrometry analysis	46
4.3.3	Gene expression analysis	50
4.4	Biofilm assay	52
5	Discussion	53
5.1	Evolutionary tolerance of ErCu strain against CSB	53
5.2	Factors involved in the tolerance of CSB in ErCu strain	55
5.3	Increased Biofilm formation in ErCu	56
5.4	Interrelation of agr system and SpoVG in <i>S.aureus</i>	60
5.5	Biofilm formation and its role in heavy metal stress tolerance in ErCu	61

5.6	Usage of CSB as an anti-microbial polymer in healthcare domain	63
6	References	64
7	Appendix	81
7.1	Superoxide anion measurement data	81
7.2	Cellular copper concentration measurement data	81
7.3	Gene expression measurement, RT-PCR data	81
7.4	Biofilm formation assay	83
7.5	PCR experiment to confirm microevolved <i>S.aureus</i>	83
7.6	Spectrometry MASCOT search data from 2D-DIGE	84
7.7	Screen shot of student's T-test score from 2d-DIGE experiment	90
7.8	Protein expression data from nano LC-MALDI	91
Figure Nr	Figure titles	Page Nr
Figure 1	Molecular structure of CSB (bis(N-allylsalicylideneiminato)-copper)	1
Figure 2	Life cycle of a <i>C.elegan</i> at 25 °C	18
Figure 3	Growth of CSB sensitive <i>MSSA476</i> and CSB tolerant ErCu strain	32
Figure 4	Graphical representation of CSB tolerance of sensitive and tolerant strains	33
Figure 4.1	Agarose gel electrophoresis showing 270bp fragment of nuc gene in <i>MSSA476</i> , ErCu, <i>S.carnosus</i>	34
Figure 4.2	Cultures grown in mannitol agar media	35
Figure 5	Intracellular superoxide anion measurement in ErCu and <i>MSSA476</i> strains	36

Figure 6	Concentration of copper ions measured by ICP-MS present in the <i>MSSA476</i> and ErCu cells	37
Figure 7	Hemolytic test of ErCu and <i>MSSA476</i> on blood agar	38
Figure 8	<i>C. elegans</i> growth assay to test the virulence of ErCu and <i>MSSA476</i> strains	39
Figure 9A	Protein pattern of ErCu and <i>MSSA476</i> grown in 0.5mM CSB obtained by 2D-DIGE	41
Figure 9B	Protein pattern of ErCu and <i>MSSA476</i> grown in 0.5mM CSB obtained by 2-DIGE showing SpoVG spot	44
Figure 10	3D view representation of 2D-DIGE expression of SpoVG in case of ErCu as in relation to the <i>MSSA476</i> strain	44
Figure 11	Mass spectrometry data MASCOT search results for SpoVG protein	45
Figure 12	Expressions of the genes <i>agrA</i> , <i>clfA</i> , <i>copZ</i> , <i>spa</i> in case of <i>MSSA476</i> and ErCu	50
Figure 13	Biofilm assay: Optical density measurement of ErCu and <i>MSSA476</i> strains stained with crystal violet (0.1%)	52
Figure 14	Schematic representation of molecular adaptation by ErCu, which will lead to enhanced biofilm formation	56
Figure 15	Schematic representation of interrelation of SpoVG and <i>agr</i> system	60
Table Nr	Table titles	Page Nr
Table 1	List of forward and reverse primers used for the gene amplification	29
Table 2	List of down regulated proteins in ErCu revealed by 2D-DIGE	42
Table 3	Protein expression revealed in nano LC-MALDI	48

VII Summary

The molecular adaptation of *S.aureus* to copper Schiff's base (CSB) was studied by comparative proteome analysis. Proteome analysis was performed by employing nano LC-MALDI mass spectrometry with isobaric tags (iTRAQ) and 2D-DIGE techniques. In CSB adapted *MSSA476* (ErCu), considerable decrease in Cu ion concentration and copZ protein is observed as compared to non-CSB adapted *MSSA476* strain by ICP-MS and nano LC-MALDI experiments respectively. CopZ protein is a copper transport protein, which aids the export of Cu^+ across the membrane. Decreased Cu^+ and CopZ suggest reduced Cu^+ influx in to the cell. It has been already established that repression of Putative septation protein SpoVG leads to repressed biofilm formation in *S. aureus*. Approximately two fold increase in SpoVG in CSB adapted *MSSA476* as observed by 2D-DIGE experiment suggests enhanced ability for biofilm formation in the adapted strain. Enhanced biofilm formation is further confirmed by biofilm assay experiment. Contrary to popular belief, it has been demonstrated previously that repression of accessory gene regulatory (agr) system is necessary to form a biofilm. Repression of agr system is confirmed by reduced agrA protein observed by nano LC-MALDI experiment in ErCu. Because of the agr repression, reduced virulence in ErCu strain was demonstrated and was further confirmed by virulence analysis experiments on *C.elegans*. SpoVG is known to be positively regulated by sigmaB factor; on the other hand sigmaB has a negative effect on agr system. Therefore, sigmaB can be proposed as a common factor, which is involved in the interrelation of SpoVG expression and agr system expression in ErCu. However, the proteomics analysis was not able to conclusively determine the expression of sigmaB in case of ErCu. Nevertheless, up-regulation of SpoVG and down-regulation of agr system in ErCu

were proved beyond doubt, which facilitates enhanced biofilm formation in ErCu. The extracellular matrix of *S.aureus* biofilm is known to immobilize toxic metals by ionic interaction of opposite charges (DNA), by precipitation, biosorption etc. It has been established that enhanced biofilm formation is the likely cause of oxidative stress tolerance towards excess copper concentration in this strain. It can be proposed that CSB adapted *MSSA476* has developed a mechanism to increase biofilm formation which prevents excess Cu^+ influx in to the cell and therefore prevents excess oxidative stress exerted by excess Cu^+ within the cell. It is demonstrated that *MSSA476* required only few generations to achieve tolerance to inhibitory concentrations of CSB due to enhanced biofilm formation properties. This emphasizes once again the importance of dealing with biofilms as a prime target for *S.aureus* therapies.

1. Introduction

1.1 Background

In our study, we were interested in the generation of evolutionary resistance in bacteria and characterisation of the response at the proteome level. Therefore, we used methicillin susceptible *Staphylococcus aureus* 476 strains (MSSA476) as a prototype for a clinically relevant bacterial strain and a novel antibacterial substance Copper Schiff's Base (CSB) synthesised by N. Poulter *et al.*, University of Bath, UK (1).

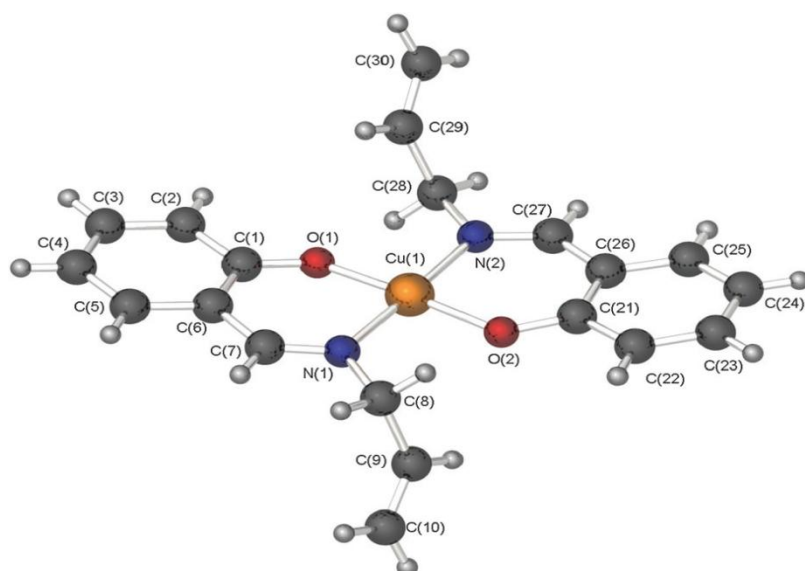


Figure 1: Molecular structure of CSB (bis(N-allylsalicylideneiminato)-copper). (Artwork from N. Poulter *et al.* (1))

Staphylococcus aureus (*S. aureus*) is an opportunistic gram-positive bacterium that is responsible for a spectrum of diseases including endocarditis, wound infections, meningitis, pulmonary infections, toxic shock syndrome (2-6). Its ability to adapt and

develop resistance to the antibiotics makes the organism one of the most successful pathogens (7-9).

Several factors are known to be related to anti-microbial resistance in *S.aureus* especially with respect to antibiotic resistance. In case of vancomycin and teicoplanin glycopeptides antibiotic resistance in *S.aureus*, thickening of cell wall prevents the antibiotics to diffuse in to the division septum of the cell to achieve resistance (10-12). *YabJ-spoVG* operon is known to control resistance of glycopeptides antibiotics in *S.aureus* (13, 14). Putative septation protein SpoVG (not *yabJ*) controls the regulation of the operon (15). SpoVG is known to be involved in the barrier septum assembly (www.uniprot.org) and capsule formation (16). Eventhough exact underlying molecular mechanism of cell wall thickening in antibiotic resistance is unknown, role of SpoVG can be suspected. Some antibiotic resistance is also seen in 'accessory gene regulatory' (*agr*) system deficient *S. aureus* strains (17). *Agr* system controls the quorum sensing and related virulence factors in *S.aureus* (18). *S.aureus* employs *agr* mediated quorum sensing to control virulence factor expressions based on to the signals received due to on cell density and environmental changes (19, 20). *Agr* system consists mainly of 4 factors: *agrA*, *agrB*, *agrC* and *agrD*. Based on cell density and environmental changes *agrB* and *agrD* produce and excrete 'Auto inducing peptides (AIP)', which is a signal molecule of *agr*. At higher concentrations of AIPs, AIP binds to *agrC* and triggers *agrA* by His-dependent phosphorylation. *AgrA* in turn, induces the expression of RNAIII and RNAII transcripts of *agrA*, *agrB*, *agrC* and *agrD* to establish a feedback loop (21-23). On the other hand, RNAIII induces the extracellular virulence factors by repressing the cell wall related proteins (24, 25). Therefore, in resistant, *agr* deficient *S.aureus*,

evidences for reduced extra cellular virulence factors can be observed (17) and increased cell wall associated proteins like those that SpoVG can be expected.

Resistant strains tend to have a fitness advantage over non resistant strains in presense of antibiotic stress and because of the fitness advantage, bacteria survives when the environmental pressure is exerted, perhaps at the cost of reduced virulence gene expression (23, 26-28). Eventhough in presence of antibiotics reduced virulence factor expressions may serve no advantage to the bacteria itself at first, it is required to survive and attain a certain cell density to establish infection with in the host system (23, 28).

Clumping factor A (clfA), immunoglobulin G-binding protein a (spa), are adhesion virulence factors located on the cell wall and are released extra cellularly establishing infection in the the host system (www.uniprot.org) (29). As mentioned above, when the antibiotic stress is applied on *S.aureus*, stress resistant *S. aureus* survives because of it's fitness advantage at the cost of reduced virulence factors (23, 26-28). Therefore, reduced expression of clfA and spa are expected in antibiotic stress resistant *S.aureus*.

Biofilm formation is another factor, which is often associated with ant-microbial resistance in bacteria. It has been established that increased biofilm formation leads to enhanced oxidative stress tolerance in bacteria (30-32). SpoVG and agr are shown to play a role in biofim formation in *S.aureus*. (33-38) (39).

Because of the ability of *S.aureus* to quickly adapt and bring resistance to a range of antibiotics, the treatment of infectious diseases caused by *S. aureus* is becoming a major problem in health care. Hence, the incidence of infectious diseases has increased significantly (40-42) . Therefore, there is always a demand for more

effective and safer chemotherapeutic agents. It is known that heavy metals can be good candidates for the therapeutic agents. Metal coordination complexes have been widely studied for their antimicrobial properties (43) (44). This has given a scope for the research of new metal complexes as bioactive compounds.

Benefits of different copper complexes against diseases such as tuberculosis, rheumatoid arthritis and infectious diseases have been demonstrated (45) (46). The treatment with copper complexes containing nitrogen and oxygen donor ligands show significantly better pharmacological effects than the regular inorganic forms of copper (47). The complexes also show stronger antimicrobial activity than the free ligands (48). Copper complexes using Schiff's base ligands are of major interest because of their biological importance (49). In this study the resistance mechanism of *S. aureus* against copper Schiff's base (bis (N-allylsalicylideneiminato)-copper) (synthesized and provided by N. Poulter *et al.* at University of Bath, UK) (1) was studied. Plasma deposited copper Schiff's base complex (CSB) can be used as an antimicrobial coating (1). Such coatings on various objects like fabrics, clinical tools like catheters can help to solve the infection related issues in our day-to-day life. It was also shown that Schiff's base alone can be antimicrobial as well; however the concentration of Schiff's base required to exert stress on *S. aureus* cells is much higher than the concentration of CSB that has been used by N. Poulter *et al.* (1).

It is a known fact that *S. aureus* has the ability to adapt quickly to different conditions and thus survive in adverse conditions such as stress by heavy metals (50). It has been shown that the presence of genes encoded by plasmid confer resistance to heavy metals like cadmium and mercury (51). It has also been described that the presence of the plasmid is not necessary to develop resistance to some other heavy

metals like zinc, copper, cobalt (52). Some of these heavy metals are essential for the cells to survive but only in trace amounts. So far, not much is known about the molecular mechanisms of adaptation to increased cellular heavy metal concentrations.

Copper is needed for many metabolic processes taking place in the cells e.g. the electron transport chain (53) (54) but only in trace amounts. It has been shown that an increase in the copper level beyond the physiological limits can be toxic to the cell (55). But when a constant pressure is created by the heavy metals like copper in the bacterial environment, it leads to selection of new variant bacterial strains which are resistant to the heavy metals (56, 57). So it becomes important to understand the mechanism by which *S. aureus* evolves and adapts to the pressure created by the copper complexes.

1.2 Methodology

Our study is focused on understanding the quantitative and qualitative changes of the proteome and corresponding gene expressions in a microevolved *MSSA476* strain, which is resistant against antibacterial CSB complex (ErCu strain). The study of the proteome changes in ErCu strain helps to investigate the molecular mechanism of the adaptation of *MSSA476* against CSB. This study was further extended to investigate the virulence of the resistant strain on the host *Caenorhabditis elegans* (*C.elegans*).

For the comparison of the complete proteome of *MSSA476* and ErCu strain, 2-Dimensional Differential In Gel Electrophoresis (2D-DIGE) and nano Liquid Chromatography –Matrix Associated Laser Desorption Ionisation (nano LC-MALDI) with isobaric tags for relative and absolute quantitation (iTRAQ) was used. 2D-gel

electrophoresis is a technique used to resolve individual proteins from a complex protein cocktail. The resolution of proteins is based on their respective isoelectric points and molecular weights. 2D-DIGE is a 2D gel electrophoresis technique, which uses fluorescent dyes (CyDyes) to label the proteins. CyDye labelling with multiple dyes (Cy2, Cy3, Cy5) allows to run the proteome from the multiple sources on the same gel. The individual proteome pattern on the gel can be compared with each other up on scanning the gel with the respective CyDye wavelengths. In this study, Cy3 and Cy5 dyes (GE Healthcare, Upsala, Sweden) were used to compare proteome of *MSSA476* and ErCu strain and typhoon scanner (GE Healthcare, Upsala, Sweden) was used to scan the gels.

First dimensional protein separation is a horizontal separation of proteins based on their respective isoelectric point. The process is also known as iso electric focusing (IEF). IEF resolved proteins are further subjected to second dimensional vertical separation of proteins based on their molecular weight. Based on the internet sources (<http://www.appliedbiomics.com/support/2d-dige-vs-2d-gel.html>) and protocols published by A. Görg and colleagues (Two-Dimensional Electrophoresis with Immobilized pH Gradients for Proteome Analysis; A laboratory manual, www.wzw.tum.de/proteomik), the advantages of fluorescent labeling over regular 2D gel electrophoresis are listed below.

Higher sensitivity: CyDye labeling gives sensitivity of 0.2ng/spot. This allows us to use smaller amounts of protein sample.

High accuracy: Differences in protein expression up to 10% can be detected.

Fluorescent labeling allows software aided accurate quantification of proteins.

Cost and time effectiveness: CyDye labeling allows multiple protein samples run on a same gel, this allows fewer number of gel runs per study. This also allows fewer number of gel runs for the statistical analysis.

Nano LC-MALDI analysis is based on differential labelling of N-terminus of the peptides by isobaric tags. Tagged samples are further analysed by tandem mass spectrometry for the relative quantification (58) and it is expected to provide wider range of protein data as compared to 2D gel electrophoresis due to the employment of isobaric tags for the relative and absolute quantification of peptides and Liquid chromatography technique for the resolution of peptides from the complex protein mixture.

For comparative proteomics analysis, both 2D-DIGE and nano LC-MALDI technique were used to achieve the best results possible.

1.3 Motivation

This research thesis was part of research project called EMBEK1, which was funded by the European Research Council (ERC). The aim of EMBEK1 was to develop antimicrobial surfaces usable in medicine. For fabrication of such surfaces novel anti-microbial monomers, this can be used for plasma assisted vapour depositon to coat various surfaces in health care. As some of the surfaces, such of implants, surgical knives, sutures, catheters, do come in contact with the patient's body, the criteria of selecting an anti-microbial substance is mainly based on 2 factors. 1) Strong anti-microbial property and 2) compatibility with human cells/tissues. In copper Schiff's base complex, N. Poulter *et al.* at University of Bath, UK (1) developed a substance, which passes both the criteria.

There are ever increasing reports of evolution of bacterial resistance against anti-microbial substances in health care domain. EMBEK1 addresses the problem by aiming to improve the design of the chosen anti-microbial substances like copper-Schiff's base complex (CSB). To better the design of anti-microbial substance, this study attempts to understand the molecular mechanisms involved in the adaptation of pathogenic bacteria like *S.aureus* to anti-microbial substance like CSB.

To achieve the insights in to the molecular mechanism involved in the adaptation of *S.aureus* to CSB, comparative proteomics study was performed, as protein is the executive apparatus of the cell. It is more complex and closer to function of a biological system than the gene. Most of the previous studies on the issue are mostly focused at the genome level and on the knock out strains. But with this study we not only aim to gain the proteomic insights in to the adaptation mechanism of micro evolved *S. aureus* strain against heavy metal ions like copper ions, but we also aim to translate the proteomics data in to one broad unifying theory at a physiological level with the help of state of the art iTRAQ labeled nano LC- MALDI analysis and 2D-DIGE analysis to analyse complete proteome of the micro evolved bacteria (*S. aureus*), whereas most of the previous proteomic studies relied only on comparatively primitive techniques like 2D-Gel Electrophoresis.

2. Materials

2.1 Chemicals

Acetonitrile (Sigma-Aldrich)

Agar (Fluka)

Amonium sulphate ($\geq 98\%$, Roth)

CaCl₂ ($\geq 98\%$, Roth)

CHAPS (GE Healthcare, Uppsala, Sweden)

Cholesterol ($\geq 99\%$, Sigma-Aldrich)

Coagulase disc (Fluka)

Colloidal coomassie blue G-250 (GE Healthcare, Uppsala, Sweden)

Copper Schiff's base (CSB) (University of Bath, UK) (59)

Crystal violet (Sigma-Aldrich)

Dimethylsulfoxide (DMSO) ($\geq 99.9\%$, for molecular biology, Sigma-Aldrich)

Dithiothreitol (DTT) (99.0%, PlusOne, GE Healthcare)

Ethanol (Merk KGaA)

Ethidiumbromide (Sigma-Aldrich)

Formic acid ((Sigma-Aldrich)

Glycerol (85 % PlusOne, GE Healthcare)

Hydroethidine (Sigma-Aldrich)

K_2HPO_4 ($\geq 98.0\%$, Carl Roth)

KH_2PO_4 ($\geq 99.0\%$, Carl Roth)

LB Agar (Luria/Miller) for molecular biology (Carl Roth)

LB medium (Luria/Miller) for molecular biology (Carl Roth)

Lysostaphin (5mg/ml, Sigma-Aldrich)

Methanol (HPLC grade, Carl Roth)

$MgSO_4$ (Ultra pure, Carl Roth)

Na_2HPO_4 ($> 99.0\%$, Roth)

NaCl (Merk, extra pure)

Nucleases (Sigma-Aldrich)

Nystatin suspension (10,000 units/ml, Sigma-Aldrich)

Peptone from casein, tryptic digests (Fluka)

Pharmalyte (GE Healthcare, Uppsala, Sweden)

Protease inhibitor (Sigma-Aldrich)

Sodium dodecyl sulphate (SDS) (99.0%, Carl Roth, PlusOne, GE Healthcare)

Thiourea (Carl Roth)

Triethylammonium bicarbonate (TEABC) (Sigma-Aldrich)

Tris (99.9%, Carl Roth, PlusOne, GE Healthcare)

Tween 20 (Carl Roth)

Ultra pure water

Urea (PlusOne, GE Healthcare)

2.2 Kits and special reagents

2D-clean up kit	GE Healthcare, Uppsala, Sweden
------------------------	--------------------------------

2D-quant kit	GE Healthcare, Uppsala, Sweden
---------------------	--------------------------------

ampholytes pH 4–7	GE Healthcare, Uppsala, Sweden
--------------------------	--------------------------------

RevertAid H Minus First Strand cDNA synthesis kit	Thermo Fisher Scientific, Germany
--	--------------------------------------

CyDye™ DIGE Fluor minimal labelling kit	GE Healthcare, Uppsala, Sweden
--	--------------------------------

IPG strips	GE Healthcare, Uppsala, Sweden
-------------------	--------------------------------

iTRAQ reagents (114 , 116)	AB Sciex, Germany
-----------------------------------	----------------------

RNA isolation kit	Quiagen universal tissue kit, Germany
------------------------------	--

Sybgreen dye	Abi Prism 7000, Applied Biosystems, Germany
---------------------	--

2.3 Special solutions and buffers

Bromophenol blue stock solution

1% bromophenol blue (w/v), 50mM tris-base volume made up by double distilled water.

Colloidal coomassie blue G-250 dye stock solution

50g ammonium sulphate, 6 ml phosphoric acid 85% (w/w), 10 ml 5% coomassie blue G-250 stock made up to 500 ml with double distilled water.

Lysis buffer for nano LC-MALDI proteomics analysis

4% SDS, 0.1M DTT and 30mM Tris HCl (pH 7.5)

M9 buffer

0.02M KH_2PO_4 , 0.04 M Na_2HPO_4 , 0.08M NaCl (autoclave for 20 min at 121°C), add 1 ml 1M MgSO_4

NGM media

2.5 g/l bacto peptone, 3 g/l NaCl, 17 g/l agar (autoclave at 121°C for 20 min). In sterile condition add 10 ml 0.1 M CaCl_2 , 10 ml 0.1 M MgSO_4 and 1 ml 5mg/ml cholesterol, 2.5 ml 10000 units/ml nystatin, make the volume to 1L by adding 25 ml of 1 M sterile phosphate buffer, pH 6.0.

Rehydration solution for 2D-DIGE analysis

7M Urea, 2M thiourea, 2% (w/v) CHAPS, 0.5% pharmalyte , 0.002% bromophenol blue, double distilled water. 7 mg/ 2.5 ml DTT added just prior to use.

2.4 Organisms used

Caenorhabditis elegans (NCBI taxonomy ID: 6239)

Provided by : Prof. Dr. Björn Schumacher,CECAD Forschungszentrum, Cologne, Germany.

Escherichia coli OP50 (NCBI taxonomy ID: 637912)

Provided by : Prof. Dr. Björn Schumacher,CECAD Forschungszentrum, Cologne, Germany.

ErCu (Evolutionarily resistant to copper *MSSA476*)

Prepared by : Vishwas Kaveeshwar, University of Bonn, Bonn, Germany. Currently, stored in Institute for Rechtsmedizin, University Clinic Cologne, Germany.

Methicilin Sensitive Staphylococcus aureus 476 (NCBI taxonomy ID: 282459)

Provided by Dr. Toby Jenkins, University of Bath, Bath, United Kingdom.

Staphylococcus carnosus (NCBI taxonomy ID: 147448)

Provided by Prof.Dr.E.A.Galinski, IFMB, University of Bonn, Germany.

3. METHODS

3.1 Evolution of CSB resistance in *MSSA476*

Ten μL of an overnight culture of *MSSA476* were inoculated in 6 ml LB medium with different concentrations of CSB in culture tubes. The tubes were incubated at 37°C for 18 h. After incubation, the optical density (OD) at 600 nm was determined. Resistance against CSB was achieved by passaging the cultures using LB medium containing final concentration of 0.6 mM CSB (concentration at which the culture shows 95% inhibition with respect to the control (MIC 95). 6 tubes of 6 ml LB medium with MIC95 of CSB (final concentration 0.6 mM dissolved in LB medium containing 1% DMSO) were inoculated with 60 μL of *MSSA476* (1% of culture inoculation) and incubated for 18 h at 37°C . After 18 h the cultures were passaged into 6 fresh tubes containing 6 ml of LB with MIC95 of CSB. The tubes were incubated again at 37°C for 18 h. After 6 passages (Approx. 135 generations) the cultures had grown to optical densities of 6 at 600nm. These cultures were plated out on LB agar plate, which contained 0.7 mM CSB. After the incubation at 37°C overnight, a single colony was picked and passaged again in an overnight culture at 37°C in 6 ml LB mixed with 0.7 mM CSB. This stock was again passaged in LB containing 0.8 mM CSB overnight at 37°C . Tolerance against 0.8mM CSB was achieved in approximately 7 days. The adapted cultures were stored in 20% (v/v) Glycerol at -80°C until use for further experiments. We called the adapted strain 'ErCu'.

3.1.1 Microevolved *S.aureus* strain confirmation

To check for the contaminations, and to confirm that microevolved cultures are still *S.aureus*, PCR experiment was performed to detect *nuc* gene. Presence of *nuc* gene

was tested in *MSSA476* (Positive control), microevolved ErCu and *Staphylococcus carnosus* (Negative control). PCR experiment was performed as per the protocol published by Brakstad *et al* (60) with the modified conditions and settings as mentioned below.

Amplification of the gene was performed in over all of 40 cycles.

- 95°C for 5 min.
- 20 s at 95°C, annealing for 45s starting at 63°C and decreasing by 0.5°C. For each of the subsequent 19 cycles, followed by extension of 72°C. .
- 20 s at 95°C, 45 s at 56°C and 45 s at 72°C for remaining 20 cycles.
- Amplified products detected by 1.5% agarose gel electrophoresis.

The microevolved cultures were further grown on LB Agar and mannitol salt agar (Fluka) to check the contamination. Only when microevolved cultures were confirmed that the cultures are essentially still *S.aureus* with PCR experiments and mannitol agar test the cultures were further processed. Single colony of ErCu grown in mannitol agar media was picked and cultured for further experiments.

3.2 Characterisation of ErCu strain

3.2.1 Intracellular superoxide anion measurement

Superoxide dismutase (SODM), which is a marker of oxidative stress, catalyses detoxification of superoxide anion to H₂O₂ which is further broken down to H₂O by the enzyme catalase (61, 62).

Measurement of superoxide anion was performed using hydroethidine (HE) (63). Superoxide anions formed by the bacterial cell metabolism oxidize HE to ethidium bromide (EB) (64) which can be detected and quantified.

Two hundred μ l of an overnight culture of *MSSA476* and CSB adapted MSSA strains with the OD of 6 were inoculated in 20 ml LB medium separately. The cultures were grown to the same OD of 3 at 600nm. 200 μ l of each culture were transferred to a 96 well micro titre plate, then final concentration of 0.5 mM of CSB and final concentration of 10 μ M HE were introduced to the culture containing wells. Both cultures were further incubated for another 30 min. At this point EB fluorescence was scanned using typhoon trio scanner (GE Healthcare) at 488 nm excitation and 610 band pass filter, data was further analysed using Image Quant TL 7.0 (GE Healthcare). *MSSA476* and ErCu strains, which were not incubated with 0.5 mM CSB, were also analysed for EB fluorescence and used to normalise the EB fluorescence in *MSSA476* and ErCu strains, which were incubated with 0.5 mM CSB

3.2.2 Cellular copper concentration measurement

Two hundred μ l of an overnight culture of *MSSA476* and CSB adapted MSSA strains with the OD of 6 are inoculated in a flask each of 20 ml LB medium separately. The cultures were then incubated at 37°C for 4 hours. After 4 hours, 0.5 mM of CSB was introduced to all the test tubes. The cultures were further incubated for another 30 min. At this point cultures were harvested which are in the log phase and are grown to the same OD of 3 at 600nm. Reference cultures were also prepared in the same way, but the cultures were not intoxicated with CSB. The media was devoid of any external copper.

All the bacterial pellets, which were harvested including reference culture, were washed 3 times with the phosphate buffer. Pellets were subjected for vacuum drying. Once the bacterial pellets were completely dried, green coloured copper residue which is attached to the surface of the pellet was removed manually and discarded. Equal amounts of dry pellets (5.6 mg) were taken for the further analysis. The dry pellets were re-suspended in 150 µl of 100µg/ml lysostaphin and incubated for 10 min at 37°C. Each of the suspensions was made up to 1 ml with 30mM Tris HCL (pH 7.5). Suspensions were boiled at 100°C for 15 min. Copper measurement in *MSSA476* strain, ErCu strain and reference was performed using inductively coupled plasma mass spectrometry (ICP-MS) according to the protocol published by A. Lotz *et al.*(65). Actual ICP-MS measurement was performed by Dr. A. Lotz, Max Planck Institute for Polymer Research, Mainz, Germany.

3.2.3 Phenotypic expression of virulence factors in *MSSA476* and in ErCu

3.2.3.1 Slide coagulase test (test for clumping factor)

The test was performed with *MSSA476* strain as a positive control sample, ErCu strain, *Staphylococcus carnosus* (*S. carnosus*) as a negative control on 3 different glass slides each. One drop of ultra pure water was given onto a glass microscope slide. A high concentrated suspension of the respective organism was then prepared. One coagulase disc (Fluka) was added and rubbed on the suspension with the tip of an inoculation loop. Subsequently, a second drop of ultra pure water was added and mixed again.

3.2.3.2 Blood agar test

LB agar containing 5% human blood was prepared. Overnight cultures of *MSSA476* and evolutionary ErCu strains were plated out on the prepared blood agar medium and incubated at 37° C for 18 h.

3.2.3.3 Virulence test of ErCu in comparison with *MSSA476* strain on *Caenorhabditis elegans*

C. elegans life cycle contains 4 larval stages (Fig. 2). At 25°C, it takes approximately 24 h to attain L4 stage from L1 stage. When there is food deficiency, starving larvae go in *dauer* phase. After supplying the food, dauer larvae will reach L4 stage. In *C.elegan* growth assay, the number of survived L4 staged larvae was determined, when L1 stage larvae were inoculated on a lawn of *MSSA476* and ErCu strain in a given time.

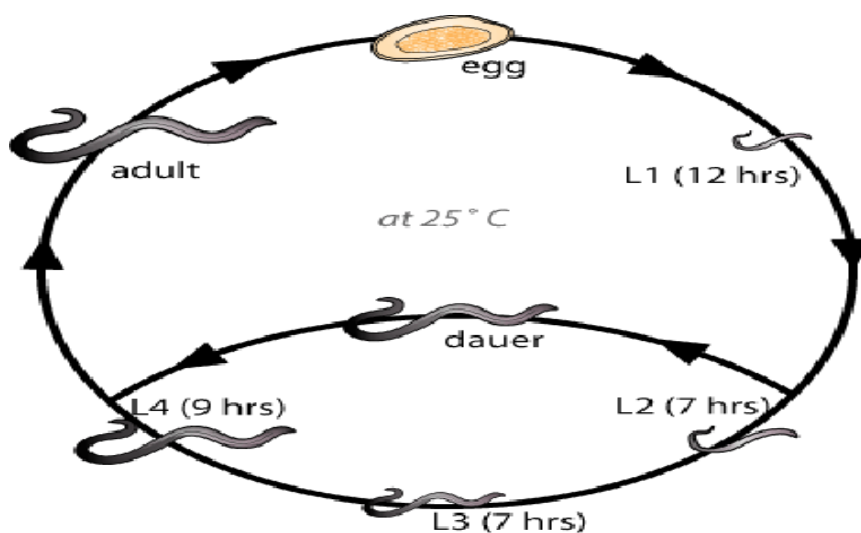


Figure 2: Life cycle of a *C.elegan* at 25 °C (From Miranda Klees *et al.*, Department of Biological Sciences, Clemson University, United States of America, artwork from www.scq.ubc.ca/geneUc-studies-of-aging-and-longevity-in-model-organisms)

A lawn of *MSSA476*, a lawn of ErCu strain and a lawn of *E. coli op 50* (control, nutrition factor of *C. elegans*) were grown on nematode growth medium (NGM) plates. Plates with *MSSA476* were used as positive control (inhibition of *C. elegans* growth is expected) and *E.coli op 50* as a negative control (no inhibition of *C. elegans* growth is expected), respectively.

A plate of fully starved *C. elegans* was washed with 10 ml of M9 buffer. The collected buffer fraction containing the *C.elegans* was then filtered through a nylon filter (NY11 Milipore, 11 μ m) and the L1 stage *C. elegans* containing filtrate was collected in falcon tubes. 500 μ l of the filtrate was used to culture the *C. elegans* on each bacterium inoculated NGM plate. Each plate contained 20 L1 staged *C. elegans*. All three plates were incubated at 25°C for 24h. No L4 staged *C.elegans* were found either in *MSSA476* or in ErCu. *C.elegans* were further incubated for another 24h at 25°C. In this time, healthy nematodes grow into L4 stage. After 48 h all three plates were examined under the microscope and the number of L4 staged *C. elegans* was counted. The experiment was repeated 3 times.

3.3 Comparative studies between *MSSA476* and ErCu with respect to protein and gene expression

3.3.1 Two-Dimensional Differential In Gel Electrophoresis analysis

Two-hundred μ l of an overnight culture of *MSSA 476* and CSB adapted *MSSA* strains with the OD₆₀₀ of 6 were inoculated in 20 ml LB medium separately. The cultures were then incubated at 37°C for 4 h. After 4 h 0.5 mM of CSB was introduced to all test tubes. Both the cultures were further incubated for another 30 min. The cultures were harvested by centrifugation at an OD just above 3 at 600nm (log phase).

Both the bacterial pellets were washed at least 3 times with phosphate buffer. Pellets were re-suspended in 1 ml lyses buffer (7 M urea, 2 M thiourea, 30 mM TRIS (pH 7.5), 4% v/v CHAPS) and subjected to a pressure of 2.70 lbs/m² in the Constant cell disruption system. After the lysis, the samples were incubated at 37°C for 15 min containing a final concentration of 1 x nuclease mix and 1 x protease inhibitor. Further, proteome analysis of ErCu and *MSSA476* strains was performed mostly according to the protocols from A. Görg and colleagues (Two-Dimensional Electrophoresis with Immobilized pH Gradients for Proteome Analysis; A laboratory manual, www.wzw.tum.de/proteomik). Some modifications were made as mentioned in the protocol published by P. Cierniak *et al* (66). The samples were centrifuged at 8000 g for 20 min at 4°C to remove insoluble material after incubation. The supernatant was then transferred into 1.5 ml centrifuge tubes and centrifuged again at 25000 g for 45 min at 4°C. Subsequently, proteins were isolated from the crude extracts by the 2-D Clean-Up Kit (GE Healthcare, Uppsala, Sweden) according to manufacturer's instructions and dissolved in lysis buffer (7 M urea, 2 M thiourea, 4% (v/v) CHAPS, 30 mM tris (pH 7.5)). The pH of the dissolved samples was adjusted to 8.5 on ice with 0.1 M NaOH (analytical grade, Carl Roth, Karlsruhe, Germany) and the protein concentration was photometrically determined using the 2-D Quant kit (GE Healthcare, Uppsala, Sweden).

The protein samples were then CyDye labelled. 50 µg of protein from each sample was labelled using the CyDye™ DIGE Fluor minimal labelling kit (GE Healthcare, Uppsala, Sweden) as suggested in the manufacturer's instructions. 1.1 µl of Cydye was used to label the 50µgs of protein each. After labelling, sample buffer (7 M urea, 2 M thiourea, 4% (v/v) CHAPS, 2% (v/v) ampholytes pH 4–7) was added to the labelled protein sample in the ratio of 1:1 and pooled. Each pooled sample consisted

of an array of the non-adapted MSSA 476 proteome, an array of the adapted ErCu proteome and a mixture of all samples (internal standard). The dye labelling order was reversed from one sample to the next. The swapping of dyes balances the effect of label factor and permits ANOVA (Analysis of Variance) estimation. The samples were then subjected to Iso electric focusing (IEF).

IEF was performed on an immobilized pH gradient (IPG) 18 cm strips, pH 4–7 (GE Healthcare, Uppsala, Sweden). Dry IPG 18cms strips were rehydrated over night in rehydration solution. The samples were then applied at the cathode end onto IPG strips using cup loading method (GE Healthcare, Uppsala, Sweden). IEF separated samples were further subjected for the additional separation in the second dimension (Ettan DALTsix, GE Healthcare, Uppsala, Sweden) for 5 h. SDS PAGE gel on which second dimensional separation was performed is scanned using a fluorescent scanner (Typhoon Trio, GE Healthcare, Uppsala, Sweden). Three different wavelengths corresponding to the Cydyes, with associated band pass filters, were used to scan the gels. Experimental groups were analysed by DeCyder™ V6 (GE Healthcare, Uppsala, Sweden). Protein spots with Student's T-test score $p < 0.01$, false discovery rate correction ($q < 0.01$) were considered and picked for the further mass spectrometry analysis. Null hypothesis for these proteins was rejected. Once the protein spots which are significantly differentially expressed were identified, the spots were manually picked from the colloidal coomassie blue (GE Healthcare, Uppsala, Sweden) stained 2DE gels. These gels were run parallel to 2D-DIGE gels. The gels were prepared and stained as per the instructions from the manufacturers. The picked protein spots were further digested by trypsin and the resulting peptides were analysed using ultra high performance liquid chromatography-mass spectrometry. Further MS analysis is performed according to the protocol explained

by P. Cierniak *et al.* (66) by Dr. Stephan Mueller at the Center for Molecular Medicine Cologne, University Hospital Cologne, Germany.

3.3.2 Nano LC- MALDI analysis

3.3.2.1 Bacterial growth conditions and sample preparations

Two-hundred μ l of an overnight culture of *MSSA476* and *ErCu* strains with the OD of 6 were inoculated in 3 flasks each of 20 ml LB medium separately. The cultures were then incubated at 37°C for 4 hours. After 4 hours, CSB was introduced to all test tubes making the final concentration of the CSB to 0.5 μ M and then all 6 cultures were further incubated for another 30 min. As next step, the cultures were harvested by centrifugation at an OD of 3. All the bacterial pellets were washed 3 times with phosphate buffer. Both adapted and the non-adapted strains were re suspended in 150 μ l of 100 μ g/ml lysostaphin and incubated for 10 min at 37°C. Afterwards the suspension was subjected to ultra sonication (Bandelin). Four percent Sodium dodecyl sulfate (SDS) and 0.1 M Dithiothreitol (DTT) (final concentration) were added to each of the crude extracts and the suspensions were made up to 1 ml with 30mM Tris HCl (pH 7.5). Suspensions were boiled at 100°C for 15 min to lyse the cells completely. A mild centrifugation step of 3000 g for 5 min was performed. The resulting pellets were discarded and the supernatants, which contain the proteins, were analysed with the nano LC- MALDI mass spectrometry.

3.3.2.2 Filter assisted sample preparation (FASP)

FASP was performed on crude lysates to obtain tryptic digested peptides for LC-MS experiments as per the protocols of J.R Wisniewski *et al.* (67) with some minor modifications. Lysates were centrifuged at 14.000 rcf for 5 min at 20°C. 20 μ l of the

supernatants corresponding to 60 µg protein were transferred to Amicon Ultra™ centrifugal filter units (0.5 ml, 10K). FASP was performed by using 1 µg of sequential endoproteinase Lys C. In addition, 1 µg of trypsin was used for the peptide digestion as demonstrated by Wisniewski JR *et al.* (67). In all the buffers used, TrisHCl with the concentration of 0.1 M was replaced by 0.1 M triethylammonium bicarbonate pH 8.5 (TEABC). However, in initial lysis buffer, buffer replacement is avoided. After the digestion, centrifugation of digested samples was performed and resulting filtrates were collected. 120 µl of 10% acetonitrile in ultrapure water were added to the filtrate, mixed with the residual sample and centrifuged again. Thus, obtained combined filtrates were applied on a C18 SD cartridge (4 mm, 1 ml). After the filtrate was applied on the SD cartridge, the SD cartridge was activated with Methanol. SD cartridge was then washed with 80% acetonitrile and equilibrated to 0.1 M TEABC. The cartridge was washed two times with 200 µl 0.1 M TEABC and the desalted peptides were eluted with 100 µl 80% acetonitrile in 0.1 M TEABC.

3.3.2.3 Isobaric tags for relative and absolute quantitation (iTRAQ)

iTRAQ peptide labeling is performed based on the protocols by Effertz.C *et al* (68). 15 µl of 1 M TEABC was added to the peptide sample prepared by FASP procedure, volume of which was reduced to 10 µl using centrifugal evaporator before adding 15 µl of 1 M TEABC. Sample volumes were further adjusted to 30 µl with water. iTRAQ reagents 114 and 116 (AB Sciex) were dissolved in 70 µl ethanol and mixed with the corresponding samples immediately. Samples with iTRAQ reagents were incubated for 2 h at ambient temperature in the dark. After the incubation, the iTRAQ labeled samples were combined. The desalting of the samples was achieved using a C18 SD cartridge as described above. 0.1 M TEABC was replaced by 0.1% formic acid

in all steps. Peptides labeled with iTRAQ from 3 different culture lysates were pooled for the further chromatographic peptide separation and MALDI analysis.

3.3.2.4 Strong Cation Exchange HPLC

Strong Cation Exchange (SCX) Chromatography was performed on an Ettan micro LC system (GE Healthcare) in split mode for iTRAQ labeled peptide fractionation before MALDI spotting. LC column with the dimensions of 0.5 mm x 150 mm was used. The column was packed with BioBasic SCX 5 μ m (Thermo). The column was equilibrated in 25% acetonitrile in 0.1% formic acid. The sample flow rate of 20 μ l/min on the column was achieved with the combination of a “0.8 mm ID” restriction capillary (Dionex) and 125 μ l/min pump flow. The samples were resuspended in 50 μ l of 40% acetonitrile containing 0.1% formic acid and were injected onto the column. Peptide separation was achieved by using a gradient of 0 M to 250 mM sodium chloride in 12 min. The fractions were collected every 60 sec. Acetonitrile from the samples was removed by subjecting the samples to brief vacuum centrifugation. 0.1% TFA (Trifluoroacetic acid) was added to the samples to adjust the volume of the sample to 20 μ l.

3.3.2.5 MALDI Spotting

MALDI spotting is performed according to the protocol mentioned by Effertz.C *et al* (68) and S. Staubach *et al* (69). Reversed phase HPLC on an Eksigent nano LC 1D plus system (Axel Semrau GmbH, Sprockhövel, Germany) is employed to separate the peptides obtained in the SCX fractions by using a vented column setup comprising a 0.1-mm/20-mm trapping column and a 0.075mm/200-mm analytical column (68). Both the trapping and analytical column were packed with ReproSil-Pur C18-AQ, 5 μ m (Dr. Maisch, Ammerbuch, Germany) at 40°C. Sample fractions were

aspirated into the sample loop and were loaded onto the trap column with a volume of 18 μ l and 30 μ l respectively. Sample was loaded on trap column using a flow rate of 6 μ l/min. 0.1 % TFA was used as loading pump buffer. Peptide elution from the column was performed over the period of 70 min with a flow rate of 300 nl/min. Peptide elution from the column was brought about by an eluting solution, which was a gradient of 5 % to 35% acetonitrile in 0.1% TFA. Post column T-union was injected with 0.7 mg/ml alpha-Cyano-4-hydroxycinnamic acid (HCCA) in 95% acetonitrile in 0.1% TFA, 1 mM ammonium phosphate using a syringe pump. The rate of syringe pump injection was maintained at 150 μ l/h. Probot™ (Dionex, Idstein, Germany) fraction collector was used to deposit 384 fractions (12 seconds) of elute on a MTB AnchorChip 384-800™ MALDI target (Bruker Daltonics, Bremen, Germany).

3.3.2.6 LC-MALDI MS/MS analysis

MALDI MS and MS/MS analysis were carried out according to the protocols followed by Effertz.C *et al* (68), S. Staubach *et al* (69), S. Feldkirchner *et al* (70) on an Ultraflex™ MALDI ToF ToF mass spectrometer (Bruker Daltonics) operated with a laser repetition rate of 1 Ghz. MALDI MS spectra data were acquired with the help of Flexcontrol 3.0 and WarpLC. Spectra calibration was performed externally on the designated target calibration spots using the Peptide Calibration Standard II (all Bruker Daltonics). MS spectra data acquired peptide mass ranging from 700 Da – 4000 Da. The laser was used with a fixed energy setting and 3000 shots/spectrum were collected from random raster points. Criteria for selecting precursor ions for MS/MS analysis was based on the signal to noise ration. Signal to noise ratio ≥ 10 was used as a cut of for selecting precursor ion further MS/MS analysis. Identical peaks in adjacent spots were measured only once, preferentially from the spot with

maximum peak intensity. Each spot was restricted to maximum of 20 MS/MS spectra. With above mentioned restriction, if the alternative position is not witnessed, in that case the restriction is relaxed and the value of 20 MS/MS spectra per spot is exceeded. If the polymer signals and peaks appear on all spots atleast more than 40%, those signals and peaks were filtered out. After the instrument calibration MS/MS spectra for 3500 shots were acquired. Internal recalibration was performed by using iTRAQ reporter ions and peptide immonium ions.

3.3.2.7 Database Searches

Database search for MS/MS spectra acquired was carried out as mentioned by S. Feldkirchner *et al* (70) and was performed using University Hospital, Cologne internet source (uni-koeln.de). A composite decoy database was generated for MS/MS spectra acquired during LC-MS/MS experiment. Perl script makeDecoyDB (Bruker Daltonics, Bremen, Germany) was used to generate the composite decoy database from Uniprot database (August 10. 2010). The uniprot data composed of 519348 sequences and 183273162 residues. To calculate the false positive rates, Perl script makeDecoyDB added a shuffled sequence and a tagged accession number for each entry is calculated in Proteinscape 2.1. The composite decoy database was further submitted to MASCOT 2.2 (Matrix Science Ltd, London, UK). MASCOT 2.2 via Proteinscape (Bruker Daltonics, Bremen, Germany) was used to search the decoy database. MASCOT 2.2 was employed with the parameter settings as listed below.

MASCOT 2.2 parameter settings:

1. Enzyme: "Trypsin" with 1 missed cleavage;

2. Fixed modifications: “carbamidomethyl”, “iTRAQ4plex (K)”, “iTRAQ4plex (N-term)” Optional modifications: “Methionine oxidation”, “iTRAQ4plex (Y)”, “Cation:Na (DE)”, “Acetyl (Protein N-term)” and “Gln>Pyro-Glu (N-Term Q)”.
3. Mass tolerance: 20 ppm for MS and 1.0 Da for MS/MS spectra
4. Species filter: “*S. aureus*”

Proteinscape was used to compile the protein list generated from MASCOT 2.2 search engine. Ion score value > 25 was used as criteria to accept the peptide hits. Protein hits required at least one peptide hit exceeding a peptide score of 40. In addition, the hits to decoy entries were used to calculate a Minimal protein score, was calculated using the hits to decoy entries. The false positive rate was kept <2% on the protein level. False positive rate <2% was achieved with the help of minimal protein score.

Nano-LC MALDI experiments were performed at Center for Molecular Medicine Cologne, Germany with the help of Dr. Stephan Mueller.

3.3.3 Gene expression analysis

Two-hundred μ l of an overnight culture of *MSSA476* and CSB adapted *MSSA* strains with the OD of 6 were inoculated in 20 ml LB medium separately. The cultures were then incubated at 37°C for 4 hours. After 4 hours 0.5 mM of CSB was introduced to all the test tubes. Both the cultures were further incubated for another 30 min. The cultures were then harvested by centrifugation at an OD₆₀₀ just above 3 (log phase). Both the bacterial pellets were washed at least 3 times with phosphate buffer. Both adapted and the non-adapted strains were resuspended in 150 μ l of 100 μ g/ml lysostaphin and incubated for 10 min at 37°C. Suspensions were made up to 1 ml

with 30mM Tris HCL (pH 7.5). Suspensions were boiled at 100°C for 15 min. After lyses, the samples were further used for RNA isolation.

3.3.3.1 Isolation of RNA

Quiagen universal tissue kit was used to isolate the RNA from the suspension. Protocol suggested by the manufacturer was used to isolate the RNA. An additional purification protocol was included to get rid of the genomic DNA contamination completely. The manufacturer's protocol by RevertAid H Minus First Strand cDNA synthesis kit was followed to remove the genomic DNA from RNA preparation. (For 1µg of RNA 1u RNase free DNase I was used.).

3.3.3.2 c-DNA preparation

Fifty ng of RNA from each sample was used to prepare cDNA. Reverse transcription reaction was performed using RevertAid H Minus First Strand cDNA Synthesis Kit and 30 µl of cDNA was prepared. The cDNA was further used to measure the relative quantities of m-RNA.

3.3.3.3 Primers

Using online primer designing software (BatchPrimer3 v1.0), primers were designed for the genes of interest. List of primer sequences for the respective genes is listed in Table 1.

Gene	Primer	Sequence (5'-3')
<i>copZ</i>	<i>copZ</i> -F	GAGCTGTGGTCACTGCAAAA
	<i>copZ</i> -B	CGTCAGCTGAAGTGACACC
<i>agrA</i>	<i>agrA</i> -F	TCACAGACTCATTGCCATT
	<i>agrA</i> -B	CACCGATGCATAGCAGTGTT
<i>clfA</i>	<i>clfA</i> - F	AGCGAGCGATTCAGATTCAG
	<i>clfA</i> -B	GTCGGAATCACTGTCGGAGT
<i>Spa</i>	<i>spa</i> - F	GTTCGTCATGATGAGCGTGT
	<i>spa</i> – B	TGAGGAGCCTCAACTTTTGG

Table 1: List of forward (F) and reverse (B) primers used for the respective gene amplification.

3.3.3.4 Real time PCR assay

The mRNA levels of copper chaperon Z, clumping factor A, accessory gene regulatory protein A were quantified by using real time PCR assay using Sybgreen (Abi Prism 7000, Applied Biosystems). Housekeeping 16s rRNA gene product was also quantified and used to normalise the quantities of the other mRNAs. The Ct values were analysed, quality controlled and graphs of gene expression were plotted using the software qbase plus. The experiment was performed in both *MSSA476* and ErCu in triplicates. Gene expression analysis experiments were performed

under the supervision of Dr.E. Gomes, Institute for Legal Medicine, University Hospital, Cologne.

3.4 Biofilm assay in *MSSA476* and ErCu strain

The microtiter dish biofilm assay is performed using static growth conditions, therefore the mature biofilm formation can be avoided and the early stages in bacterial biofilm formation can be studied (71).

Overnight cultures of *MSSA476* and ErCu with the same OD of 5 were 1:100 diluted in LB medium. 100 µl of each diluted culture was transferred into each well in a fresh tissue culture untreated 24 well microtiter plate. Microtitre plate was covered with the lid and incubated at 37°C over night. Planktonic bacteria from each microtiter dish were removed by briskly shaking the dish out in a waste tray. Wells were further washed by submerging the plate in the tray with 1-2 inches of water. Thus, filled water was removed in the wash tray by vigorously shaking out the liquid. Water was replaced when it became cloudy. 125 µl of 0.1% crystal violet solution is added to each well. Micro titer plate was incubated for 10 min at room temperature. Each micro titer dish was shaken and crystal violet solution is removed over the waste tray. Dishes were further washed again 2 more times in the water trays and as much liquid as possible is removed from the dish after each wash. Micro titer dish was inverted and vigorously tapped on paper towels to remove any excess liquid. Plates are air-dried. 200 µl of 95% ethanol is added to each stained well. Dye is allowed to solubilize by covering plates and incubating 10 to 15 min at room temperature. The contents of each well were mixed by pipetting, and then 125 µl of the crystal violet/ethanol solution from each well is transferred to a separate new clear flat-

bottom 96-well plate. Optical density (OD) of the samples was measured at a wavelength of 600 nm.

4. Results

4.1 Evolution of CSB resistance in *MSSA476*

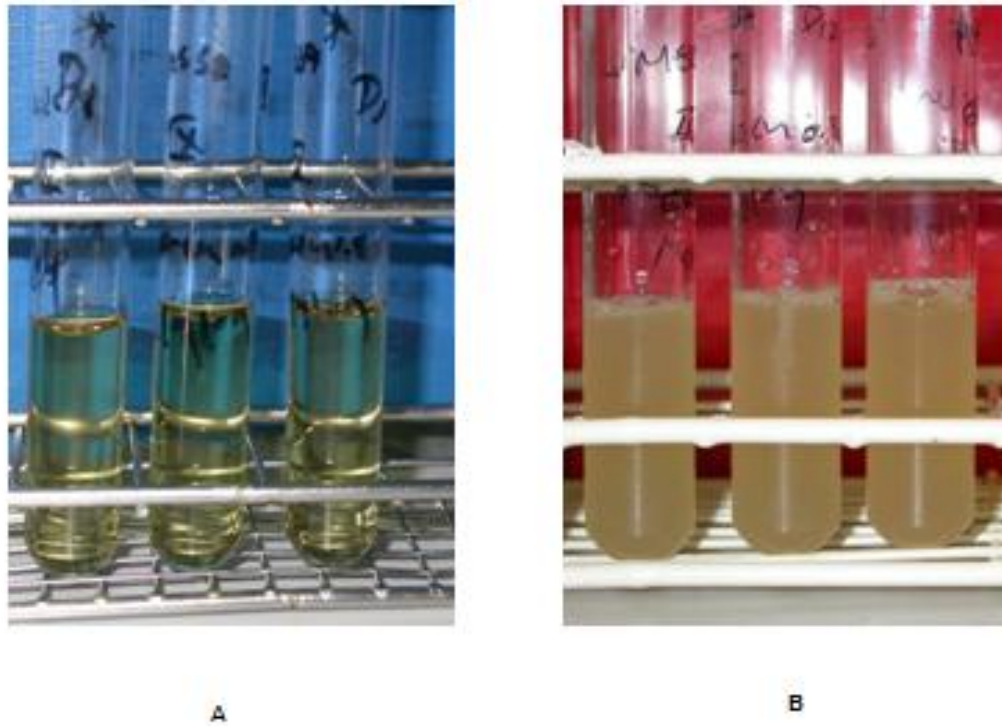


Figure 3: Growth of CSB sensitive *MSSA476* and CSB tolerant ErCu strain A) No growth was observed in CSB tolerant *MSSA476* incubated in LB with 0.8mM CSB at 37 °C for 18h B) Growth observed in CSB adapted ErCu strain incubated in LB with 0.8mM CSB at 37 °C for 18 h

Non passaged wild type *MSSA476* showed no significant growth when incubated in LB media with 0.8mM CSB at 37°C for 18 h as shown by clear green solution in Fig. 3A, whereas CSB passaged *MSSA476* showed after the microevolution experiment significant growth when incubated in LB media with 0.8mM CSB at 37°C for 18 h represented by the turbid solution in Fig. 3B.

Bacterial growth was determined by measuring Optical Density (OD) of the cultures at 600nm wavelength at various concentrations of CSB.

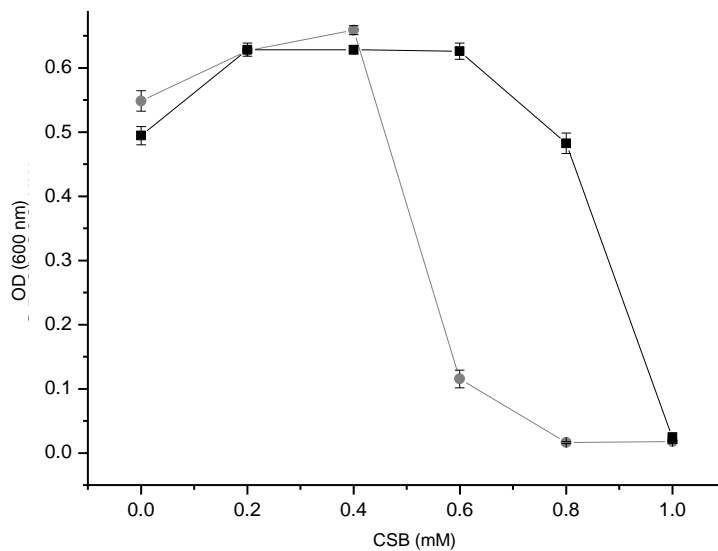


Figure 4: Graphical representation of CSB tolerance of sensitive and tolerant strains. Optical density at 600 nm after 18 h of incubation of non-adapted (grey circles) and adapted *MSSA476* (ErCu) (black squares) at different concentration of CSB in LB medium. Samples were diluted 1:10 before the readings were taken (n=3).

After the microevolution, experiments the tolerance against CSB was compared between the CSB adapted ErCu and its non-CSB adapted ancestral strain MSSA 476. Fig. 4 shows the optical densities at different CSB concentrations after 18 h. As depicted both the cultures grow in a medium lacking CSB to an OD of about 5 to 5.5 (Fig. 4). With increasing CSB concentration up to 0.4 mM, the OD of both the cultures increases slightly to about 6. At a concentration of 0.6 mM of CSB, a

marked difference in copper tolerance was observed. At 0.8 mM, nearly no growth could be determined for the *MSSA476*. In contrast to that, the CSB adapted ErCu was still able to grow to an OD_{600} of 5 at 0.8 mM of CSB concentration.

As shown in the Fig. 3 and 4, ErCu strain is able to grow better than, wildtype *MSSA476* at 0.6 mM and up to 0.8 mM of CSB.

4.1.1 Confirmation of microevolved *S.aureus* strain

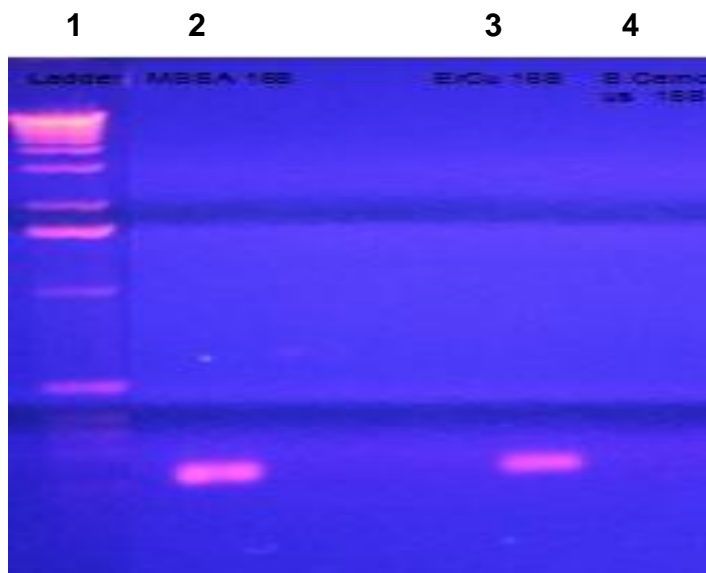
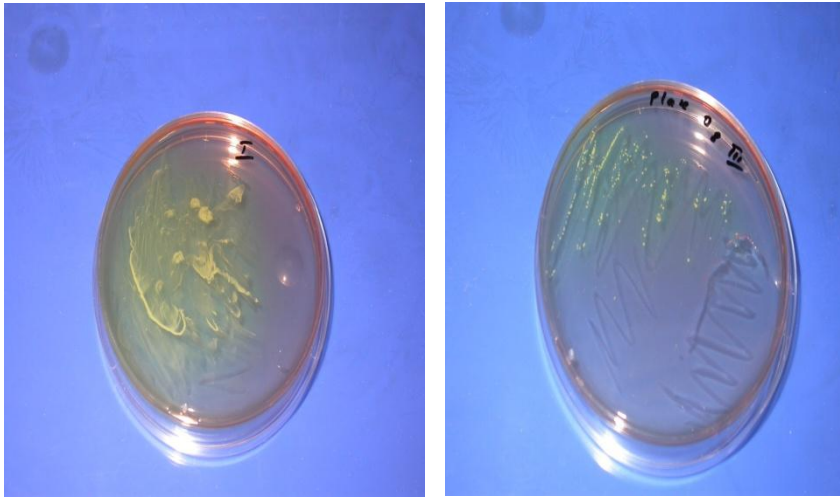


Figure 4.1: Agarose gel electrophoresis showing 270bp fragment of *nuc* gene in *MSSA476*, ErCu (Lane 2 and 3), and in *S.carnosus* as the negative control (Lane 4), 1Kbp ladder (Lane 1). Picture has been edited to remove the non-relevant lanes. Non edited figure can be referred in appendix (7.5)

Fig. 4.1 shows amplified *nuc* gene fragment band in *MSSA476* (positive control) and ErCu strains. No *nuc* gene band can be seen for *S.carnosus* (negative control) as expected.



A

B

Figure 4.2: Cultures grown in mannitol agar media. A) *MSSA476* culture B) ErCu cultures

Fig. 4.2 shows growth of yellow *MSSA476* (positive control) and ErCu colonies in mannitol agar medium which is used to pick the non-contaminated *S.aureus* colonies.

4.2 Characterisation of ErCu strain

4.2.1 Intracellular superoxide anion measurement

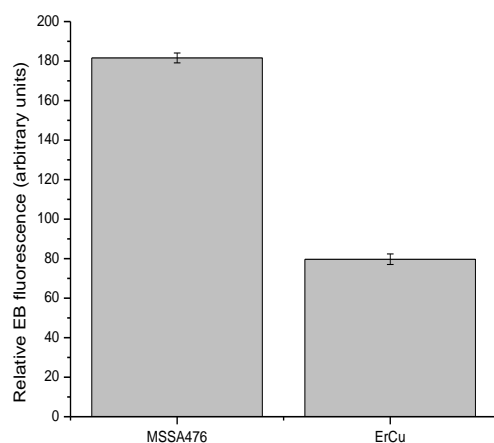


Figure 5: Intracellular superoxide anion measurement in ErCu and *MSSA476* strains grown in the presence of 0.5 mM CSB. Fluorescence reading of EB can be referred in appendix 7.1

Fig. 5 shows the fluorescence of EB originating from the relative amounts of superoxide in *MSSA476* and ErCu, it can be seen that the production of EB is considerably higher in case of *MSSA476* than ErCu. This suggests that, there is a higher superoxide anion production in *MSSA476* than in ErCu.

Superoxide dismutase is a marker of oxidative stress created by toxic reactive oxygen species (ROS) like superoxide anion (61) (62). Therefore, the generation of superoxide was measured. Decreased superoxide anion in ErCu is a clear indication of reduced Superoxide dismutase in ErCu, which was further, confirmed in comparative proteomics experiment as well (Table 3). Reduced Superoxide dismutase indicates lower oxidative stress in ErCu.

4.2.2 Cellular copper concentration measurement

Insights in to the copper hemostasis mechanism in ErCu are possible by comparing the cellular copper concentration of ErCu with *MSSA476*.

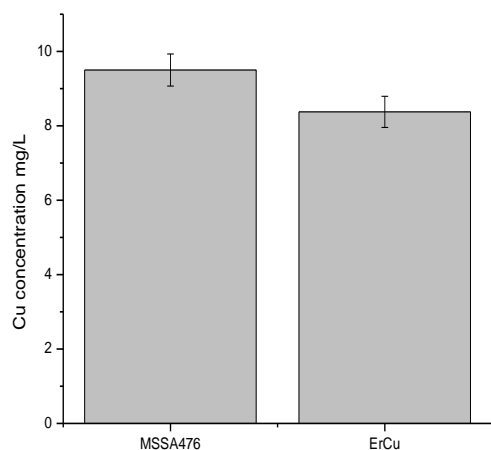


Figure 6: Concentration of copper ions measured by ICP-MS present in the *MSSA476* and ErCu cells grown in 0.5mM CSB. Measurement is expressed in mg/L of sample processed. Error bars indicate the deviation of 3 independent experiments. ICP-MS reading and standard deviation calculated can be referred in appendix 7.2

The copper concentration for the ErCu strain is at an average of 8.37 mg/L of lysate, where as *MSSA476*, showed an average concentration of 9.5 mg/L of lysate. Student's T test was performed to validate the data. T test gave the value of 0.041, which can be taken as a proof that the experimental data are statistically significant.

From the observations, it is clear that ErCu is able to maintain cellular copper homeostasis better than *MSSA476*. The molecular mechanism of copper homeostasis in case of ErCu is further determined by comparative proteomics experiments (Chapter, 4.3.2).

4.2.3 Phenotypic expression of virulence factors.

It is well recorded that under heavy metal stress, virulence of *S.aureus* is diminished (72, 73). To understand the virulence ability of ErCu and *MSSA476*, slide coagulase test, blood agar test and *Caenorhabditis elegans* (*C.elegan*) growth assay were performed. Slide coagulase test helps detecting virulence factors like clumping factor in bacteria, whereas blood agar test determines the hemolytic activity of bacteria. Virulence bio-assay is based on the larval development of *C.elegans*.

Coagulase test (clumping factor test) showed a microscopic clumping within 30 sec. in *MSSA476* (positive control). In contrast, the ErCu did not show such an effect, nor did *S. carnosus*, which was used as negative control.

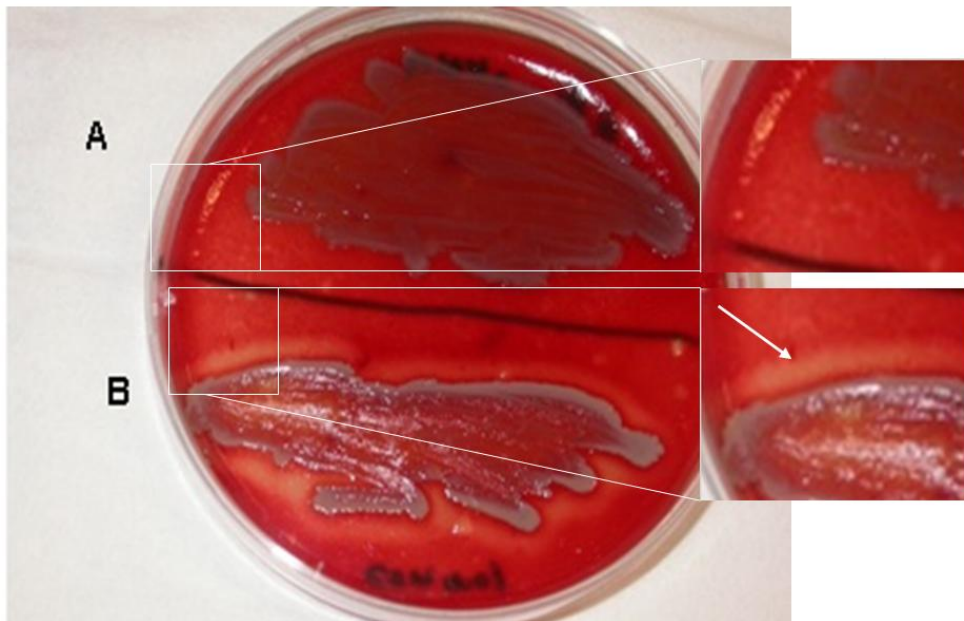


Figure 7: Hemolytic test on blood agar. A: ErCu on LB Agar containing human blood. B: *MSSA476* on LB Agar containing human blood, white arrow indicates the hemolytic zone

In hemolytic test, when *MSSA476* culture (positive control) is compared to the ErCu strain on the same blood agar plate (Fig. 7), a significant hemolytic zone can be seen around the *MSSA476* culture (Fig. 7 B) as compared to the ErCu strain (Fig. 7 A). This indicates the release of toxins causing hemolysis in case of *MSSA476* strain only. In conclusion ErCu does not show hemolytic activity and no bound coagulase activity (clumping factor). These indications for reduced virulence in ErCu were confirmed In *C.elegan* growth assay.

The number of living L4 nematode stages are shown after incubation together with *MSSA476* or ErCu or *E. coli* op 50, respectively (Fig. 8).

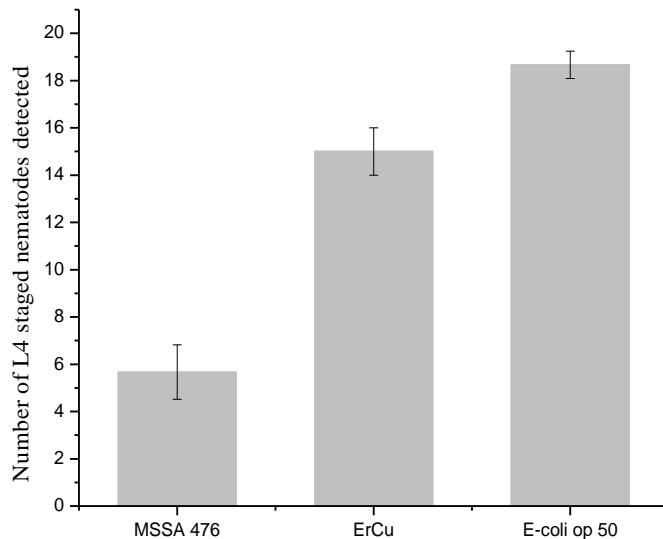


Figure 8: *C. elegan* growth assay to test the virulence of ErCu and *MSSA476* strains: In the presence of virulent *MSSA476* (positive control) only a few viable L4 staged nematodes were detected after 48 h of incubation. In contrast, in cultures with ErCu strain a large number of L4 staged nematodes were detected. The same is found for *E. coli* op 50 (negative control). n=3

As shown in the graph in Fig. 8, far more living individuals of *C. elegans* in L4 stage were detected which were grown on CSB adapted ErCu strain in comparison to the *C. elegans* grown on the wild type strain. The highest number of *C. elegans* (on average 19 nematodes) in L4 stage was counted after feeding on *E. coli* op 50 (negative control).

Comparative proteomics experiments were performed to obtain further insights in to this phenomenon.

4.3 Comparative Studies between *MSSA476* and ErCu strain with respect to protein and gene expression

For the comparison of the complete proteome of *MSSA476* and ErCu strain, 2D-Differential In Gel Electrophoresis (2D-DIGE) and nano Liquid Chromatography – Matrix Associated Laser Desorption Ionisation (nano LC-MALDI) with isobaric tags for relative and absolute quantitation (iTRAQ) were used. Differential labelling of N-terminus of the peptides by isobaric tags is the principle behind nano LC-MALDI technique. Tagged samples are further analysed by tandem mass spectrometry for the relative quantitation (58).

4.3.1 Two- Dimensional Differential In Gel Electrophoresis (2D-DIGE) analysis

2D-gel electrophoresis is a technique used to resolve individual proteins from a complex protein cocktail. The resolution of proteins is based on their respective isoelectric points and molecular weights. The proteins observed in this study are limited to the iso electric points ranging from pH 4-7. Therefore, extremely acidic or basic proteins could not be resolved.

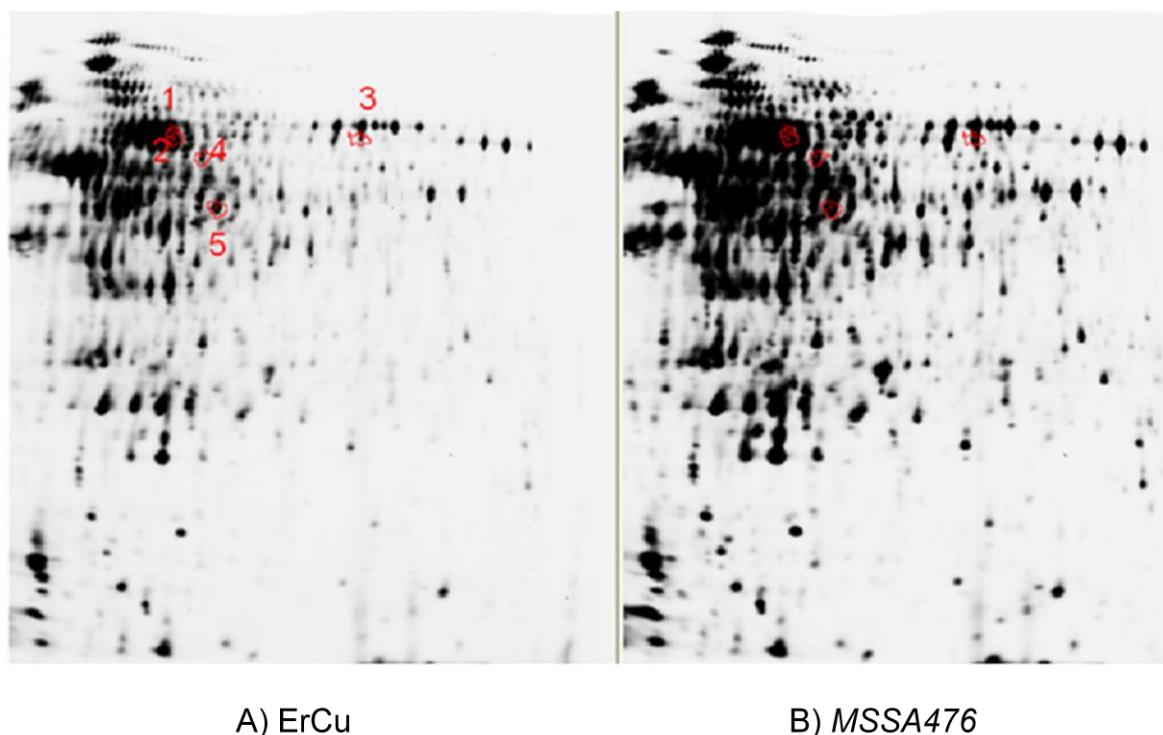


Figure 9A: Protein pattern of A) ErCu and B) *MSSA476* parent strains grown in 0.5mM CSB obtained by 2D-DIGE. 5 down regulated protein spots are marked and numbered in the ErCu gel.

With 2D-DIGE analysis, over 2000 protein spots were found on the gel. Student's t test was performed to validate the statistical significance of obtained data. On the out set several hundred proteins seem to be differentially expressed in ErCu. However, up on analysis by 'Decyder' image analysis software and Student's t test only 6 proteins were revealed to be statistically verified differentially expressed in ErCu (five down-regulated and one up-regulated). Out of six, five proteins were revealed to be down-regulated in ErCu with the Student's t test score under 0.01 (Proteins with student's t test score ≤ 0.01 are generally considered statistically significant in case of 2D-DIGE experiments globally). Five down regulated proteins, with their expression levels as compared to *MSSA476*, statistical analysis scores and functions are listed in table 2.

	Protein name	T-test	Protein expression	Functions
1	Aspartyl/glutamyl-tRNA amidotransferase subunit A	0.0039	-1.62	Purine biosynthesis
2	Aldehyde dehydrogenase like protein	0.0039	-1.71	Production of ATP and maintain energy pool
3	Inositol monophosphate dehydrogenase	0.0039	-1.91	Maintaining the guanine nucleotide pool
4	Fumarate hydratase	0.0039	-1.56	Production of ATP and maintain energy pool
5	Ornithine-oxo-acid transaminase	0.0066	-1.98	L-proline biosynthesis

Table 2: List of down regulated proteins in ErCu, with their expression levels as compared to *MSSA476*, statistical analysis scores and functions. Functions of the proteins listed were referred from uniprot (www.uniprot.org)

Spectrometry data MASCOT search results and screen shot for Student's t test analysed by 'DeCyder' software for above mentioned proteins can be referred in appendix (7.6, 7.7).

According to www.uniprot.org, the functions of the 5 down regulated proteins mentioned in the table 2 indicate, the involvement of the proteins in bacterial metabolism and metabolic energy pool. However, the role of down-regulated proteins in the adaptation mechanism is unclear. Further investigation is required to determine whether the down-regulation of above listed proteins is a random event or they play a role in CSB tolerance in ErCu.

2D-DIGE analysis also revealed one up-regulated protein in ErCu (Fig. 9B) which is statistically significant based on student's t test.

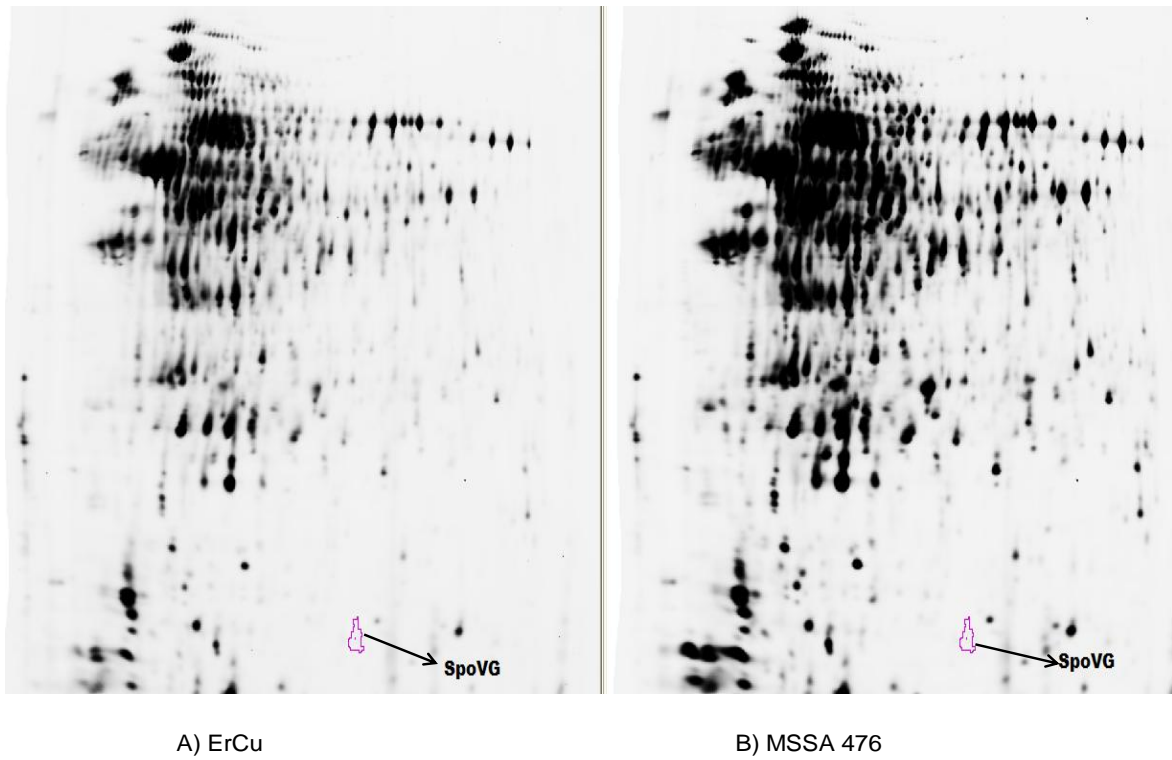


Figure 9B: Protein pattern of A) ErCu and B) *MSSA476* grown in 0.5mM CSB obtained by 2D-DIGE showing SpoVG spot.

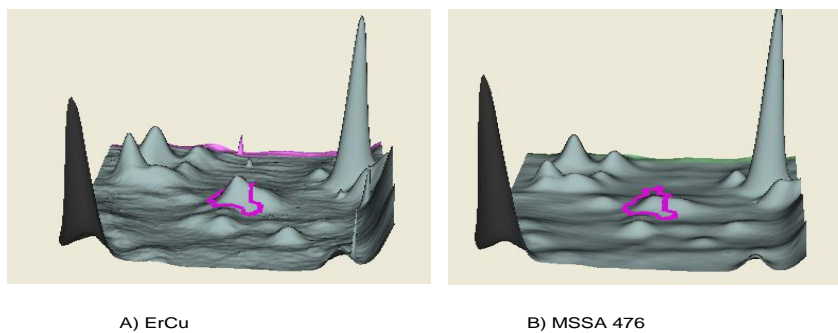


Figure 10: 3D view representation of 2D-DIGE expression of SpoVG in case of A) ErCu as in relation to the B) *MSSA476* strain.

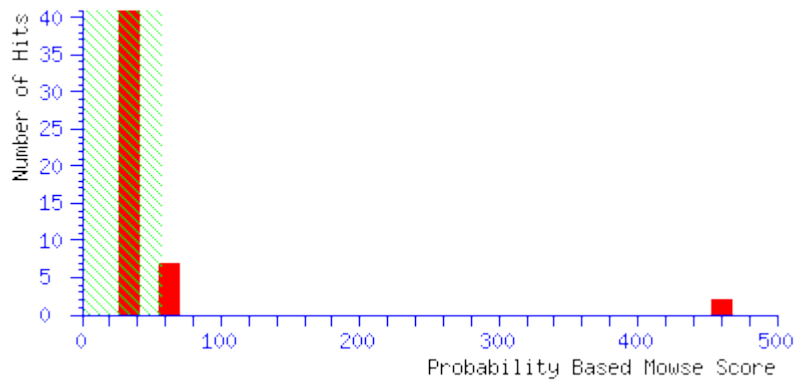


Figure 11: Mass spectrometry data MASCOT search results for SpoVG protein.

Number of hits suggests number peptide hits, which could have a similar peptide sequence. However, the hits obtained could be the result of random events due to false positives and other background sequences. Probability based mowse (Molecular Weight SEarch) score is $-10 \cdot \log(P)$, where P is the probability that the observed match is a random event. Mowse scores > 67 indicate identity or extensive homology ($p < 0.05$). Protein scores are derived from ions scores as a non-probabilistic basis for ranking protein hits. Scores in the green shaded region are not significant (at a level of $p = 5\%$).

In Fig. 11, putative septation protein SpoVG scores the highest Mowse score of 460, which is much higher than the cut off score of 67. The higher the mowse score, the lower is the probability that the identified protein is a random event. Therefore, identified protein can be confirmed as SpoVG with the highest score of 460.

2D-DIGE analysis shows 1.90 times increase in the Putative septation protein SpoVG (protein ID: Q5HIH8 /SP5G_STAAC) in ErCu as compared to *MSSA476*. Student's t test analysis was performed to validate the statistical significance of the data obtained. Student's t test analysis gave the value of 0.011, which can be considered as proof that the experimental data obtained are statistically significant.

Only 2 times increase in SpoVG expression itself is generally not considered enough to make all the differences seen in ErCu and *MSSA476*. However, increase in the expression is consistent in 4 different ErCu cultures, indicating its role in CSB tolerance in ErCu. Further comparative studies were performed to identify other factors involved in the tolerance against CSB. The role of down-regulated proteins in the adaptation mechanism is unclear. Further investigation is required to determine whether the down-regulation of above listed proteins is a random event or they play a role in CSB tolerance in ErCu.

4.3.2 Nano LC- MALDI mass spectrometry analysis

Protein resolution with nano LC-MALDI is based on the principle of differential labelling of N-terminus of the peptides by isobaric tags. Tagged samples are further analysed by tandem mass spectrometry for the relative quantitation (58).

After 2D-DIGE proteome analysis, nano-LC MALDI technique was employed for further proteome analysis based on the advantages of nano-LC MALDI over 2D-DIGE (Chapter 1).

Using nano LC-MALDI mass spectrometry, we could analyse 457 proteins quantitatively (supplement). We were able to compare the expression of these proteins between ErCu and *MSSA476*. Out of 457 proteins, 23 proteins were found to be up regulated more than 1.5 times in ErCu. 56 proteins in ErCu were found to have the expression levels below 70% as compared to the ancestral *MSSA476 strain*. In table 3, some of the proteins and their expressions in relation to the *MSSA476 strain* and their functions are listed which appear to be relevant with respect to heavy metal stress, oxidative stress, virulence and biofilm formation.

Protein /ID	Protein ID (Uniprot)	Gene symbol	Protein expression (in relation to the ancestral strain)	Functions
Copper chaperon Z	Q6GDP0/ COPZ_ST AAR	<i>Copz</i>	Expressed at 38% level	CopZ chaperon plays an important role in the export of copper across the cell membrane. (74).
Superoxide dismutase	Q2YUU9/ SODM2_ STAAB	<i>SODM2</i>	Expressed at 69% level	Superoxide dismutase is a marker of oxidative stress, which helps the cells to cope up with toxic reactive oxygen species (ROS) like superoxide anion (61) (62)
Immunoglobulin G-binding protein A	P02976 S PA_STAA 8	<i>Spa</i>	expressed at 14% level	Surface Protein present in the cell wall of the bacteria <i>S. aureus</i> . It helps to inhibit phagocytosis, <i>S. aureus</i> lacking this protein show

				a diminished virulence.
Accessory gene regulatory protein A	Q5HEG2/ AGRA_ST AAC	<i>agrA</i>	expressed at 57% level	Accessory gene regulatory protein A is an important regulator of virulence factors of <i>S. aureus</i> .
Clumping factor A	Q6GB45 /CLFA_ST AAS	<i>clfA</i>	expressed at 12% level	Activates platelets aggregation, Helps the bacteria to attach to the fibrinogen hence forming bacterial clumps. Convincingly associated with pathogenicity of <i>S.aureus</i>

Table 3: Protein expression revealed in nano LC-MALDI; Proteins with decreased expression, in case of evolutionarily CSB adapted *MSSA476* (ErCu) in relation to the *MSSA476* strain which appear to be relevant with respect to heavy metal stress, oxidative stress, virulence and biofilm formation. Protein functions were referred from the data base uniprot. (www.uniprot.com).

Nano LC-MALDI analysis showed a significant decrease in copper chaperone copZ and superoxide dismutase (SODM2) expression. It can also be noticed that

expression of virulence factors immunoglobulin G-binding protein A (*spa*), accessory gene regulatory protein A (*agrA*) and clumping factor A (*clfA*), are also reduced to a great extent. (See table 3).

Nano LC-MALDI data of *agrA*, *clfA*, *spA*, and *copZ* were further confirmed by gene expression analysis as well. Increased level of SODM2 in *MSSA476* than that of ErCu found in nano LC-MALDI data was already indicated by the superoxide anion measurement experiments (Fig. 5).

Analysis with nano LC-MALDI mass spectrometry revealed a decrease in the protein Copper chaperone CopZ (expressed only at 38% level) in ErCu strains. CopZ chaperon is responsible for the intracellular sequestration of Cu^+ (74)(www.uniprot.org). The corresponding gene *copZ* forms an important component of *copAZ* operon and plays an important role in homeostasis of copper in the cell (74).

In previously performed slide coagulase test, blood agar test and *C.elegan* growth analysis, reduced virulence in ErCu was observed (Fig. 7, 8 and 12). Complimentary to the virulence analysis results, nano LC-MALDI proteomics was also able to identify some of the virulence factors, which were affected by the adaptation. Accessory gene regulatory protein A (*agrA*) is a component of accessory gene regulatory system (*agr*) which is shown to be reduced in ErCu. Agr system plays an important role in the virulence of *S. aureus* (75). Reduced virulence factors like clumping factor A (*clfA*) and reduced *agrA* protein indicates reduced virulence in ErCu cells.

4.3.3 Gene expression analysis

Nano LC-MALDI experiment was performed on protein samples, which were pooled together from 3 different cultures. However, the experiment was run only once as an identification step. Because of the preliminary and therefore only indicative character of the nano LC-MALDI experiments (see chapter 3.3.2), statistical analysis cannot be applied to confirm the data. To confirm the nano LC-MALDI data, gene expression analysis as complementary experiments was carried out on selected proteins from nano LC-MALDI data, which appear to be relevant to our study.

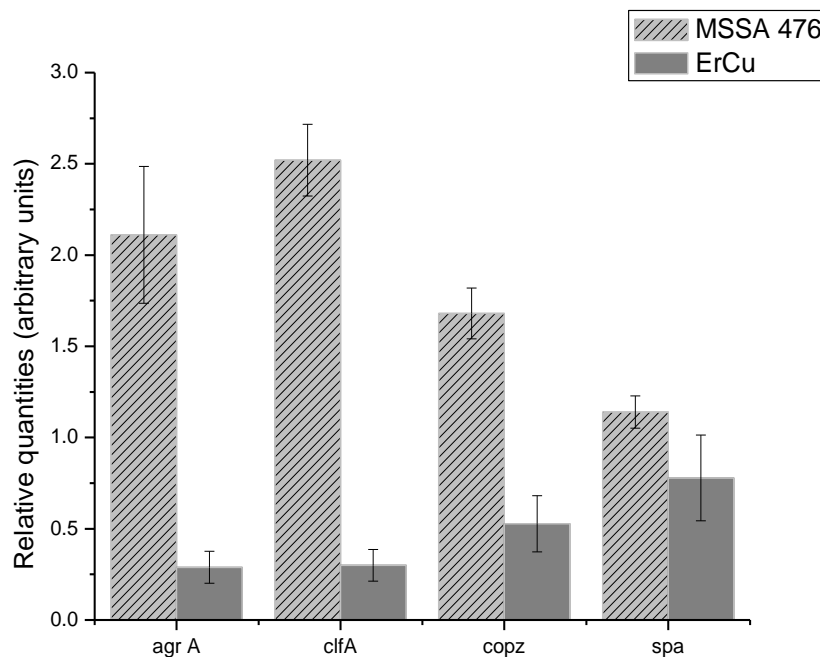


Figure 12: Expressions (arbitrary unit) of the genes *agrA*, *clfA*, *copZ*, *spa* in case of *MSSA476* (oblique line filling) and ErCu (solid bars). Graph was generated with the software 'qbase plus', by Dr.Eva Gomez at the Institute of Legal Medicine, University Hospital Cologne, Germany. Cq value readings from real time RT-PCR can be referred in appendix 7.3

Fig. 12 shows the relative expression of the genes *agrA*, *clfA*, *copZ* and *spa* in relation to each other. Gene expression of copper chaperon Z (*copZ*), clumping factor A (*clfA*), accessory gene regulatory protein A (*agrA*) were reduced respectively in case of ErCu strain as compared to the expression in *MSSA476*. In case of ErCu strain Immunoglobulin G binding protein A (*spa*) gene showed decreased expression, but we observed high quantification cycle values (Cq values) for the *spa* gene. Student's t-test p value for *spa* gene did not fall in the significance range ($p \leq 0.05$). This suggests that the differences in gene expression were not sufficient for the detection. However, it is possibility that the gene expression signals may not fall in the limit of detection of the RT-PCR. The high Cq values which are out of limit signal for the detection of RT-PCR were excluded as the same RNA and amplification conditions were also used for the other target genes analysed. However, expression of *spa* protein is shown to be down regulated in nano LC-MALDI experiments.

With a shadow of doubt on *spa* gene expression, the remaining determined gene expressions are in good accordance with the proteomics results mentioned above (nano LC-MALDI). Therefore, nano LC-MALDI data can be confirmed and used for further analysis. SODM2, which is highlighted in nano LC-MALDI data, is already confirmed in the intracellular superoxide anion measurement experiment (Fig. 5).

4.4 Biofilm assay

This experiment was designed to confirm increase in biofilm formation due to increase in SpoVG protein in ErCu as suggested by 2D-DIGE analysis.

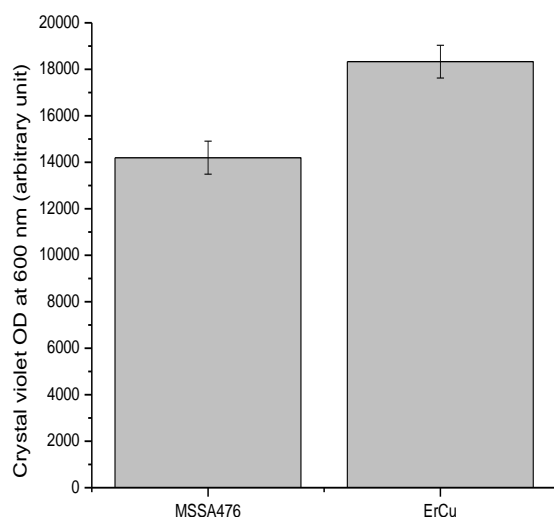


Figure 13: Biofilm assay: Optical density measurement of ErCu and *MSSA476* strains stained with crystal violet (0.1%). OD values for crystal violet intensity with the standard deviations can be referred in appendix 7.4

Fig. 13 shows higher OD measurement of 0.1% crystal violet at 600nm in case of ErCu as compared to *MSSA476* strain. Higher OD values of 0.1% crystal violet staining of ErCu proves that ErCu has the higher ability of forming biofilm as compared to *MSSA476* strain.

The earlier stages of biofilm due to static growth conditions were measured by crystal violet stain. Early stage biofilm formation assay appropriately fitted our study, as bacterial growth conditions used in proteomics study were at the exponential growth phase. .

5. Discussion

5.1 Evolutionary tolerance of ErCu strain against CSB

When a constant pressure is created by heavy metals like copper in the bacterial environment, it leads to selection of new variant bacterial strains, which are resistant to the heavy metals (56, 57). Comparative studies between micro evolved *S. aureus* (ErCu) against copper and the wild type *S.aureus* (*MSSA476*) at the molecular level will provide insights in to the mechanism by which *S. aureus* evolves and adapts to the pressure created by the copper complexes. Therefore, experiments were designed of microevolution of *MSSA476* in order to obtain resistance against copper-Schiff's base (CSB).

As depicted in Fig. 3 and 4 ErCu is clearly more tolerant to CSB than *MSSA476* strain. Minimal Inhibitory concentration (MIC) experiments conducted by N. Poulter *et al.* on CSB against *MSSA476* strain exhibited MIC₁₀₀ at 0.5 mM (1). In this study, MIC₁₀₀ for CSB against *MSSA476* was found to be close to 0.8 mM. Along with the experimental conditions and the laboratory conditions, the difference in MIC₁₀₀ could be due to the different concentration of DMSO used in the preparation of CSB solution. Eventhough, our preliminary experiments (results not shown) did not show any significant anti-microbial activity for 1% DMSO. Anti-microbial activity of higher concentration of DMSO needs to be investigated. Therefore, 2% DMSO used by N. Poulter *et al.* could be one of the reasons for lower MIC₁₀₀ as compared to the MIC₁₀₀ achieved by using 1% DMSO in this study.

To confirm whether microevolved *S.aureus* is essentially still *S.aureus* and to rule out the possibility of selection of false bacteria during microevolution, PCR and mannitol agar tests were performed.

PCR tests were run to confirm presence of *nuc* gene in ErCu. *Nuc* gene is a 270 bp DNA fragment which codes for thermo stable nuclease in *S.aureus* which is highly conserved (60). Hence , it is a good candidate which can be used to detect *S.aureus* (60). Mannitol is a fermentable carbohydrate. And *S.aureus* is the only bacterium which is known to ferment mannitol. Phenol red a pH indicator present in mannitol agar media indicates the change in the pH of the media. Due to fermentation of mannitol salt *S.aureus* colonies appear yellow in colour with yellow zones surrounding the colonies (76).

Presence of *nuc* gene band in PCR experiments (Fig 4.1) and the mannitol agar tests clearly confirm that microevolved ErCu is still essentially an *S.aureus* strain. Picking a single yellow ErCu colony from mannitol agar media for further culturing and storage assures non-contaminated cultures for further experiments.

Microevolution experiment results indicate that due to the constant pressure created by copper in the bacterial environment, adapted *MSSA476* attained better fitness to copper stress environment which shows more tolerance to higher concentrations of copper.

Stress by heavy metals is often directly related to oxidative stress in *S. aureus*. (77-80). If ErCu strain has indeed developed an adaptation to CSB, then it should also be able to cope better with oxidative stress. Superoxide dismutase (SODM2), which is a marker of oxidative stress, catalyses detoxification of superoxide anion to H_2O_2 which is further broken down to H_2O by the enzyme catalase (61, 62). Nano LC-MALDI results, show decreased level of SODM2 in ErCu cells. This suggests that ErCu strain experiences reduced oxidative stress as compared to *MSSA476* strain when exposed to super-physiological concentrations of copper or CSB. To confirm

this result, concentration of superoxide anion present within the cell was also measured. The results are in agreement with the proteomics results. (Fig. 5). A lower amount of copper ions present in ErCu cells as in non-adapted MSSA 476 cells was confirmed by ICP-MS experiments (Fig. 6). This suggests that less copper ion are entering the cells and therefore the ROS cascade usually triggered by super-physiological copper concentrations is not activated as observed in case of the nonadapted MSSA 476.

5.2 Factors involved in the tolerance of CSB in ErCu strain

When there is an increase in the cellular copper level above physiological levels, bacteria activates the mechanism of copper homeostasis in the cell perhaps by activating copAZ operon (74). Analysis with nano LC-MALDI mass spectrometry revealed a decrease in the protein Copper chaperone CopZ (expressed only at 30% level) in ErCu strains as compared to *MSSA476* strain. This result was further confirmed by using real time reverse transcription (RT) -PCR (12). CopZ chaperon is responsible for the intracellular sequestration of Cu^+ and the corresponding gene *copZ* forms an important component of copAZ operon. When there is an increase in cellular copper above physiological levels, copZ is activated leading to a cascade that activates copB, which removes copper from the cell, hence maintaining the copper homeostasis in the cell (74).

According to our ICP-MS experiments (Fig. 6), it is evident that the copper levels were found to be lower in ErCu cells than in the *MSSA476* cells. Reduced copper concentration in ErCu cells suggests that either the export of copper is more efficient or entrance of the copper is inhibited in the ErCu cells. As shown in the results, reduced expression of copZ in the ErCu cells strongly suggests that the adapted

bacterial strain has developed mechanisms, which does not improve export but block the entry of excess copper ions in to the bacterial cells. Together with the results on oxidative stress, this becomes even more evident.

5.3 Increased Biofilm formation in ErCu

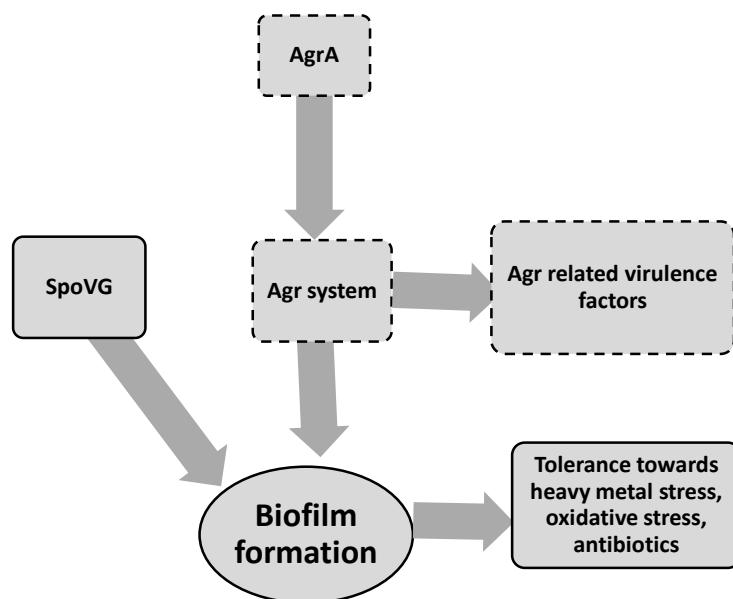


Figure 14: Schematic representation of molecular adaptation by ErCu, which will lead to enhanced biofilm formation. Dotted lines represent repression and solid lines represent elevated expression.

It has been demonstrated that the repression of regulatory protein SpoVG also represses biofilm formation in *S.aureus* (39).

In 2D-DIGE comparative proteome analysis, approximately 2 times increase in SpoVG protein is observed in ErCu strain (Fig. 9B and 10), which indicates increase in the biofilm formation in ErCu. The microtiter dish biofilm assay is performed to

analyse biofilm formation in ErCu and *MSSA476*. Biofilm assay is performed using static growth conditions, therefore the mature biofilm formation can be avoided and the early stages in bacterial biofilm formation can be studied (71). The biofilm assay confirms increased biofilm formation in ErCu (Fig. 13).

Moreover, while characterizing the ErCu strain, hemolytic tests indicated reduced release of toxins. Moreover, nano LC-MALDI and gene expression results also showed down regulation of *clfA* and *spa* in ErCu (Table 3, Fig.12). The clumping factor formation by *S. aureus* is convincingly related to the virulence of *S. aureus* (81). Therefore, hemolytic test results and reduced *clfA* protein indicates global reduction of virulence in ErCu. To confirm reduced virulence, a growth test was conducted on *C.elegans*. *C. elegans* were chosen because there is a remarkably high degree of correlation between pathogen virulence factor required for nematode killing and virulence in vertebrate models (82). Quicker growth of *C. elegans* from L1 to L4 stage in case of ErCu infected *C. elegans* as compared to the *C. elegans* infected by *MSSA476* strain confirms the reduced virulence of ErCu strain. Therefore, increased copper tolerance, enhanced biofilm formation and reduced virulence appear to coincide in ErCu. A possible unifying concept for these observations may be the following hypothesis:

It has been established that increased biofilm formation leads to enhanced oxidative stress tolerance in bacteria (30-32). Contrary to opportunistic pathogens like *Pseudomonas aeruginosa*, the repression of quorum sensing system is necessary to form a biofilm in case of *S. aureus*, and when there is a reactivation of quorum sensing in the biofilms, dispersion of the cells can be witnessed(33) (83-85). It is established that in *S.aureus*, the quorum-sensing system is regulated by agr system and a communication molecule called auto inducing peptide (AIP)(86). Blaise R.

Boles, and Alexander R. Horswill have demonstrated that repression of *agr* is necessary to form a biofilm (33-38) which co-relates to our nano LC- MALDI and real time reverse transcription (RT)-PCR results (Fig. 12). With nano LC-MALDI and RT-PCR experiments we were able to show that accessory gene regulatory protein A (*agrA*), a component of accessory gene regulatory system (*agr*) (87) is reduced in ErCu (Table 3 and Fig. 12). *AgrA* modulates *agr* system by activating RNAIII, an effector molecule of *agr* (87-90). Therefore, reduced *agrA* indicates repression of *agr* system. And repression of *agr* also means reduced virulence as explained above (75) (Fig. 7,8 and 12). Even though previous studies showed that clumping factor A (*clfA*) expression, a surface virulence protein (81), is independent of *agr* activity (91, 92), nano LC-MALDI and gene expression results of this study demonstrated down regulation of *clfA* in ErCu (Table 3 and Fig. 12). when the stress is applied on *S.aureus*, stress resistant *S. aureus* survives because of its fitness advantage at the cost of global reduction of virulence factors (23, 26-28). Therefore, reduced expression of virulence factors like *clfA* and *spa* can be attributed to the global reduction of virulence factors, which also include the virulence factors that are not regulated by *agr* system in stress adapted ErCu strain. However, in depth investigation of *clfA* protein in ErCu is required.

The major observation is that increase in SpoVG and decrease in *agr* system both explain biofilm formation, which in turn 'leads to increased copper tolerance.

Resistance against antibiotics like ciprofloxacin, mupirocin, and rifampin is seen in *agr* deficient *S.aureus* (17, 23). *Agr* deficient *S.aureus* have also exhibited intermediary level resistance against glycopeptides like vancomycin (17). And because of the deficient *Agr* system reduced extracellular virulence factors have been noticed in antibiotic resistant *S.aureus* strains (23, 93-95). The factors

observed in antibiotic resistance in *S.aureus* are similar to the observations made in the resistance mechanism of *S.aureus* against CSB in this study. In addition, increase in the cell wall thickness in vancomycin resistant *S.aureus* (10-12) indicates increase in SpoVG. An increase of SpoVG was also observed in ErCu strain. The uncanny similarities in the mechanisms of antibiotic resistance and CSB resistance in *S.aureus* suggests cross resistance for antibiotic and CSB stress on *S.aureus*. Further investigations are required to examine whether ErCu strain also exhibits resistance against a range of antibiotics like ciprofloxacin, mupirocin, rifampin and vancomycin. However, preliminary experiments were conducted to determine whether ErCu has developed a capsule or a thicker cell wall as compared to *MSSA476* using India ink staining technique. Eventhough results were only preliminary and not confirmatory, no considerable difference was observed between *MSSA476* and ErCu (results not shown).

Therefore, along with the biofilm mediated resistance theory, cell wall thickening for resistance needs to be further investigated in ErCu.

5.4. Interrelation of agr system and SpoVG in *S.aureus*

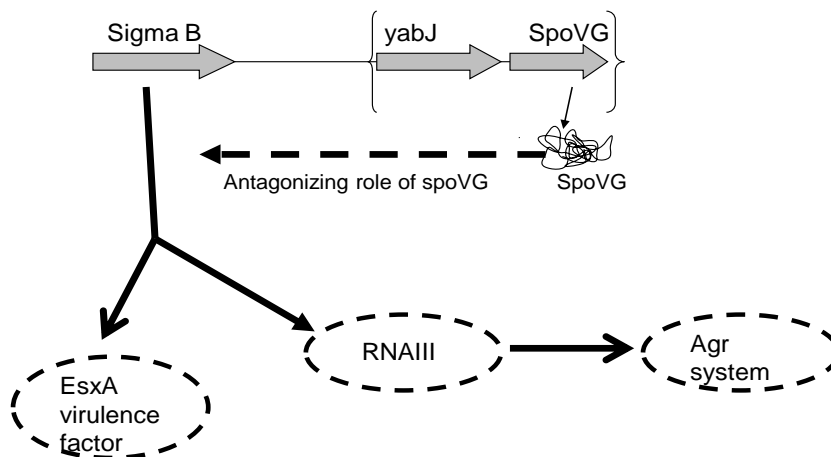


Figure 15: Schematic representation of interrelation of SpoVG and agr system as suggested by Schulthess, *et al.* (2011, 2012)

As discussed above, both increased SpoVG and repression of agr are effectors of biofilm formation. One explanation is that SpoVG has a negative effect on agr system, which facilitates biofilm formation. SpoVG as a part of *yabJ-spoVG* regulatory system it is positively modulated by sigmaB and in fact *yabJ-spoVG* locus may serve as effector that modulates sigmaB effects over sigmaB-dependent genes (16). SigmaB on the other hand is known to have a repressing effect on agr system (38, 79, 96, 97). Hence, it could be assumed that sigmaB is the common factor, which is responsible for up-regulation of SpoVG and down regulation of agr system seen in ErCu. However, expression of alkaline shock protein (*asp23*) marker of sigmaB in *S.aureus* (98-100) seems to be reduced in ErCu according to nano LC-

MALDI data (see appendix 7.8). Nano LC-MALDI analysis can be used as an identification step; hence, this puzzling result needs to be confirmed with another method like gene expression analysis. Asp23 expression revealed by nano LC-MALDI is not confirmed by gene expression data. Therefore, asp23 expression data from nano LC-MALDI is not considered conclusively. Hence, in the absence of second independent result, it cannot be concluded whether SigmaB activity is actually increased in ErCu. Nonetheless up regulation of SpoVG and down regulation of agr system are confirmed beyond doubt with the help of 2D-DIGE, nano LC-MALDI and gene expression analysis. If there is infact reduced sigmaB activity in ErCu, further investigations are required to understand the mechanism of how SpoVG is able to bypass the effect of sigmaB in ErCu. Schulthess *et al* (2012) demonstrated that depending upon the growth conditions and other environmental factors SpoVG takes an opposing role to sigmaB in regulation of virulence factor esxA protein in *S.aureus*. This demonstrates the ability of SpoVG to antagonize the effect of sigmaB on virulence factor like esxA and agr system (101, 102). It can be proposed that even if sigmaB activity is indeed reduced in ErCu, SpoVG is able to modulate the effect of sigmaB on its own expression and on agr expression. Hence, it can be concluded that irrespective of sigmaB expression, increase in SpoVG mediates repression of agr system.

5.5 Biofilm formation and its role in heavy metal stress tolerance in ErCu

It can be proposed that, at the time when bacterial cultures are harvested (in the exponential growth phase) for the experiments, ErCu cells are more advanced in biofilm formation than control cells due to increased expression of SpoVG and repression of the agr system. Because of the reduced agr system, we also observe reduced virulence in ErCu strain. To conclude the mechanism of CSB adaptation in

S.aureus, it can be suggested that ErCu has developed a mechanism, which enables the bacteria to form biofilm at an earlier stage with the help of increased SpoVG and decreased agr activity. Improved formation of biofilm coincides with adaptation of *S.aureus* against high concentrations of Cu ions. Staphylococcal biofilms are composed of N-acetyl-glucosamine-based exopolysaccharides, also known as polysaccharide intercellular adhesin (PIA), cytoplasmic proteins and polyanionic extracellular DNA (103, 104). It is well known that biofilms cause dramatically increased resistance to antibiotics. Evidence also suggests that biofilms protect from toxic metals by the combined action of physical and chemical interactions. The extracellular matrix not only impedes the diffusion of small molecules but, in addition, immobilizes toxic metals, for example by ionic interaction of opposite charges (DNA), precipitation and biosorption (105) (106).

As a whole range of factors is involved in the complex process of biofilm formation, it is difficult to pinpoint specific mutations, which cause the phenotype of the CSB tolerant phenotype of strain ErCu. The consequences of enhanced biofilm formation on stress tolerance are, nonetheless, dramatic and likely to affect a multitude of antimicrobials, including heavy metals and antibiotics. We have shown here that exposure to inhibitory concentrations of CSB will lead within only few generations to more tolerant spontaneous mutations due to enhanced biofilm formation properties. This emphasizes once again the importance of dealing with biofilms as a prime target for *S.aureus* therapies. The results also demonstrate that great care should be paid to the nowadays very common use of metal impregnated materials, especially in hospitals. The more likely cross-resistance to antibiotics could exacerbate the situation of antibiotic resistance.

5.6 Usage of CSB as an anti-microbial polymer in healthcare domain

As described above (Chapter: 1), this study is a part of EMBEK1 project. Aim of EMBEK1 project is to produce novel anti-microbial substances, which can be polymerised for variety of materials used in healthcare domain. Santo *et al.* (2012), demonstrated that copper based surfaces are effective in killing pathogenic bacteria like *Staphylococcus haemolyticus* (107). Therefore, copper based CSB monomer seems to be a good fit to be polymerised as an anti-microbial surface. Results of preliminary tests performed on CSB polymers by P.Cierniak *et al* and N. Poulter *et al.* showed that, CSB polymers were able to kill *S.aureus* effectively. As demonstrated in this study, anti-microbial effect of CSB monomer on *S.aureus* is seen at 0.6mM or higher concentration of CSB, which is considerably a high concentration as compared to the concentration required by other metallic complex based monomers like zinc (1, 66). It was also demonstrated that, only 135 generations were required for an opportunistic bacteria like *S.aureus* to develop tolerance against CSB. Vuong *et al.* (2000), demonstrated that agr repressed *S.aureus* tend to adhere better to a polymer surface like polyesterene surface than the agr positive bacteria (37). Even though adhesion factor like *clfA* is reduced in ErCu, Vuong *et al.* hypothesize that down regulation of δ -toxin surfactant helps in better adhesion of bacteria which exhibit reduced expression of agr system like in case of ErCu (37, 108). δ -toxin is known to be a part of inflammatory polypeptide complex regulated by agr system, which acts as a surfactant and prevents adherence of bacterial cells to the surfaces (109). Therefore, decrease in agr expression also decreases the δ -toxin expression which facilitates the adherence of bacterial cell to the surfaces (37, 110). However, for the better understanding, similar kind of study on CSB polymer is necessary.

6. References

1. Poulter N, Donaldson M, Mulley G, Duque L, Waterfield N, Shard AG, et al. Plasma deposited metal Schiff-base compounds as antimicrobials. *New Journal of Chemistry*. 2011;35(7):1477-84.
2. Bayer AS, Lam K, Ginzton L, Norman DC, Chiu CY, Ward JI. Staphylococcus aureus bacteremia. Clinical, serologic, and echocardiographic findings in patients with and without endocarditis. *Arch Intern Med*. 1987 Mar;147(3):457-62. PubMed PMID: 3103561.
3. Kim JH, van der Horst C, Mulrow CD, Corey GR. Staphylococcus aureus meningitis: review of 28 cases. *Rev Infect Dis*. 1989 Sep-Oct;11(5):698-706. PubMed PMID: 2682944.
4. Gonzalez C, Rubio M, Romero-Vivas J, Gonzalez M, Picazo JJ. Bacteremic pneumonia due to Staphylococcus aureus: A comparison of disease caused by methicillin-resistant and methicillin-susceptible organisms. *Clin Infect Dis*. 1999 Nov;29(5):1171-7. PubMed PMID: 10524959.
5. Boyce JM. MRSA patients: proven methods to treat colonization and infection. *J Hosp Infect*. 2001 Aug;48 Suppl A(14):S9-14. PubMed PMID: 11759035.
6. Davis JP, Chesney PJ, Wand PJ, LaVenture M. Toxic-shock syndrome: epidemiologic features, recurrence, risk factors, and prevention. *N Engl J Med*. 1980 Dec 18;303(25):1429-35. PubMed PMID: 7432401.
7. Suller MTE, Russell AD. Triclosan and antibiotic resistance in Staphylococcus aureus. *Journal of Antimicrobial Chemotherapy*. 2000 July 1, 2000;46(1):11-8.
8. Irish D, Eltringham I, Teall A, Pickett H, Farelly H, Reith S, et al. Control of an outbreak of an epidemic methicillin-resistant Staphylococcus aureus also resistant to mupirocin. *Journal of Hospital Infection*. 1998;39(1):19-26.

9. Cookson BD, Farrelly H, Stapleton P, Garvey RP, Price MR. Transferable resistance to triclosan in MRSA. *Lancet*. 1991 Jun 22;337(8756):1548-9. PubMed PMID: 1675398.
10. Liu C, Chambers HF. Staphylococcus aureus with Heterogeneous Resistance to Vancomycin: Epidemiology, Clinical Significance, and Critical Assessment of Diagnostic Methods. *Antimicrobial Agents and Chemotherapy*. 2003;47(10):3040-5. PubMed PMID: PMC201119.
11. Howden BP, Davies JK, Johnson PDR, Stinear TP, Grayson ML. Reduced Vancomycin Susceptibility in Staphylococcus aureus, Including Vancomycin-Intermediate and Heterogeneous Vancomycin-Intermediate Strains: Resistance Mechanisms, Laboratory Detection, and Clinical Implications. *Clinical Microbiology Reviews*. 2010;23(1):99-139. PubMed PMID: PMC2806658.
12. Renzoni A, Andrey DO, Jousselin A, Barras C, Monod A, Vaudaux P, et al. Whole Genome Sequencing and Complete Genetic Analysis Reveals Novel Pathways to Glycopeptide Resistance in Staphylococcus aureus. *PLoS ONE*. 2011 06/27;6(6):e21577. PubMed PMID: PMC3124529.
13. Meier S, Goerke C, Wolz C, Seidl K, Homerova D, Schulthess B, et al. sigmaB and the sigmaB-dependent arlRS and yabJ-spoVG loci affect capsule formation in Staphylococcus aureus. *Infection and immunity*. 2007 Sep;75(9):4562-71. PubMed PMID: 17635871. Pubmed Central PMCID: PMC1951174. Epub 2007/07/20.
14. Schulthess B, Meier S, Homerova D, Goerke C, Wolz C, Kormanec J, et al. Functional characterization of the sigmaB-dependent yabJ-spoVG operon in Staphylococcus aureus: role in methicillin and glycopeptide resistance. *Antimicrob*

Agents Chemother. 2009 May;53(5):1832-9. PubMed PMID: 19223635. Pubmed Central PMCID: PMC2681525. Epub 2009/02/19.

15. Schulthess B, Bloes DA, Francois P, Girard M, Schrenzel J, Bischoff M, et al. The sigmaB-dependent yabJ-spoVG operon is involved in the regulation of extracellular nuclease, lipase, and protease expression in Staphylococcus aureus. Journal of bacteriology. 2011 Sep;193(18):4954-62. PubMed PMID: 21725011. Pubmed Central PMCID: PMC3165683. Epub 2011/07/05.

16. Meier S, Goerke C, Wolz C, Seidl K, Homerova D, Schulthess B, et al. $\sigma(B)$ and the $\sigma(B)$ -Dependent arlRS and yabJ-spoVG Loci Affect Capsule Formation in Staphylococcus aureus. Infection and immunity. ;75(9):4562-71. PubMed PMID: PMC1951174.

17. Sakoulas G, Eliopoulos GM, Moellering RC, Jr., Wennersten C, Venkataraman L, Novick RP, et al. Accessory gene regulator (agr) locus in geographically diverse Staphylococcus aureus isolates with reduced susceptibility to vancomycin. Antimicrob Agents Chemother. 2002 May;46(5):1492-502. PubMed PMID: 11959587. Pubmed Central PMCID: PMC127153. Epub 2002/04/18.

18. Recsei P, Kreiswirth B, O'Reilly M, Schlievert P, Gruss A, Novick RP. Regulation of exoprotein gene expression in Staphylococcus aureus by agar. Molecular & general genetics : MGG. 1986 Jan;202(1):58-61. PubMed PMID: 3007938. Epub 1986/01/01.

19. Ji G, Beavis RC, Novick RP. Cell density control of staphylococcal virulence mediated by an octapeptide pheromone. Proceedings of the National Academy of Sciences of the United States of America. 1995 Dec 19;92(26):12055-9. PubMed PMID: 8618843. Pubmed Central PMCID: PMC40295. Epub 1995/12/19.

20. Antunes LC, Ferreira RB, Buckner MM, Finlay BB. Quorum sensing in bacterial virulence. *Microbiology*. 2010 Aug;156(Pt 8):2271-82. PubMed PMID: 20488878. Epub 2010/05/22.
21. Novick RP, Geisinger E. Quorum sensing in staphylococci. *Annu Rev Genet*. 2008;42:541-64. PubMed PMID: 18713030. Epub 2008/08/21.
22. Novick RP. Autoinduction and signal transduction in the regulation of staphylococcal virulence. *Mol Microbiol*. 2003 Jun;48(6):1429-49. PubMed PMID: 12791129. Epub 2003/06/07.
23. Paulander W, Nissen Varming A, Bæk KT, Haaber J, Frees D, Ingmer H. Antibiotic-Mediated Selection of Quorum-Sensing-Negative *Staphylococcus aureus*. *mBio*. 2012 Nov-Dec;3(6):e00459-12. PubMed PMID: PMC3509436.
24. Queck SY, Jameson-Lee M, Villaruz AE, Bach TH, Khan BA, Sturdevant DE, et al. RNAIII-independent target gene control by the agr quorum-sensing system: insight into the evolution of virulence regulation in *Staphylococcus aureus*. *Molecular cell*. 2008 Oct 10;32(1):150-8. PubMed PMID: 18851841. Pubmed Central PMCID: PMC2575650. Epub 2008/10/15.
25. Chevalier C, Boisset S, Romilly C, Masquida B, Fechter P, Geissmann T, et al. *Staphylococcus aureus* RNAIII binds to two distant regions of *coa* mRNA to arrest translation and promote mRNA degradation. *PLoS Pathog*. 2010 Mar 12;6(3):e1000809. PubMed PMID: 20300607. Pubmed Central PMCID: PMC2837412. Epub 2010/03/20.
26. Paulander W, Maisnier-Patin S, Andersson DI. The fitness cost of streptomycin resistance depends on *rpsL* mutation, carbon source and RpoS (σ^S). *Genetics*. 2009 Oct;183(2):539-46, 1SI-2SI. PubMed PMID: 19652179. Pubmed Central PMCID: PMC2766315. Epub 2009/08/05.

27. Rudkin JK, Edwards AM, Bowden MG, Brown EL, Pozzi C, Waters EM, et al. Methicillin resistance reduces the virulence of healthcare-associated methicillin-resistant *Staphylococcus aureus* by interfering with the agr quorum sensing system. *The Journal of infectious diseases*. 2012 Mar 1;205(5):798-806. PubMed PMID: 22301683. Pubmed Central PMCID: PMC3318674. Epub 2012/02/04.
28. Sturm A, Heinemann M, Arnoldini M, Benecke A, Ackermann M, Benz M, et al. The cost of virulence: retarded growth of *Salmonella Typhimurium* cells expressing type III secretion system 1. *PLoS Pathog*. 2011 Jul;7(7):e1002143. PubMed PMID: 21829349. Pubmed Central PMCID: PMC3145796. Epub 2011/08/11.
29. Bronner S, Monteil H, Prévost G. Regulation of virulence determinants in *Staphylococcus aureus*: complexity and applications. *FEMS Microbiology Reviews*. 2004;28(2):183-200.
30. Boles BR, Thoendel M, Singh PK. Rhamnolipids mediate detachment of *Pseudomonas aeruginosa* from biofilms. *Mol Microbiol*. 2005 Sep;57(5):1210-23. PubMed PMID: 16101996. Epub 2005/08/17.
31. Fux CA, Wilson S, Stoodley P. Detachment Characteristics and Oxacillin Resistance of *Staphylococcus aureus* Biofilm Emboli in an In Vitro Catheter Infection Model. *Journal of Bacteriology*. 2004 July 15, 2004;186(14):4486-91.
32. Hall-Stoodley L, Stoodley P. Biofilm formation and dispersal and the transmission of human pathogens. *Trends in Microbiology*. 2005;13(1):7-10.
33. Boles BR, Horswill AR. agr-Mediated Dispersal of *Staphylococcus aureus* Biofilms. *PLoS Pathog*. 2008;4(4):e1000052.

34. Beenken KE, Blevins JS, Smeltzer MS. Mutation of sarA in *Staphylococcus aureus* limits biofilm formation. *Infection and immunity*. 2003 Jul;71(7):4206-11. PubMed PMID: 12819120. Pubmed Central PMCID: PMC161964. Epub 2003/06/24.
35. Beenken KE, Dunman PM, McAleese F, Macapagal D, Murphy E, Projan SJ, et al. Global Gene Expression in *Staphylococcus aureus* Biofilms. *Journal of bacteriology*. ;186(14):4665-84. PubMed PMID: PMC438561.
36. Vuong C, Gerke C, Somerville GA, Fischer ER, Otto M. Quorum-sensing control of biofilm factors in *Staphylococcus epidermidis*. *The Journal of infectious diseases*. 2003 Sep 1;188(5):706-18. PubMed PMID: 12934187. Epub 2003/08/23.
37. Vuong C, Saenz HL, Gotz F, Otto M. Impact of the agr quorum-sensing system on adherence to polystyrene in *Staphylococcus aureus*. *The Journal of infectious diseases*. 2000 Dec;182(6):1688-93. PubMed PMID: 11069241. Epub 2000/11/09.
38. Lauderdale KJ, Boles BR, Cheung AL, Horswill AR. Interconnections between Sigma B, agr, and Proteolytic Activity in *Staphylococcus aureus* Biofilm Maturation. *Infection and immunity*. 2009 02/0277(4):1623-35. PubMed PMID: PMC2663138.
39. Qin N, Tan X, Jiao Y, Liu L, Zhao W, Yang S, et al. RNA-Seq-based transcriptome analysis of methicillin-resistant *Staphylococcus aureus* biofilm inhibition by ursolic acid and resveratrol. *Scientific reports*. 2014;4:5467. PubMed PMID: 24970710. Pubmed Central PMCID: PMC4073122. Epub 2014/06/28.
40. Jarvis WR, Schlosser J, Chinn RY, Tweeten S, Jackson M. National prevalence of methicillin-resistant *Staphylococcus aureus* in inpatients at US health care facilities, 2006. *Am J Infect Control*. 2007 Dec;35(10):631-7. PubMed PMID: 18063126.

41. Charlebois ED, Bangsberg DR, Moss NJ, Moore MR, Moss AR, Chambers HF, et al. Population-based community prevalence of methicillin-resistant *Staphylococcus aureus* in the urban poor of San Francisco. *Clin Infect Dis*. 2002 Feb 15;34(4):425-33. PubMed PMID: 11797167.
42. Al-Rawahi GN, Schreader AG, Porter SD, Roscoe DL, Gustafson R, Bryce EA. Methicillin-resistant *Staphylococcus aureus* nasal carriage among injection drug users: six years later. *J Clin Microbiol*. 2008 Feb;46(2):477-9. PubMed PMID: 18039800.
43. Kamalakannan P, Venkappayya D. Synthesis and characterization of cobalt and nickel chelates of 5-dimethylaminomethyl-2-thiouracil and their evaluation as antimicrobial and anticancer agents. *Journal of Inorganic Biochemistry*. 2002 May 21;90(1-2):22-37.
44. Rodriguez-Arguelles MC, Mosquera-Vazquez S, Touron-Touceda P, Sanmartin-Matalobos J, Garcia-Deibe AM, Belicchi-Ferrari M, et al. Complexes of 2-thiophenecarbonyl and isonicotinoyl hydrazones of 3-(N-methyl)isatin. A study of their antimicrobial activity. *Journal of Inorganic Biochemistry*. 2007 Jan;101(1):138-47.
45. Sorenson JRJ. Copper chelates as possible active forms of antiarthritic agents. *Journal of Medicinal Chemistry*. 1976 1976;19(1):135-48.
46. Brown DH, Smith WE, Teape JW, Lewis AJ. Antiinflammatory effects of some copper complexes. *Journal of Medicinal Chemistry*. 1980 2012/03/09;23(7):729-34.
47. Sorenson JRJ. Copper-complexes in biochemistry and pharmacology. *Chemistry in Britain*. 1984 1984;20(12):1110-3.

48. Raman N, Joseph J, Sakthivel A, Jeyamurugan R. Synthesis, structural characterization and antimicrobial studies of novel schiff base copper(ii) complexes. *Journal of the Chilean Chemical Society*. 2009;54:354-7.
49. Lv J, Liu T, Cai S, Wang X, Liu L, Wang Y. Synthesis, structure and biological activity of cobalt(II) and copper(II) complexes of valine-derived schiff bases. *Journal of Inorganic Biochemistry*. 2006;100(11):1888-96.
50. Groves DJ, Short H, Thewaini AJ, Young FE. Epidemiology of Antibiotic and Heavy Metal Resistance in Bacteria: Resistance Patterns in Staphylococci Isolated from Populations in Iraq Exposed and Not Exposed to Heavy Metals or Antibiotics. *Antimicrobial Agents and Chemotherapy*. 1975 May 1, 1975;7(5):622-8.
51. Silver S, Phung LT. Bacterial heavy metal resistance: new surprises. *Annu Rev Microbiol*. 1996;50:753-89. PubMed PMID: 8905098.
52. Xiong A, Jayaswal RK. Molecular characterization of a chromosomal determinant conferring resistance to zinc and cobalt ions in *Staphylococcus aureus*. *J Bacteriol*. 1998 Aug;180(16):4024-9. PubMed PMID: 9696746.
53. Mason HS. Binuclear copper clusters as active sites for oxidases. *Advances in experimental medicine and biology*. 1976 1976;74:464-9. PubMed PMID: MEDLINE:183478.
54. Nicholas KM, Wentworth P, Harwig CW, Wentworth AD, Shafton A, Janda KD, editors. A cofactor approach to copper-dependent catalytic antibodies. *Proceedings of the National Academy of Sciences of the United States of America*; 2002 Mar 5.
55. Gaetke LM, Chow CK. Copper toxicity, oxidative stress, and antioxidant nutrients. *Toxicology*. 2003 Jul 15;189(1-2):147-63. PubMed PMID: 12821289. eng.

56. Baquero F, Negri MC, Morosini MI, Blazquez J. Antibiotic-selective environments. *Clin Infect Dis*. 1998 Aug;27 Suppl 1:S5-11. PubMed PMID: 9710666. Epub 1998/08/26.
57. Genetic Relationship Between Heavy Metals Resistance and β - Lactamase Production In E. Coli and Staphylococcus Aureus. *Ibn Al-Haitham Journal For Pure And Applied Science*. 2012;25(1):49-54.
58. Wiese S, Reidegeld KA, Meyer HE, Warscheid B. Protein labeling by iTRAQ: a new tool for quantitative mass spectrometry in proteome research. *Proteomics*. 2007 Feb;7(3):340-50. PubMed PMID: 17177251. Epub 2006/12/21. .
59. Poulter N, Donaldson M, Mulley G, Duque L, Waterfield N, Shard AG, et al. Plasma deposited metal Schiff-base compounds as antimicrobials. *New Journal of Chemistry*.35(7).
60. Brakstad OG, Aasbakk K, Maeland JA. Detection of Staphylococcus aureus by polymerase chain reaction amplification of the nuc gene. *Journal of Clinical Microbiology*. 1992;30(7):1654-60. PubMed PMID: PMC265359.
61. Clements MO, Watson SP, Foster SJ. Characterization of the Major Superoxide Dismutase of Staphylococcus aureus and Its Role in Starvation Survival, Stress Resistance, and Pathogenicity. *Journal of Bacteriology*. 1999 July 1, 1999;181(13):3898-903.
62. Fridovich I. Superoxide Radical and Superoxide Dismutases. *Annual Review of Biochemistry*. 1995;64(1):97-112.
63. Carter WO, Narayanan PK, Robinson JP. Intracellular hydrogen peroxide and superoxide anion detection in endothelial cells. *Journal of Leukocyte Biology*. 1994 February 1, 1994;55(2):253-8.

64. Rothe G, Valet G. Flow cytometric analysis of respiratory burst activity in phagocytes with hydroethidine and 2',7'-dichlorofluorescein. *Journal of Leukocyte Biology*. 1990 May 1, 1990;47(5):440-8.
65. Lotz A, Heller M, Dohm N, Cierniak P, Bender K, Jansen B, et al. Antimicrobial efficacy and optimized cell adhesion from defined plasma polymerised multilayer structures involving zinc acetylacetonate and allylamine. *Journal of Materials Chemistry*. 2012;22(37):19455 - 61.
66. Cierniak P, Jübner M, Müller S, Bender K. Insights into Mechanisms and Proteomic Characterisation of *Pseudomonas aeruginosa* Adaptation to a Novel Antimicrobial Substance. *PLoS ONE*. 2013;8(7):e66862.
67. Wisniewski JR, Zougman A, Nagaraj N, Mann M. Universal sample preparation method for proteome analysis. *Nature methods*. 2009 May;6(5):359-62. PubMed PMID: 19377485. Epub 2009/04/21.
68. Effertz C, Muller S, Elert E. Differential peptide labeling (iTRAQ) in LC-MS/MS based proteomics in *Daphnia* reveal mechanisms of an antipredator response. *Journal of proteome research*. 2015 Feb 6;14(2):888-96. PubMed PMID: 25494525. Epub 2014/12/17.
69. Staubach S, Pekmez M, Hanisch FG. Differential Proteomics of Urinary Exovesicles from Classical Galactosemic Patients Reveals Subclinical Kidney Insufficiency. *Journal of proteome research*. 2016 Jun 3;15(6):1754-61. PubMed PMID: 27103203. Epub 2016/04/23.
70. Feldkirchner S, Schessl J, Muller S, Schoser B, Hanisch FG. Patient-specific protein aggregates in myofibrillar myopathies: laser microdissection and differential proteomics for identification of plaque components. *Proteomics*. 2012 Dec;12(23-24):3598-609. PubMed PMID: 23044792. Epub 2012/10/10.

71. O'Toole GA. Microtiter dish biofilm formation assay. *Journal of visualized experiments : JoVE*. 2011 (47). PubMed PMID: 21307833. Pubmed Central PMCID: PMC3182663. Epub 2011/02/11.
72. Baker J, Sitthisak S, Sengupta M, Johnson M, Jayaswal RK, Morrissey JA. Copper Stress Induces a Global Stress Response in *Staphylococcus aureus* and Represses *sae* and *agr* Expression and Biofilm Formation. *Applied and Environmental Microbiology*. ;76(1):150-60. PubMed PMID: PMC2798663.
73. Michel A, Agerer F, Hauck CR, Herrmann M, Ullrich J, Hacker J, et al. Global regulatory impact of ClpP protease of *Staphylococcus aureus* on regulons involved in virulence, oxidative stress response, autolysis, and DNA repair. *Journal of bacteriology*. 2006 Aug;188(16):5783-96. PubMed PMID: 16885446. Pubmed Central PMCID: PMC1540084. Epub 2006/08/04.
74. Sitthisak S, Knutsson L, Webb JW, Jayaswal RK. Molecular characterization of the copper transport system in *Staphylococcus aureus*. *Microbiology*. 2007 Dec;153(Pt 12):4274-83. PubMed PMID: 18048940.
75. Abdelnour A, Arvidson S, Bremell T, Ryden C, Tarkowski A. The accessory gene regulator (*agr*) controls *Staphylococcus aureus* virulence in a murine arthritis model. *Infect Immun*. 1993 Sep;61(9):3879-85. PubMed PMID: 8359909.
76. Ali R, Al-Achkar K, Al-Mariri A, Safi M. Role of Polymerase Chain Reaction (PCR) in the detection of antibiotic-resistant *Staphylococcus aureus*. *Egyptian Journal of Medical Human Genetics*. 2014 7//;15(3):293-8.
77. Baker J, Sitthisak S, Sengupta M, Johnson M, Jayaswal RK, Morrissey JA. Copper stress induces a global stress response in *Staphylococcus aureus* and represses *sae* and *agr* expression and biofilm formation. *Appl Environ Microbiol*. 2009 Jan;76(1):150-60. PubMed PMID: 19880638.

78. Horsburgh MJ, Ingham E, Foster SJ. In *Staphylococcus aureus*, Fur Is an Interactive Regulator with PerR, Contributes to Virulence, and Is Necessary for Oxidative Stress Resistance through Positive Regulation of Catalase and Iron Homeostasis. *Journal of Bacteriology*. 2001 January 15, 2001;183(2):468-75.
79. Horsburgh MJ, Aish JL, White IJ, Shaw L, Lithgow JK, Foster SJ. sigmaB modulates virulence determinant expression and stress resistance: characterization of a functional rsbU strain derived from *Staphylococcus aureus* 8325-4. *Journal of bacteriology*. 2002 Oct;184(19):5457-67. PubMed PMID: 12218034. Pubmed Central PMCID: PMC135357. Epub 2002/09/10.
80. Soutourina O, Dubrac S, Poupel O, Msadek T, Martin-Verstraete I. The Pleiotropic CymR Regulator of *Staphylococcus aureus* Plays an Important Role in Virulence and Stress Response. *PLoS Pathog*.6(5):e1000894.
81. Moreillon P, Entenza JM, Francioli P, McDevitt D, Foster TJ, Francois P, et al. Role of *Staphylococcus aureus* coagulase and clumping factor in pathogenesis of experimental endocarditis. *Infect Immun*. 1995 Dec;63(12):4738-43. PubMed PMID: 7591130.
82. Begun J, Sifri CD, Goldman S, Calderwood SB, Ausubel FM. *Staphylococcus aureus* virulence factors identified by using a high-throughput *Caenorhabditis elegans*-killing model. *Infect Immun*. 2005 Feb;73(2):872-7. PubMed PMID: 15664928.
83. Beenken KE, Blevins JS, Smeltzer MS. Mutation of sarA in *Staphylococcus aureus* Limits Biofilm Formation. *Infection and Immunity*. 2003 July 1, 2003;71(7):4206-11.

84. Davies DG, Parsek MR, Pearson JP, Iglewski BH, Costerton JW, Greenberg EP. The Involvement of Cell-to-Cell Signals in the Development of a Bacterial Biofilm. *Science*. 1998 April 10, 1998;280(5361):295-8.
85. Vuong C, Saenz HL, Götz F, Otto M. Impact of the agr Quorum-Sensing System on Adherence to Polystyrene in *Staphylococcus aureus*. *Journal of Infectious Diseases*. 2000 December 1, 2000;182(6):1688-93.
86. Ji G, Beavis R, Novick RP. Bacterial Interference Caused by Autoinducing Peptide Variants. *Science*. 1997 June 27, 1997;276(5321):2027-30.
87. Reyes D, Andrey DO, Monod A, Kelley WL, Zhang G, Cheung AL. Coordinated regulation by AgrA, SarA, and SarR to control agr expression in *Staphylococcus aureus*. *Journal of bacteriology*. 2011 Nov;193(21):6020-31. PubMed PMID: 21908676. Pubmed Central PMCID: PMC3194896. Epub 2011/09/13.
88. Tegmark K, Morfeldt E, Arvidson S. Regulation of agr-dependent virulence genes in *Staphylococcus aureus* by RNAIII from coagulase-negative staphylococci. *Journal of bacteriology*. 1998 Jun;180(12):3181-6. PubMed PMID: 9620969. Pubmed Central PMCID: PMC107820. Epub 1998/06/11.
89. Koenig RL, Ray JL, Maleki SJ, Smeltzer MS, Hurlburt BK. *Staphylococcus aureus* AgrA binding to the RNAIII-agr regulatory region. *Journal of bacteriology*. 2004 Nov;186(22):7549-55. PubMed PMID: 15516566. Pubmed Central PMCID: PMC524880. Epub 2004/11/02.
90. Adhikari RP, Arvidson S, Novick RP. A nonsense mutation in agrA accounts for the defect in agr expression and the avirulence of *Staphylococcus aureus* 8325-4 traP::kan. *Infection and immunity*. 2007 Sep;75(9):4534-40. PubMed PMID: 17606604. Pubmed Central PMCID: PMC1951176. Epub 2007/07/04.

91. Wolz C, McDevitt D, Foster TJ, Cheung AL. Influence of agr on fibrinogen binding in *Staphylococcus aureus* Newman. *Infection and immunity*. 1996 Aug;64(8):3142-7. PubMed PMID: 8757845. Pubmed Central PMCID: PMC174199. Epub 1996/08/01.
92. Xue T, You Y, Shang F, Sun B. Rot and Agr system modulate fibrinogen-binding ability mainly by regulating clfB expression in *Staphylococcus aureus* NCTC8325. *Medical microbiology and immunology*. 2012 Feb;201(1):81-92. PubMed PMID: 21701848. Epub 2011/06/28.
93. Fowler VG, Jr., Sakoulas G, McIntyre LM, Meka VG, Arbeit RD, Cabell CH, et al. Persistent bacteremia due to methicillin-resistant *Staphylococcus aureus* infection is associated with agr dysfunction and low-level in vitro resistance to thrombin-induced platelet microbicidal protein. *The Journal of infectious diseases*. 2004 Sep 15;190(6):1140-9. PubMed PMID: 15319865. Epub 2004/08/21.
94. Sakoulas G, Eliopoulos GM, Fowler VG, Jr., Moellering RC, Jr., Novick RP, Lucindo N, et al. Reduced susceptibility of *Staphylococcus aureus* to vancomycin and platelet microbicidal protein correlates with defective autolysis and loss of accessory gene regulator (agr) function. *Antimicrob Agents Chemother*. 2005 Jul;49(7):2687-92. PubMed PMID: 15980337. Pubmed Central PMCID: PMC1168700. Epub 2005/06/28.
95. Moise PA, Forrest A, Bayer AS, Xiong YQ, Yeaman MR, Sakoulas G. Factors influencing time to vancomycin-induced clearance of nonendocarditis methicillin-resistant *Staphylococcus aureus* bacteremia: role of platelet microbicidal protein killing and agr genotypes. *The Journal of infectious diseases*. 2010 Jan 15;201(2):233-40. PubMed PMID: 20001853. Pubmed Central PMCID: PMC2819315. Epub 2009/12/17.

96. Bischoff M, Entenza JM, Giachino P. Influence of a functional sigB operon on the global regulators sar and agr in *Staphylococcus aureus*. *Journal of bacteriology*. 2001 Sep;183(17):5171-9. PubMed PMID: 11489871. Pubmed Central PMCID: PMC95394. Epub 2001/08/08.
97. Bischoff M, Dunman P, Kormanec J, Macapagal D, Murphy E, Mounts W, et al. Microarray-based analysis of the *Staphylococcus aureus* sigmaB regulon. *Journal of bacteriology*. 2004 Jul;186(13):4085-99. PubMed PMID: 15205410. Pubmed Central PMCID: PMC421609. Epub 2004/06/19.
98. Gertz S, Engelmann S, Schmid R, Ohlsen K, Hacker J, Hecker M. Regulation of sigmaB-dependent transcription of sigB and asp23 in two different *Staphylococcus aureus* strains. *Molecular & general genetics : MGG*. 1999 Apr;261(3):558-66. PubMed PMID: 10323238. Epub 1999/05/14.
99. Giachino P, Engelmann S, Bischoff M. Sigma(B) activity depends on RsbU in *Staphylococcus aureus*. *Journal of bacteriology*. 2001 Mar;183(6):1843-52. PubMed PMID: 11222581. Pubmed Central PMCID: PMC95078. Epub 2001/02/27.
100. Kullik I, Giachino P, Fuchs T. Deletion of the alternative sigma factor sigmaB in *Staphylococcus aureus* reveals its function as a global regulator of virulence genes. *Journal of bacteriology*. 1998 Sep;180(18):4814-20. PubMed PMID: 9733682. Pubmed Central PMCID: PMC107504. Epub 1998/09/12.
101. Schulthess B, Bloes DA, Berger-Bächi B. Opposing roles of σ B and σ B-controlled SpoVG in the global regulation of esxA in *Staphylococcus aureus*. *BMC Microbiology*. 2012;12(1):1-11.
102. Schulthess B, Bloes DA, François P, Girard M, Schrenzel J, Bischoff M, et al. The σ (B)-Dependent yabJ-spoVG Operon Is Involved in the Regulation of

Extracellular Nuclease, Lipase, and Protease Expression in *Staphylococcus aureus*. *Journal of bacteriology*. 2011 ;193(18):4954-62. PubMed PMID: PMC3165683.

103. Lister JL, Horswill AR. *Staphylococcus aureus* biofilms: recent developments in biofilm dispersal. *Frontiers in Cellular and Infection Microbiology*. 2014 ;4:178. PubMed PMID: PMC4275032.

104. Otto M. Staphylococcal Biofilms. *Current topics in microbiology and immunology*. 2008;322:207-28. PubMed PMID: PMC2777538.

105. Archer NK, Mazaitis MJ, Costerton JW, Leid JG, Powers ME, Shirtliff ME. *Staphylococcus aureus* biofilms: properties, regulation, and roles in human disease. *Virulence*. 2011 Sep-Oct;2(5):445-59. PubMed PMID: 21921685. Pubmed Central PMCID: PMC3322633. Epub 2011/09/17.

106. Harrison JJ, Ceri H, Turner RJ. Multimetal resistance and tolerance in microbial biofilms. *Nature reviews Microbiology*. 2007 Dec;5(12):928-38. PubMed PMID: 17940533. Epub 2007/10/18.

107. Santo CE, Quaranta D, Grass G. Antimicrobial metallic copper surfaces kill *Staphylococcus haemolyticus* via membrane damage. *MicrobiologyOpen*. 2012;1(1):46-52. PubMed PMID: PMC3426407.

108. Vuong C, Kocianova S, Yao Y, Carmody AB, Otto M. Increased colonization of indwelling medical devices by quorum-sensing mutants of *Staphylococcus epidermidis* in vivo. *The Journal of infectious diseases*. 2004 Oct 15;190(8):1498-505. PubMed PMID: 15378444. Epub 2004/09/21. .

109. Mehlin C, Headley CM, Klebanoff SJ. An Inflammatory Polypeptide Complex from *Staphylococcus epidermidis*: Isolation and Characterization. *The Journal of Experimental Medicine*. 1999;189(6):907-18.

110. Vacheethasanee K, Marchant RE. Surfactant polymers designed to suppress bacterial (*Staphylococcus epidermidis*) adhesion on biomaterials. *Journal of Biomedical Materials Research*. 2000;50(3):302-12.

7. APPENDIX

7.1 Superoxide anion measurement in *MSSA476* and ErCu

MSSA	Mean	Std er	ErCu	Mean	Std er
181.38	181.62	2.5111	84	79.71	2.645
185.29			77.13		
178.2			78		

Table 4: EB fluorescence of *MSSA476* and ErCu strain grown in 0.5 mM CSB at 488 nm excitation and 610-band pass filter. (Single measurement from 3 independent experiments).

7.2 Cellular copper concentration measurement

Strains	sample 1	sample 2	sample 3	Mean	Stdev	Std er
MSSA 476	9.12	9.18	10.2	9.5	0.60696	0.429185
ErCu	8.92	7.75	8.46	8.376667	0.589435	0.416793

Table 5: Measurement of cellular copper concentration in *MSSA476* and ErCu strain grown in 0.5 mM CSB using ICP-MS. (Single measurement from 3 independent experiments).

7.3 Gene expression measurement

Gene	MSSA	ErCu
16S rRNA	13,206	15,402
	13,592	18,651
	13,431	17,816
AgrA	25,975	34,388

	26,381	34,045
	26,842	34,475
CopZ	23,349	29,833
	23,214	29,664
	23,234	29,785
CifA	23,116	31,000
	23,116	30,959
	23,738	31,072
Spa	29,386	34,916
	29,385	34,513
	28,838	34,862

Table 6: Cq values measured in qRT- PCR experiments for respective genes.

Cq value is a n arbitrary units representing time taken to express the gene in the respective organism. Higher the Cq value, lower is the gene expression. Each gene expression is internally normalised by 16S rRNA gene and accordingly graph is created. The software qbase plus is used to normalise and generate the graph. Graphical representation is also based on an arbitrary unit, with higher values for higher gene expression.

7.4 Biofilm formation assay

Strains	Sample 1	Sample 2	Sample 3	Sample 4	Mean	Stdev	Std er
MSSA 476	15710.8 4	13268.4 3	13109.2 9	14704.3 9	14198.2 4	1237.53 9	714.493 2
ErCu	17135.2 9	18111.4 5	18030.3	20027.2 8	18326.0 8	1217.32 1	702.820 8

Table 7: Optical density measurement of ErCu and *MSSA476* strains stained with crystal violet (0.1%).

7.5 PCR experiment to confirm the microevolved *S.aureus*

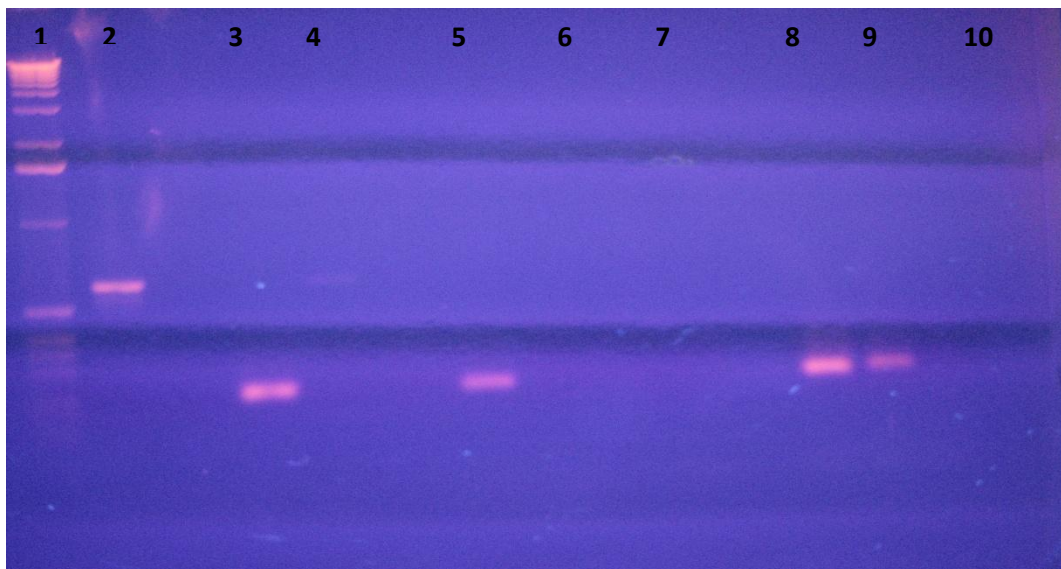


Figure 16: Agrose gel electrophoresis showing amplified bands (Lane 1: 1Kb marker ladder; Lane 2: 16S rRNA gene from *MSSA476*; Lane 3: *Nuc* gene from *MSSA476*; Lane 4: 16S rRNA from ErCu; Lane 5: *Nuc* gene from ErCu; Lane 6 and 7: 16S rRNA gene and *nuc* gene respectively from *S.carnosus*; Lane 8,9 and 10: Multiplex PCR products containing *nuc* gene and *mecA* gene from *MSSA476*, ErCu and *S.Carnosus* respectively).

In the lane 4, DNA concentration used for PCR was much lesser than the other lanes. Hence, a very light intensity band can be seen. *MecA* gene was used check the presence of MRSA strain in multiplex PCR lane.

7.6 Spectrometry MASCOT search data for 5 down regulated proteins from 2D-DIGE experiments

A) Mass spectrometry data MASCOT search results for Aspartyl/glutamyl-tRNA amidotransferase subunit A protein.

{*MATRIX* Mascot Search Results ***SCIENCE***

User : zba
 Email :
 Search title : HCT_bacteria_NCBI
 MS data file : 5066549580983709.mgf
 Database : NCBIInr 20100531 (11112683 sequences; 3786819628 residues)
 Taxonomy : Bacteria (Eubacteria) (6309942 sequences)
 Timestamp : 15 Jul 2010 at 09:26:14 GMT
 Protein
 hits : [gi|21](#) aspartyl/glutamyl-tRNA amidotransferase subunit A
 [283570](#) [Staphylococcus aureus subsp. aureus MW2]

[gi|23](#)
[963804](#) glutamyl-tRNA (Gln) amidotransferase subunit A
[3](#) [Staphylococcus warneri L37603]

[gi|27](#) glutamyl-tRNA Gln amidotransferase subunit A [Staphylococcus
[468503](#) epidermidis ATCC 12228]

[gi|28](#) Aspartyl-tRNA (Asn) amidotransferase subunit A/Glutamyl-
[955038](#) tRNA (Gln) amidotransferase subunit A [Staphylococcus
[2](#) lugdunensis HKU09-01]

[gi|25](#)
[373054](#) indole-3-pyruvate decarboxylase [Staphylococcus aureus
[1](#) subsp. aureus USA300_TCH959]

[gi|15](#) aldehyde dehydrogenase-like protein [Staphylococcus aureus
[923157](#) subsp. aureus Mu50]

[gi|15](#) glycine dehydrogenase subunit 1 [Staphylococcus aureus
[924526](#) subsp. aureus Mu50]

[gi|23](#) aspartyl/glutamyl-tRNA amidotransferase subunit A
[098220](#) [Oceanobacillus iheyensis HTE831]

[gi|15925112](#) dihydrolipoamide dehydrogenase [Staphylococcus aureus subsp. aureus Mu50]

Probability Based Mowse Score

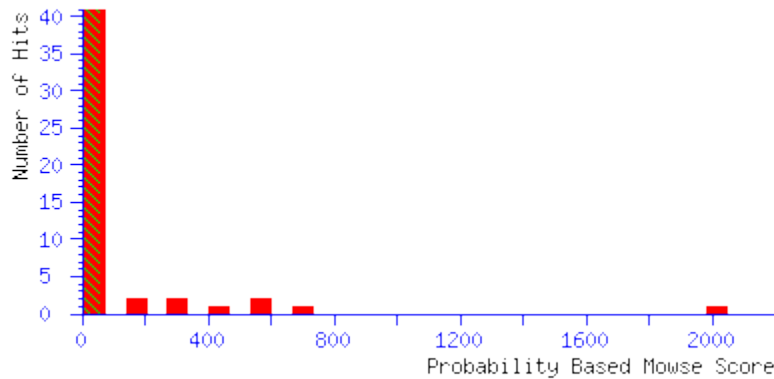


Figure 17: MS MASCOT data search probability based mowse score chart for Aspartyl/glutamyl-tRNA amidotransferase subunit A protein.

B) Mass spectrometry data MASCOT search results for Aldehyde dehydrogenase like protein.

{MATRIX} *{SCIENCE}* Mascot Search Results

```

User           : zba
Email          :
Search title   : HCT_bacteria_NCBI
MS data file   : 5066549580983696.mgf
Database       : NCBIInr 20100531 (11112683 sequences; 3786819628 residues)
Taxonomy       : Bacteria (Eubacteria) (6309942 sequences)
Timestamp      : 15 Jul 2010 at 07:32:19 GMT
Protein        : gi|15925112 aldehyde dehydrogenase-like protein [Staphylococcus
hits           : 23157 aureus subsp. aureus Mu50]

               gi|15925112 aldehyde dehydrogenase [Staphylococcus aureus subsp.
               25112 aureus Mu50]

               gi|103487892 ABC transporter related [Sphingopyxis alaskensis RB2256]

               gi|260221788 Glycine-rich RNA-binding protein GRP1A [Curvibacter
               221788 putative symbiont of Hydra magnipapillata]

```

Probability Based Mowse Score

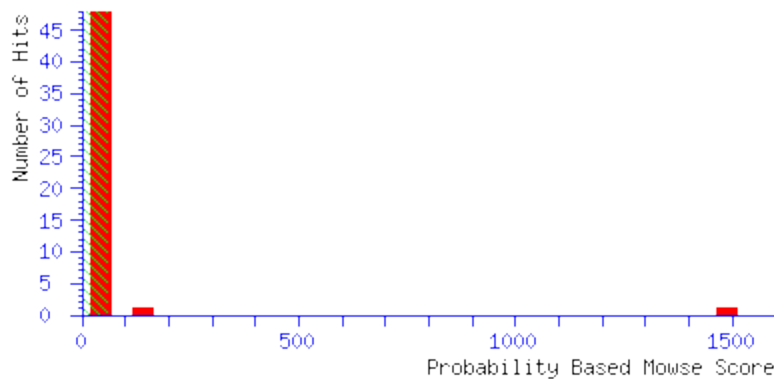


Figure 18: MASCOT data search probability based mowse score chart for Aldehyde dehydrogenase like protein.

C) Mass spectrometry data MASCOT search results for Inositol monophosphate dehydrogenase protein.

MATRIX
SCIENCE Mascot Search Results

```

User           : zba
Email          :
Search title   : HCT_bacteria_NCBI
MS data file   : 5066549580983622.mgf
Database       : NCBIInr 20100531 (11112683 sequences; 3786819628 residues)
Taxonomy       : Bacteria (Eubacteria) (6309942 sequences)
Timestamp      : 14 Jul 2010 at 10:17:29 GMT
Protein hits   :
                 gi|15 inositol-monophosphate dehydrogenase [Staphylococcus aureus
                 923380 subsp. aureus Mu50]
                 :
                 gi|70 inositol-monophosphate dehydrogenase [Staphylococcus
                 727582 haemolyticus JCSC1435]
                 gi|21 formate--tetrahydrofolate ligase [Staphylococcus aureus
                 283404 subsp. aureus MW2]
                 gi|89 inositol-5-monophosphate dehydrogenase [Bacillus sp. NRRL B-
                 100965 14911]
                 gi|22 glycine dehydrogenase [decarboxylating]
                 304309 (Glycinedecarboxylase) (Glycine cleavage system P-protein)
                 4 [Staphylococcus capitis SK14]

```

Probability Based Mowse Score

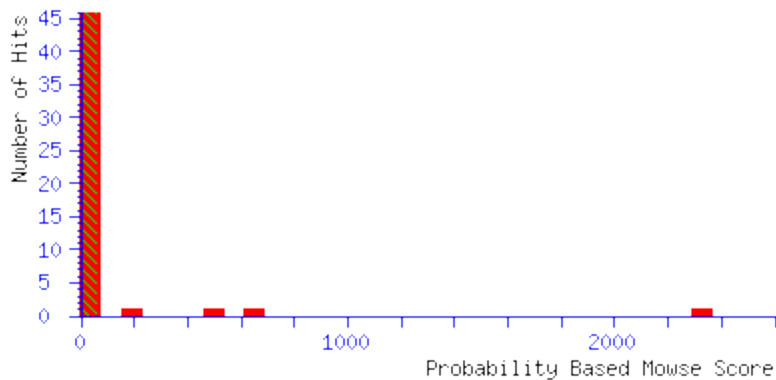


Figure 19: MS MASCOT data search probability based mowse score chart for Inositol monophosphate dehydrogenase protein.

D) Mass spectrometry data MASCOT search results for Fumarate hydratase protein.

{MATRIX} *{SCIENCE}* Mascot Search Results

```

User           : zba
Email          :
Search title   : HCT_bacteria_NCBI
MS data file   : 5066549580983697.mgf
Database       : NCBI nr 20100531 (11112683 sequences; 3786819628 residues)
Taxonomy       : Bacteria (Eubacteria) (6309942 sequences)
Timestamp      : 15 Jul 2010 at 07:40:54 GMT
Protein        : gi|25373 fumarate hydratase [Staphylococcus aureus subsp.
hits          : 5269 aureus TCH130]

               gi|22447 fumarate hydratase, class-II [Staphylococcus carnosus
               6910 subsp. carnosus TM300]

               gi|91787
               923 fumarate hydratase [Polaromonas sp. JS666]

               gi|23885
               4888 ComF operon protein 1 [Lactobacillus jensenii 269-3]

               gi|23801 hypothetical protein VEIDISOL_01556 [Veillonella
               9682 dispar ATCC 17748]

```

Probability Based Mowse Score

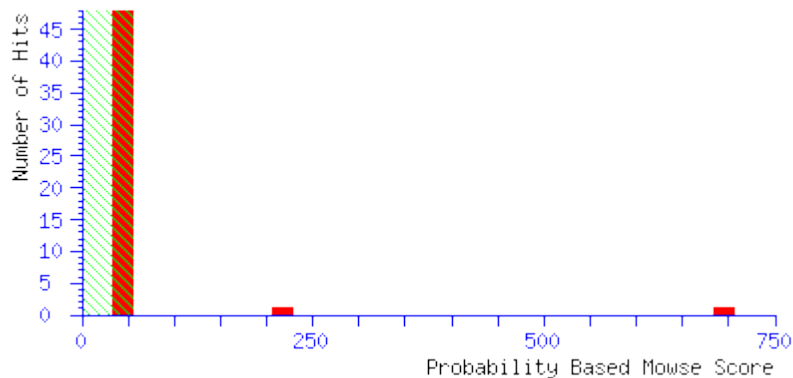


Figure 20: MS MASCOT data search probability based mowse score chart for Fumarate hydratase protein.

E) Mass spectrometry data MASCOT search results for Ornithine-oxo-acid transaminase protein.

{MATRIX} Mascot Search Results *{SCIENCE}*

```

User           : zba
Email          :
Search title   : HCT_bacteria_NCBI
MS data file   : 5066549580983698.mgf
Database       : NCBIInr 20100531 (11112683 sequences; 3786819628 residues)
Taxonomy       : Bacteria (Eubacteria) (6309942 sequences)
Timestamp      : 15 Jul 2010 at 07:37:49 GMT
Protein        : gi|1592 ornithine--oxo-acid transaminase [Staphylococcus aureus
hits           : 3947 subsp. aureus Mu50]

                gi|2834 ornithine--oxo-acid transaminase [Staphylococcus aureus
                70156 subsp. aureus ST398]

                gi|2518 ornithine--oxo-acid transaminase [Staphylococcus
                10330 epidermidis BCM-HMP0060]

                gi|1592 putative NADH-dependent flavin oxidoreductase
                3946 [Staphylococcus aureus subsp. aureus Mu50]

                gi|1608 ornithine--oxo-acid transaminase [Bacillus subtilis
                1086 subsp. subtilis str. 168]

```


Probability Based Mowse Score

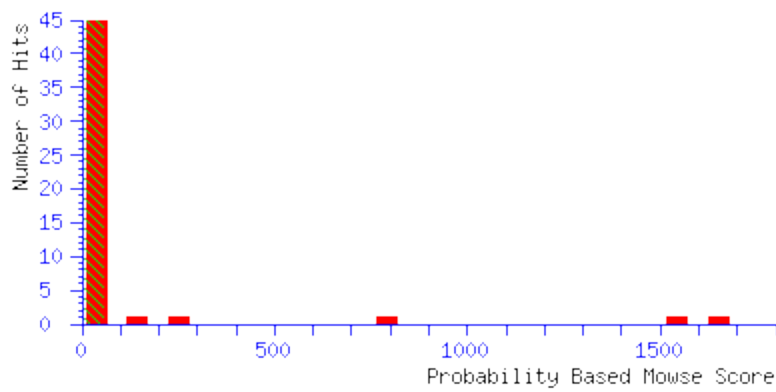
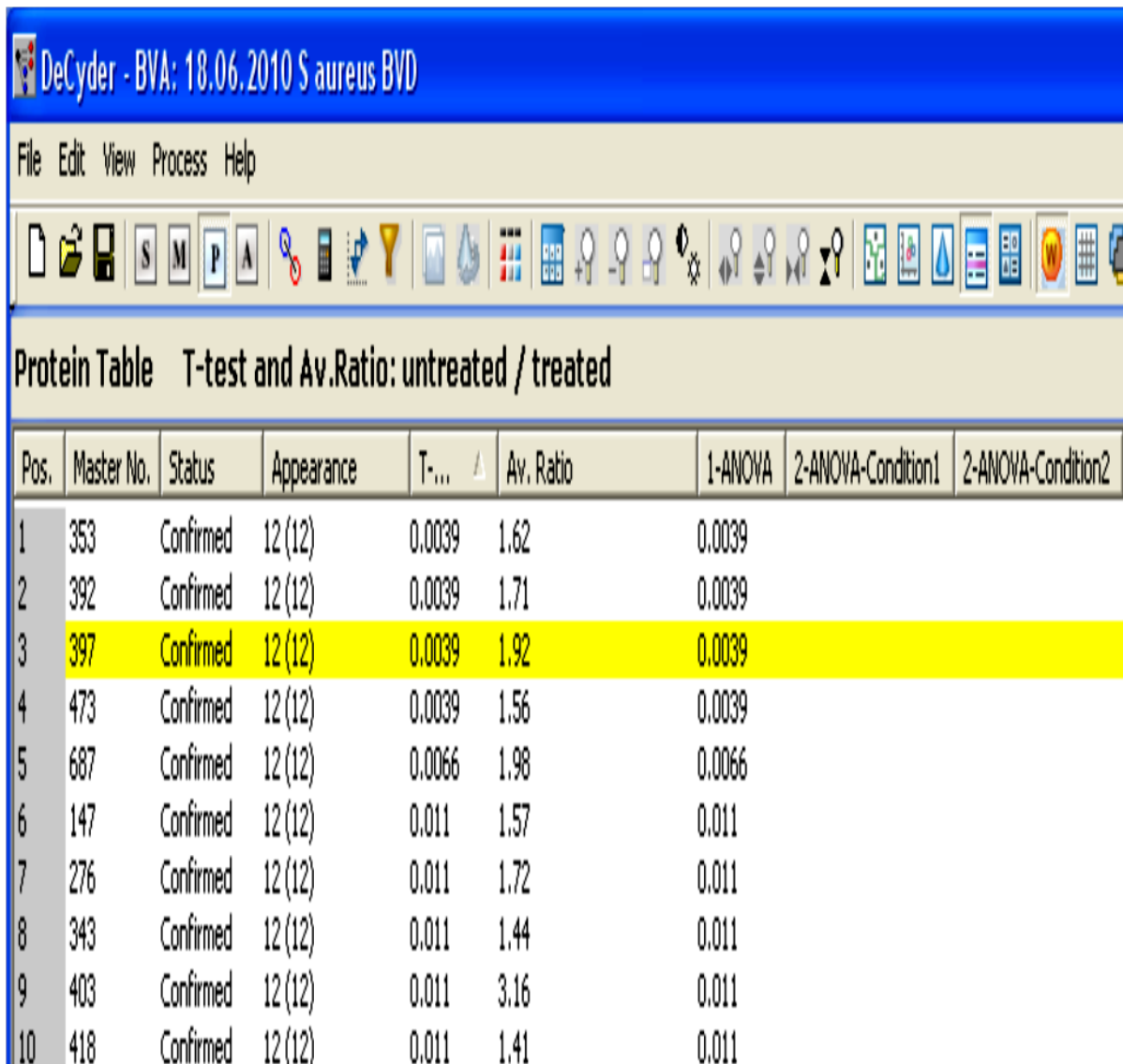


Figure 21: MS MASCOT data search probability based mowse score chart for Ornithine-oxo-acid transaminase protein.

7.7 Screen shot of student's T-test score from 2D-DIGE experiment



DeCyder - BVA: 18.06.2010 S aureus BVD

File Edit View Process Help

Protein Table T-test and Av.Ratio: untreated / treated

Pos.	Master No.	Status	Appearance	T-...	Av. Ratio	1-ANOVA	2-ANOVA-Condition1	2-ANOVA-Condition2
1	353	Confirmed	12 (12)	0.0039	1.62	0.0039		
2	392	Confirmed	12 (12)	0.0039	1.71	0.0039		
3	397	Confirmed	12 (12)	0.0039	1.92	0.0039		
4	473	Confirmed	12 (12)	0.0039	1.56	0.0039		
5	687	Confirmed	12 (12)	0.0066	1.98	0.0066		
6	147	Confirmed	12 (12)	0.011	1.57	0.011		
7	276	Confirmed	12 (12)	0.011	1.72	0.011		
8	343	Confirmed	12 (12)	0.011	1.44	0.011		
9	403	Confirmed	12 (12)	0.011	3.16	0.011		
10	418	Confirmed	12 (12)	0.011	1.41	0.011		

Figure 22: Screen shot picture of list of Student's T-test scores obtained by 'Decyder' software for the down-regulated proteins from 2D-DIGE experiment

7.8 Protein expression data from nano LC-MALDI analysis

Accession	Protein	Scores	Peptides	Expression
PUR1_S TAA1	Amidophosphoribosyltransferase OS=Staphylococcus aureus (strain COL) GN=purF PE=3 SV=1	810	12	2.90
RL36_S TAA1	50S ribosomal protein L36 OS=Staphylococcus aureus (strain Mu3 / ATCC 700698) GN=rpmJ PE=3 SV=1	52	1	2.34
PUR5_S TAA1	Phosphoribosylformylglycinamide cyclo-ligase OS=Staphylococcus aureus (strain MSSA476) GN=purM PE=3 SV=1	1002	16	2.16
RS15_S TAA1	30S ribosomal protein S15 OS=Staphylococcus aureus (strain Mu3 / ATCC 700698) GN=rpsO PE=3 SV=1	188	3	2.09
PURQ_ STAAS	Phosphoribosylformylglycinamide synthase 1 OS=Staphylococcus aureus (strain MSSA476) GN=purQ PE=3 SV=1	1115	15	2.09
PUR2_S TAA1	Phosphoribosylamine--glycine ligase OS=Staphylococcus aureus (strain MSSA476) GN=purD PE=3 SV=1	1216	19	2.04
PUR9_S TAA8	Bifunctional purine biosynthesis protein purH OS=Staphylococcus aureus (strain NCTC 8325) GN=purH PE=3 SV=1	1975	30	2.02
PURL_S TAA1	Phosphoribosylformylglycinamide synthase 2 OS=Staphylococcus aureus (strain COL) GN=purL PE=3 SV=1	2926	47	2.02
PUR7_S TAA1	Phosphoribosylaminoimidazole-succinocarboxamide synthase OS=Staphylococcus aureus (strain Mu3 / ATCC 700698) GN=purC PE=3 SV=1	868	13	1.81
SARV_ STAAC	HTH-type transcriptional regulator sarV OS=Staphylococcus aureus (strain COL) GN=sarV PE=3 SV=1	444	9	1.80
PUR8_S TAA3	Adenylosuccinate lyase OS=Staphylococcus aureus (strain USA300) GN=purB PE=3 SV=1	1430	27	1.71
PURK_ STAAM	Phosphoribosylaminoimidazole carboxylase ATPase subunit OS=Staphylococcus aureus (strain Mu50 / ATCC 700699) GN=purK PE=1 SV=1	578	11	1.71
PUR3_S TAA1	Phosphoribosylglycinamide formyltransferase OS=Staphylococcus aureus (strain MRSA252) GN=purN PE=3 SV=1	282	5	1.65
RL28_S TAA1	50S ribosomal protein L28 OS=Staphylococcus aureus (strain Mu3 / ATCC 700698) GN=rpmB PE=3 SV=1	161	3	1.61

PURA_ STAAC	Adenylosuccinate synthetase OS=Staphylococcus aureus (strain COL) GN=purA PE=3 SV=1	1460	22	1.60
RL331_ STAAC	50S ribosomal protein L33 1 OS=Staphylococcus aureus (strain COL) GN=rpmG1 PE=3 SV=1	285	3	1.56
RL15_S TAA1	50S ribosomal protein L15 OS=Staphylococcus aureus (strain Mu3 / ATCC 700698) GN=rplO PE=3 SV=1	476	6	1.55
LDH1_S TAA1	L-lactate dehydrogenase 1 OS=Staphylococcus aureus (strain MRSA252) GN=ldh1 PE=3 SV=1	814	12	1.54
GLYA_ STAAT	Serine hydroxymethyltransferase OS=Staphylococcus aureus (strain USA300 / TCH1516) GN=glyA PE=3 SV=1	1452	26	1.54
RS9_ST AA1	30S ribosomal protein S9 OS=Staphylococcus aureus (strain Mu3 / ATCC 700698) GN=rpsI PE=3 SV=1	849	12	1.51
GUAC_ STAAM	GMP reductase OS=Staphylococcus aureus (strain Mu50 / ATCC 700699) GN=guaC PE=1 SV=1	371	5	1.50
PFLB_S TAA1	Formate acetyltransferase OS=Staphylococcus aureus (strain bovine RF122 / ET3-1) GN=pfIB PE=3 SV=1	1437	25	1.50
GATA_ STAAS	Glutamyl-tRNA(Gln) amidotransferase subunit A OS=Staphylococcus aureus (strain MSSA476) GN=gatA PE=3 SV=1	1152	15	1.49
NTPA_S TAA1	Nucleoside-triphosphatase OS=Staphylococcus aureus (strain COL) GN=SACOL1162 PE=3 SV=1	119	1	1.48
DHA2_S TAA3	Alanine dehydrogenase 2 OS=Staphylococcus aureus (strain USA300) GN=ald2 PE=3 SV=1	1429	22	1.43
PYRC_ STAAC	Dihydroorotase OS=Staphylococcus aureus (strain COL) GN=pyrC PE=3 SV=1	426	6	1.42
DAGK_ STAAB	Diacylglycerol kinase OS=Staphylococcus aureus (strain bovine RF122 / ET3-1) GN=dagK PE=3 SV=1	86	1	1.41
RL20_S TAA1	50S ribosomal protein L20 OS=Staphylococcus aureus (strain Mu3 / ATCC 700698) GN=rplT PE=3 SV=1	265	5	1.41
URK_S TAA1	Uridine kinase OS=Staphylococcus aureus (strain bovine RF122 / ET3-1) GN=udk PE=3 SV=1	59	1	1.39
RL30_S TAA1	50S ribosomal protein L30 OS=Staphylococcus aureus (strain Mu3 / ATCC 700698) GN=rpmD PE=3 SV=1	445	6	1.39
RS12_S TAA1	30S ribosomal protein S12 OS=Staphylococcus aureus (strain Mu3 / ATCC 700698) GN=rpsL PE=3 SV=1	565	11	1.38
ATPA_S TAA1	ATP synthase subunit alpha OS=Staphylococcus aureus (strain bovine RF122 / ET3-1) GN=atpA PE=3 SV=1	1390	22	1.38

PYRR_ STAAC	Bifunctional protein pyrR OS=Staphylococcus aureus (strain COL) GN=pyrR PE=3 SV=1	179	2	1.37
IDH_ ST AAC	Isocitrate dehydrogenase [NADP] OS=Staphylococcus aureus (strain COL) GN=icd PE=3 SV=1	1476	25	1.36
NDK_ S TAAS	Nucleoside diphosphate kinase OS=Staphylococcus aureus (strain MSSA476) GN=ndk PE=3 SV=1	672	9	1.36
DTD_ ST AAB	D-tyrosyl-tRNA(Tyr) deacylase OS=Staphylococcus aureus (strain bovine RF122 / ET3-1) GN=dtd PE=3 SV=1	43	1	1.36
Y811_ S TAAS	NADH dehydrogenase-like protein SAS0811 OS=Staphylococcus aureus (strain MSSA476) GN=SAS0811 PE=3 SV=1	1315	19	1.36
COAE_ STAAR	Dephospho-CoA kinase OS=Staphylococcus aureus (strain MRSA252) GN=coaE PE=3 SV=1	123	2	1.35
RL23_ S TAA1	50S ribosomal protein L23 OS=Staphylococcus aureus (strain Mu3 / ATCC 700698) GN=rplW PE=3 SV=1	451	7	1.35
RL2_ ST AA1	50S ribosomal protein L2 OS=Staphylococcus aureus (strain Mu3 / ATCC 700698) GN=rplB PE=3 SV=1	910	12	1.35
OTCC_ STAAC	Ornithine carbamoyltransferase, catabolic OS=Staphylococcus aureus (strain COL) GN=arcB PE=3 SV=1	468	8	1.33
CSD_ ST AAC	Probable cysteine desulfurase OS=Staphylococcus aureus (strain COL) GN=csd PE=3 SV=1	167	2	1.32
AZO1_ S TAA3	FMN-dependent NADPH-azoreductase OS=Staphylococcus aureus (strain USA300) GN=azo1 PE=3 SV=1	191	4	1.32
RS10_ S TAA2	30S ribosomal protein S10 OS=Staphylococcus aureus (strain JH1) GN=rpsJ PE=3 SV=1	347	6	1.31
DRP35_ STAA3	Lactonase drp35 OS=Staphylococcus aureus (strain USA300) GN=drp35 PE=3 SV=2	126	3	1.30
ATPF_ S TAAB	ATP synthase subunit b OS=Staphylococcus aureus (strain bovine RF122 / ET3-1) GN=atpF PE=3 SV=1	445	5	1.30
ADH_ S TAAB	Alcohol dehydrogenase OS=Staphylococcus aureus (strain bovine RF122 / ET3-1) GN=adh PE=3 SV=1	379	5	1.29
FOLD_ S TAAC	Bifunctional protein folD OS=Staphylococcus aureus (strain COL) GN=folD PE=3 SV=1	1073	17	1.29
MURA1_ STAA C	UDP-N-acetylglucosamine 1-carboxyvinyltransferase 1 OS=Staphylococcus aureus (strain COL) GN=murA1 PE=3 SV=1	494	7	1.29
RPOA_	DNA-directed RNA polymerase subunit alpha	955	16	1.28

STAAC	OS=Staphylococcus aureus (strain COL) GN=rpoA PE=3 SV=1			
ATPE_S TAA1	ATP synthase epsilon chain OS=Staphylococcus aureus (strain bovine RF122 / ET3-1) GN=atpC PE=3 SV=1	132	1	1.28
RS3_ST AA1	30S ribosomal protein S3 OS=Staphylococcus aureus (strain Mu3 / ATCC 700698) GN=rpsC PE=3 SV=1	1068	19	1.28
RL22_S TAA1	50S ribosomal protein L22 OS=Staphylococcus aureus (strain Mu3 / ATCC 700698) GN=rplV PE=3 SV=1	364	5	1.28
EFTU_S TAA1	Elongation factor Tu OS=Staphylococcus aureus (strain bovine RF122 / ET3-1) GN=tuf PE=3 SV=1	3512	46	1.27
QUEF_ STAAR	NADPH-dependent 7-cyano-7-deazaguanine reductase OS=Staphylococcus aureus (strain MRSA252) GN=queF PE=3 SV=1	40	1	1.27
GLNA_ STAAC	Glutamine synthetase OS=Staphylococcus aureus (strain COL) GN=glnA PE=3 SV=1	1977	26	1.26
RL27_S TAA1	50S ribosomal protein L27 OS=Staphylococcus aureus (strain Mu3 / ATCC 700698) GN=rpmA PE=3 SV=1	403	6	1.26
UPP_ST AAB	Uracil phosphoribosyltransferase OS=Staphylococcus aureus (strain bovine RF122 / ET3-1) GN=upp PE=3 SV=1	892	12	1.26
RS18_S TAA1	30S ribosomal protein S18 OS=Staphylococcus aureus (strain Mu3 / ATCC 700698) GN=rpsR PE=3 SV=1	183	3	1.25
RL14_S TAA1	50S ribosomal protein L14 OS=Staphylococcus aureus (strain Mu3 / ATCC 700698) GN=rplN PE=3 SV=1	459	9	1.25
LDH2_S TAA3	L-lactate dehydrogenase 2 OS=Staphylococcus aureus (strain USA300) GN=ldh2 PE=3 SV=1	1328	19	1.25
RS4_ST AA1	30S ribosomal protein S4 OS=Staphylococcus aureus (strain Mu3 / ATCC 700698) GN=rpsD PE=3 SV=1	1120	21	1.25
RL19_S TAA3	50S ribosomal protein L19 OS=Staphylococcus aureus (strain USA300) GN=rplS PE=3 SV=1	428	8	1.24
CH10_S TAA1	10 kDa chaperonin OS=Staphylococcus aureus (strain Mu3 / ATCC 700698) GN=groS PE=3 SV=1	320	6	1.24
6PGD_S TAAC	6-phosphogluconate dehydrogenase, decarboxylating OS=Staphylococcus aureus (strain COL) GN=gnd PE=3 SV=1	1420	24	1.24
MURA2 _STAA B	UDP-N-acetylglucosamine 1-carboxyvinyltransferase 2 OS=Staphylococcus aureus (strain bovine RF122 / ET3-1) GN=murA2 PE=3 SV=1	314	4	1.23
FTHS_S TAAR	Formate--tetrahydrofolate ligase OS=Staphylococcus aureus (strain MRSA252) GN=fhs PE=3 SV=1	2030	31	1.23

SYS_ST AAR	Seryl-tRNA synthetase OS=Staphylococcus aureus (strain MRSA252) GN=serS PE=3 SV=1	901	14	1.23
ACON_ STAAC	Aconitate hydratase OS=Staphylococcus aureus (strain COL) GN=acnA PE=3 SV=1	3312	51	1.22!
RL6_ST AA1	50S ribosomal protein L6 OS=Staphylococcus aureus (strain Mu3 / ATCC 700698) GN=rplF PE=3 SV=1	1238	16	1.22!
HSLV_S TAAB	ATP-dependent protease subunit HslV OS=Staphylococcus aureus (strain bovine RF122 / ET3-1) GN=hslV PE=3 SV=1	264	4	1.22
RL29_S TAA1	50S ribosomal protein L29 OS=Staphylococcus aureus (strain Mu3 / ATCC 700698) GN=rpmC PE=3 SV=1	254	3	1.21
GYRA_ STAAR	DNA gyrase subunit A OS=Staphylococcus aureus (strain MRSA252) GN=gyrA PE=3 SV=1	372	7	1.21
GPMA_ STAAB	2,3-bisphosphoglycerate-dependent phosphoglycerate mutase OS=Staphylococcus aureus (strain bovine RF122 / ET3-1) GN=gpmA PE=3 SV=1	1002	15	1.21
PCKA_ STAAS	Phosphoenolpyruvate carboxykinase [ATP] OS=Staphylococcus aureus (strain MSSA476) GN=pckA PE=3 SV=1	2248	37	1.21
PEPT_S TAAR	Peptidase T OS=Staphylococcus aureus (strain MRSA252) GN=pepT PE=3 SV=1	240	5	1.21
RL5_ST AA1	50S ribosomal protein L5 OS=Staphylococcus aureus (strain Mu3 / ATCC 700698) GN=rplE PE=3 SV=1	1378	23	1.21
PDXT_S TAAB	Glutamine amidotransferase subunit pdxT OS=Staphylococcus aureus (strain bovine RF122 / ET3-1) GN=pdxT PE=3 SV=1	514	8	1.21
AMPM_ STAAC	Methionine aminopeptidase OS=Staphylococcus aureus (strain COL) GN=map PE=3 SV=1	315	3	1.20
HUTI_S TAAC	Imidazolonepropionase OS=Staphylococcus aureus (strain COL) GN=hutI PE=3 SV=1	582	9	1.20
RS5_ST AA1	30S ribosomal protein S5 OS=Staphylococcus aureus (strain Mu3 / ATCC 700698) GN=rpsE PE=3 SV=1	1000	14	1.20
RS14Z_ STAA1	30S ribosomal protein S14 type Z OS=Staphylococcus aureus (strain Mu3 / ATCC 700698) GN=rpsZ PE=3 SV=1	80	2	1.20
SECG_ STAAC	Probable protein-export membrane protein secG OS=Staphylococcus aureus (strain COL) GN=secG PE=3 SV=1	119	1	1.20
RS8_ST AA1	30S ribosomal protein S8 OS=Staphylococcus aureus (strain Mu3 / ATCC 700698) GN=rpsH PE=3 SV=1	674	9	1.20

RL32_S TAA1	50S ribosomal protein L32 OS=Staphylococcus aureus (strain Mu3 / ATCC 700698) GN=rpmF PE=3 SV=1	196	2	1.19
CARB_ STAAW	Carbamoyl-phosphate synthase large chain OS=Staphylococcus aureus (strain MW2) GN=carB PE=3 SV=1	711	13	1.19
RL21_S TAAU	50S ribosomal protein L21 OS=Staphylococcus aureus GN=rplU PE=3 SV=1	669	7	1.18
RBFA_ STAAB	Ribosome-binding factor A OS=Staphylococcus aureus (strain bovine RF122 / ET3-1) GN=rbfA PE=3 SV=1	117	2	1.18
RL3_ST AA1	50S ribosomal protein L3 OS=Staphylococcus aureus (strain Mu3 / ATCC 700698) GN=rplC PE=3 SV=1	761	12	1.18
PNP_ST AAS	Polyribonucleotide nucleotidyltransferase OS=Staphylococcus aureus (strain MSSA476) GN=pnp PE=3 SV=1	1007	16	1.18
SUCD_ STAAS	Succinyl-CoA ligase [ADP-forming] subunit alpha OS=Staphylococcus aureus (strain MSSA476) GN=sucD PE=3 SV=1	1353	20	1.18
TRXB_S TAAC	Thioredoxin reductase OS=Staphylococcus aureus (strain COL) GN=trxB PE=3 SV=1	957	15	1.17
DCUP_ STAAT	Uroporphyrinogen decarboxylase OS=Staphylococcus aureus (strain USA300 / TCH1516) GN=hemE PE=3 SV=1	291	6	1.17
TIG_ST AAC	Trigger factor OS=Staphylococcus aureus (strain COL) GN=tig PE=3 SV=1	1242	22	1.17
EFTS_S TAAM	Elongation factor Ts OS=Staphylococcus aureus (strain Mu50 / ATCC 700699) GN=tsf PE=1 SV=1	1820	28	1.17
AHPF_S TAAS	Alkyl hydroperoxide reductase subunit F OS=Staphylococcus aureus (strain MSSA476) GN=ahpF PE=3 SV=1	803	11	1.17
RL31B_ STAA1	50S ribosomal protein L31 type B OS=Staphylococcus aureus (strain Mu3 / ATCC 700698) GN=rpmE2 PE=3 SV=1	639	10	1.17
PYRH_ STAAB	Uridylate kinase OS=Staphylococcus aureus (strain bovine RF122 / ET3-1) GN=pyrH PE=3 SV=1	182	2	1.17
LIPA_S TAAB	Lipoyl synthase OS=Staphylococcus aureus (strain bovine RF122 / ET3-1) GN=lipA PE=3 SV=1	424	8	1.16
CVFB_S TAAB	Conserved virulence factor B OS=Staphylococcus aureus (strain bovine RF122 / ET3-1) GN=cvfB PE=3 SV=1	96	2	1.16
RS7_ST AA1	30S ribosomal protein S7 OS=Staphylococcus aureus (strain Mu3 / ATCC 700698) GN=rpsG PE=3 SV=1	800	13	1.16
DNLJ_S	DNA ligase OS=Staphylococcus aureus (strain bovine RF122 /	333	4	1.16

TAAB	ET3-1) GN=ligA PE=3 SV=1			
DYR_ST AAS	Dihydrofolate reductase OS=Staphylococcus aureus (strain MSSA476) GN=folA PE=3 SV=3	177	3	1.16
LUKL1_ STAAB	Uncharacterized leukocidin-like protein 1 OS=Staphylococcus aureus (strain bovine RF122 / ET3-1) GN=SAB1875c PE=3 SV=1	82	2	1.16
ENGA_ STAAC	GTP-binding protein engA OS=Staphylococcus aureus (strain COL) GN=engA PE=3 SV=1	384	6	1.16
G6PI_S TAA3	Glucose-6-phosphate isomerase OS=Staphylococcus aureus (strain USA300) GN=pgi PE=3 SV=1	1492	28	1.15
CH60_S TAA1	60 kDa chaperonin OS=Staphylococcus aureus (strain Mu3 / ATCC 700698) GN=groL PE=3 SV=1	1845	25	1.15
BINL_S TAAU	Transposon Tn552 resolvase OS=Staphylococcus aureus GN=tnpR PE=3 SV=1	74	1	1.15
PLSX_S TAAR	Phosphate acyltransferase OS=Staphylococcus aureus (strain MRSA252) GN=plsX PE=3 SV=1	167	3	1.15
ENGB_ STAAR	Probable GTP-binding protein engB OS=Staphylococcus aureus (strain MRSA252) GN=engB PE=3 SV=1	47	1	1.14
RL17_S TAA1	50S ribosomal protein L17 OS=Staphylococcus aureus (strain Mu3 / ATCC 700698) GN=rplQ PE=3 SV=1	497	6	1.14
FTSA_S TAAR	Cell division protein ftsA OS=Staphylococcus aureus (strain MRSA252) GN=ftsA PE=3 SV=1	349	4	1.14
HUTH_ STAAM	Histidine ammonia-lyase OS=Staphylococcus aureus (strain Mu50 / ATCC 700699) GN=hutH PE=3 SV=1	1037	18	1.14
DNAK_ STAAC	Chaperone protein dnaK OS=Staphylococcus aureus (strain COL) GN=dnaK PE=2 SV=1	2404	32	1.14
LDHD_ STAAC	D-lactate dehydrogenase OS=Staphylococcus aureus (strain COL) GN=ldhD PE=3 SV=1	503	9	1.13
RS13_S TAA1	30S ribosomal protein S13 OS=Staphylococcus aureus (strain Mu3 / ATCC 700698) GN=rpsM PE=3 SV=1	283	5	1.13
GCH4_ STAAR	GTP cyclohydrolase folE2 OS=Staphylococcus aureus (strain MRSA252) GN=folE2 PE=3 SV=1	347	6	1.13
RL1_ST AAR	50S ribosomal protein L1 OS=Staphylococcus aureus (strain MRSA252) GN=rplA PE=3 SV=1	727	8	1.13
WALR_ STAAB	Transcriptional regulatory protein walR OS=Staphylococcus aureus (strain bovine RF122 / ET3-1) GN=walR PE=3 SV=2	604	10	1.13

ATPB_S TAAB	ATP synthase subunit beta OS=Staphylococcus aureus (strain bovine RF122 / ET3-1) GN=atpD PE=3 SV=1	2114	31	1.13
PYRE_S TAAS	Orotate phosphoribosyltransferase OS=Staphylococcus aureus (strain MSSA476) GN=pyrE PE=3 SV=1	286	6	1.12
KAD_S TAAC	Adenylate kinase OS=Staphylococcus aureus (strain COL) GN=adk PE=3 SV=1	794	11	1.12
F16PC_ STAAS	Fructose-1,6-bisphosphatase class 3 OS=Staphylococcus aureus (strain MSSA476) GN=fbp PE=3 SV=1	1052	19	1.12
RL18_S TAA1	50S ribosomal protein L18 OS=Staphylococcus aureus (strain Mu3 / ATCC 700698) GN=rplR PE=3 SV=1	592	9	1.12
MURC_ STAAM	UDP-N-acetylmuramate--L-alanine ligase OS=Staphylococcus aureus (strain Mu50 / ATCC 700699) GN=murC PE=1 SV=1	577	8	1.12
PYRB_ STAAC	Aspartate carbamoyltransferase OS=Staphylococcus aureus (strain COL) GN=pyrB PE=3 SV=1	178	4	1.12
RL13_S TAA1	50S ribosomal protein L13 OS=Staphylococcus aureus (strain Mu3 / ATCC 700698) GN=rplM PE=3 SV=1	1179	19	1.12
Y500_S TAA9	UPF0133 protein SaurJH9_0500 OS=Staphylococcus aureus (strain JH9) GN=SaurJH9_0500 PE=3 SV=1	331	4	1.12
RF3_ST AAB	Peptide chain release factor 3 OS=Staphylococcus aureus (strain bovine RF122 / ET3-1) GN=prfC PE=3 SV=1	266	6	1.11
GLMS_ STAAC	Glucosamine--fructose-6-phosphate aminotransferase [isomerizing] OS=Staphylococcus aureus (strain COL) GN=glmS PE=3 SV=3	1355	19	1.11
RL24_S TAA1	50S ribosomal protein L24 OS=Staphylococcus aureus (strain Mu3 / ATCC 700698) GN=rplX PE=3 SV=1	128	2	1.11
Y1737_ STAAN	Uncharacterized protein SA1737 OS=Staphylococcus aureus (strain N315) GN=SA1737 PE=1 SV=1	224	3	1.11
EFG_ST AAB	Elongation factor G OS=Staphylococcus aureus (strain bovine RF122 / ET3-1) GN=fusA PE=3 SV=3	3913	60	1.11
SYI_ST AAS	Isoleucyl-tRNA synthetase OS=Staphylococcus aureus (strain MSSA476) GN=ileS PE=3 SV=1	1036	18	1.11
MQO2_ STAAC	Probable malate:quinone oxidoreductase 2 OS=Staphylococcus aureus (strain COL) GN=mqo2 PE=3 SV=1	2710	46	1.11
TAGH_ STAAM	Teichoic acids export ATP-binding protein TagH OS=Staphylococcus aureus (strain Mu50 / ATCC 700699) GN=tagH PE=1 SV=1	205	3	1.10

SYG_ST AAC	Glycyl-tRNA synthetase OS=Staphylococcus aureus (strain COL) GN=glyQS PE=3 SV=1	1274	19	1.10
RL16_S TAA1	50S ribosomal protein L16 OS=Staphylococcus aureus (strain Mu3 / ATCC 700698) GN=rpIP PE=3 SV=1	338	5	1.10
Y1885_ST AAN	Probable DEAD-box ATP-dependent RNA helicase SA1885 OS=Staphylococcus aureus (strain N315) GN=SA1885 PE=1 SV=1	611	12	1.10
RS2_ST AA1	30S ribosomal protein S2 OS=Staphylococcus aureus (strain Mu3 / ATCC 700698) GN=rpsB PE=3 SV=1	1279	17	1.10
HEM2_STAA8	Delta-aminolevulinic acid dehydratase OS=Staphylococcus aureus (strain NCTC 8325) GN=hemB PE=3 SV=1	377	7	1.10
BUTA_STAAC	Diacetyl reductase [(S)-acetoin forming] OS=Staphylococcus aureus (strain COL) GN=butA PE=3 SV=1	246	3	1.10
GRPE_STAAC	Protein grpE OS=Staphylococcus aureus (strain COL) GN=grpE PE=3 SV=1	258	3	1.10
Y408_S TAAW	UPF0753 protein MW0408 OS=Staphylococcus aureus (strain MW2) GN=MW0408 PE=3 SV=1	41	1	1.10
rndCLP B_STAAW	Chaperone protein ClpB OS=Staphylococcus aureus (strain MW2) GN=clpB PE=3 SV=1	71	2	1.09
PANC_STAAB	Pantothenate synthetase OS=Staphylococcus aureus (strain bovine RF122 / ET3-1) GN=panC PE=3 SV=1	201	2	1.09
G3P2_S TAAC	Glyceraldehyde-3-phosphate dehydrogenase 2 OS=Staphylococcus aureus (strain COL) GN=gapA2 PE=3 SV=1	1283	19	1.09
PT1_ST AAM	Phosphoenolpyruvate-protein phosphotransferase OS=Staphylococcus aureus (strain Mu50 / ATCC 700699) GN=ptsI PE=1 SV=1	1052	20	1.09
CLPP_S TAAB	ATP-dependent Clp protease proteolytic subunit OS=Staphylococcus aureus (strain bovine RF122 / ET3-1) GN=clpP PE=3 SV=1	378	7	1.09
SYK_ST AAS	Lysyl-tRNA synthetase OS=Staphylococcus aureus (strain MSSA476) GN=lysS PE=3 SV=1	977	18	1.09
ARO_A STAAB	3-phosphoshikimate 1-carboxyvinyltransferase OS=Staphylococcus aureus (strain bovine RF122 / ET3-1) GN=aroA PE=3 SV=1	180	1	1.09
FABH_STAAC	3-oxoacyl-[acyl-carrier-protein] synthase 3 OS=Staphylococcus aureus (strain COL) GN=fabH PE=3 SV=1	295	5	1.08

Y2311_ STAAN	Putative NAD(P)H nitroreductase SA2311 OS=Staphylococcus aureus (strain N315) GN=SA2311 PE=1 SV=1	569	9	1.08
RS11_S TAA1	30S ribosomal protein S11 OS=Staphylococcus aureus (strain Mu3 / ATCC 700698) GN=rpsK PE=3 SV=1	543	5	1.08
IF3_ST AA8	Translation initiation factor IF-3 OS=Staphylococcus aureus (strain NCTC 8325) GN=infC PE=3 SV=1	345	3	1.08
EFP_ST AAB	Elongation factor P OS=Staphylococcus aureus (strain bovine RF122 / ET3-1) GN=efp PE=3 SV=1	343	6	1.08
FTSZ_S TAAC	Cell division protein ftsZ OS=Staphylococcus aureus (strain COL) GN=ftsZ PE=3 SV=1	2344	30	1.08
FABG_ STAAC	3-oxoacyl-[acyl-carrier-protein] reductase OS=Staphylococcus aureus (strain COL) GN=fabG PE=3 SV=2	1025	12	1.08
CARA_ STAAC	Carbamoyl-phosphate synthase small chain OS=Staphylococcus aureus (strain COL) GN=carA PE=3 SV=1	212	4	1.07
TRAP_S TAAS	Signal transduction protein TRAP OS=Staphylococcus aureus (strain MSSA476) GN=traP PE=3 SV=1	471	8	1.07
SSB_ST AAC	Single-stranded DNA-binding protein OS=Staphylococcus aureus (strain COL) GN=ssb PE=3 SV=1	643	8	1.07
CLPX_S TAAB	ATP-dependent Clp protease ATP-binding subunit clpX OS=Staphylococcus aureus (strain bovine RF122 / ET3-1) GN=clpX PE=3 SV=1	284	6	1.07
DUS_ST AAC	Probable tRNA-dihydrouridine synthase OS=Staphylococcus aureus (strain COL) GN=dus PE=3 SV=2	102	2	1.07
DHE2_S TAAC	NAD-specific glutamate dehydrogenase OS=Staphylococcus aureus (strain COL) GN=gluD PE=3 SV=1	1585	22	1.07
FUMC_ STAAC	Fumarate hydratase class II OS=Staphylococcus aureus (strain COL) GN=fumC PE=3 SV=1	815	14	1.07
ILVE_S TAAC	Probable branched-chain-amino-acid aminotransferase OS=Staphylococcus aureus (strain COL) GN=ilvE PE=3 SV=1	778	13	1.06
SUCC_ STAAC	Succinyl-CoA ligase [ADP-forming] subunit beta OS=Staphylococcus aureus (strain COL) GN=sucC PE=3 SV=1	1735	28	1.06
FABF_S TAAC	3-oxoacyl-[acyl-carrier-protein] synthase 2 OS=Staphylococcus aureus (strain COL) GN=fabF PE=1 SV=1	1047	17	1.06
SODM1_ STAA3	Superoxide dismutase [Mn/Fe] 1 OS=Staphylococcus aureus (strain USA300) GN=sodA PE=3 SV=1	775	9	1.06
PRSA_	Foldase protein prsA OS=Staphylococcus aureus (strain	399	7	1.06

STAAR	MRSA252) GN=prsA PE=3 SV=1			
SYD_ST AAR	Aspartyl-tRNA synthetase OS=Staphylococcus aureus (strain MRSA252) GN=aspS PE=3 SV=1	854	15	1.06
ISPD1_ STAAS	2-C-methyl-D-erythritol 4-phosphate cytidyltransferase 1 OS=Staphylococcus aureus (strain MSSA476) GN=ispD1 PE=3 SV=1	496	7	1.06
PYRG_ STAA8	CTP synthase OS=Staphylococcus aureus (strain NCTC 8325) GN=pyrG PE=3 SV=1	920	14	1.06
MAZF_ STAAB	Toxin mazF OS=Staphylococcus aureus (strain bovine RF122 / ET3-1) GN=mazF PE=3 SV=1	49	1	1.05
Y989_S TAAW	UPF0637 protein MW0989 OS=Staphylococcus aureus (strain MW2) GN=MW0989 PE=3 SV=1	208	3	1.05
Y1178_ STAAN	UPF0154 protein SA1178 OS=Staphylococcus aureus (strain N315) GN=SA1178 PE=1 SV=1	84	2	1.05
MSRA2 _STAA R	Peptide methionine sulfoxide reductase msrA 2 OS=Staphylococcus aureus (strain MRSA252) GN=msrA2 PE=3 SV=1	261	4	1.05
SYT_ST AAM	Threonyl-tRNA synthetase OS=Staphylococcus aureus (strain Mu50 / ATCC 700699) GN=thrS PE=1 SV=1	1458	26	1.05
SYV_ST AAR	Valyl-tRNA synthetase OS=Staphylococcus aureus (strain MRSA252) GN=valS PE=3 SV=1	639	11	1.05
QOX1_ STAAR	Probable quinol oxidase subunit 1 OS=Staphylococcus aureus (strain MRSA252) GN=qoxB PE=3 SV=1	179	3	1.05
RNJ1_S TAAB	Ribonuclease J 1 OS=Staphylococcus aureus (strain bovine RF122 / ET3-1) GN=SAB0955c PE=3 SV=1	704	10	1.04
SYH_ST AAB	Histidyl-tRNA synthetase OS=Staphylococcus aureus (strain bovine RF122 / ET3-1) GN=hisS PE=3 SV=1	94	2	1.04
RS6_ST AA1	30S ribosomal protein S6 OS=Staphylococcus aureus (strain Mu3 / ATCC 700698) GN=rpsF PE=3 SV=1	864	17	1.04
ATPG_ STAAC	ATP synthase gamma chain OS=Staphylococcus aureus (strain COL) GN=atpG PE=3 SV=1	609	11	1.04
Y1090_ STAAB	Uncharacterized protein SAB1090 OS=Staphylococcus aureus (strain bovine RF122 / ET3-1) GN=SAB1090 PE=4 SV=1	617	10	1.04
RS1_ST AAC	30S ribosomal protein S1 OS=Staphylococcus aureus (strain COL) GN=rpsA PE=3 SV=1	1129	16	1.04
AZOR_ STAAB	FMN-dependent NADH-azoreductase OS=Staphylococcus aureus (strain bovine RF122 / ET3-1) GN=azoR PE=3 SV=2	193	4	1.04

GATB_ STAAB	Aspartyl/glutamyl-tRNA(Asn/Gln) amidotransferase subunit B OS=Staphylococcus aureus (strain bovine RF122 / ET3-1) GN=gatB PE=3 SV=1	1171	20	1.04
RL4_ST AA1	50S ribosomal protein L4 OS=Staphylococcus aureus (strain Mu3 / ATCC 700698) GN=rplD PE=3 SV=1	763	10	1.04
VRAR_ STAAC	Response regulator protein vraR OS=Staphylococcus aureus (strain COL) GN=vraR PE=3 SV=1	73	1	1.04
RS16_S TAA1	30S ribosomal protein S16 OS=Staphylococcus aureus (strain Mu3 / ATCC 700698) GN=rpsP PE=3 SV=1	459	8	1.04
RPOC_ STAAC	DNA-directed RNA polymerase subunit beta' OS=Staphylococcus aureus (strain COL) GN=rpoC PE=3 SV=1	2296	40	1.04
PTLA_S TAAC	Lactose-specific phosphotransferase enzyme IIA component OS=Staphylococcus aureus (strain COL) GN=lacF PE=3 SV=1	66	1	1.03
GCSPB _STAAS	Probable glycine dehydrogenase [decarboxylating] subunit 2 OS=Staphylococcus aureus (strain <i>MSSA476</i>) GN=gcvPB PE=3 SV=1	1204	20	1.03
DLTA_S TAAR	D-alanine--poly(phosphoribitol) ligase subunit 1 OS=Staphylococcus aureus (strain MRSA252) GN=dltA PE=3 SV=1	474	8	1.03
RS19_S TAA1	30S ribosomal protein S19 OS=Staphylococcus aureus (strain Mu3 / ATCC 700698) GN=rpsS PE=3 SV=1	444	6	1.03
SYL_ST AAB	Leucyl-tRNA synthetase OS=Staphylococcus aureus (strain bovine RF122 / ET3-1) GN=leuS PE=3 SV=1	437	8	1.03
METK_ STAAR	S-adenosylmethionine synthase OS=Staphylococcus aureus (strain MRSA252) GN=metK PE=3 SV=1	651	11	1.03
SAER_ STAAB	Response regulator saeR OS=Staphylococcus aureus (strain bovine RF122 / ET3-1) GN=saeR PE=3 SV=1	154	3	1.03
GPDA_ STAAC	Glycerol-3-phosphate dehydrogenase [NAD(P)+] OS=Staphylococcus aureus (strain COL) GN=gpsA PE=3 SV=1	240	2	1.03
RS17_S TAA1	30S ribosomal protein S17 OS=Staphylococcus aureus (strain Mu3 / ATCC 700698) GN=rpsQ PE=3 SV=1	226	5	1.02
FABD_ STAAS	Malonyl CoA-acyl carrier protein transacylase OS=Staphylococcus aureus (strain <i>MSSA476</i>) GN=fabD PE=3 SV=1	314	3	1.02
DAPA_ STAAB	Dihydrodipicolinate synthase OS=Staphylococcus aureus (strain bovine RF122 / ET3-1) GN=dapA PE=3 SV=1	52	1	1.02
NUSB_	N utilization substance protein B homolog OS=Staphylococcus	87	2	1.02

STAAB	aureus (strain bovine RF122 / ET3-1) GN=nusB PE=3 SV=1			
ATPD_S TAAR	ATP synthase subunit delta OS=Staphylococcus aureus (strain MRSA252) GN=atpH PE=3 SV=1	536	8	1.01
SRRA_ STAAC	Transcriptional regulatory protein srrA OS=Staphylococcus aureus (strain COL) GN=srrA PE=2 SV=1	519	8	1.01
RF1_ST AAB	Peptide chain release factor 1 OS=Staphylococcus aureus (strain bovine RF122 / ET3-1) GN=prfA PE=3 SV=1	135	3	1.01
RL11_S TAAB	50S ribosomal protein L11 OS=Staphylococcus aureus (strain bovine RF122 / ET3-1) GN=rplK PE=3 SV=3	516	10	1.01
ODP2_S TAAM	Dihydrolipoyllysine-residue acetyltransferase component of pyruvate dehydrogenase complex OS=Staphylococcus aureus (strain Mu50 / ATCC 700699) GN=pdhC PE=1 SV=1	1772	23	1.01
SYE_ST AAM	Glutamyl-tRNA synthetase OS=Staphylococcus aureus (strain Mu50 / ATCC 700699) GN=gltX PE=1 SV=1	1112	20	1.01
ALF2_S TAAC	Fructose-bisphosphate aldolase OS=Staphylococcus aureus (strain COL) GN=fba PE=3 SV=1	1048	18	1.01
GLMM_ STAAC	Phosphoglucosamine mutase OS=Staphylococcus aureus (strain COL) GN=glmM PE=1 SV=1	822	16	1.00
OBG_S TAAC	GTPase obg OS=Staphylococcus aureus (strain COL) GN=obg PE=3 SV=1	173	3	1.00
IF1_ST AA1	Translation initiation factor IF-1 OS=Staphylococcus aureus (strain Mu3 / ATCC 700698) GN=infA PE=3 SV=1	366	7	1.00
NUSG_ STAAC	Transcription antitermination protein nusG OS=Staphylococcus aureus (strain COL) GN=nusG PE=3 SV=1	307	5	1.00
SYFB_S TAAS	Phenylalanyl-tRNA synthetase beta chain OS=Staphylococcus aureus (strain MSSA476) GN=pheT PE=3 SV=1	609	12	1.00
SYP_ST AAS	Prolyl-tRNA synthetase OS=Staphylococcus aureus (strain MSSA476) GN=proS PE=3 SV=1	860	13	1.00
QOX2_ STAA3	Probable quinol oxidase subunit 2 OS=Staphylococcus aureus (strain USA300) GN=qoxA PE=3 SV=1	863	16	1.00
SARR_ STAAB	HTH-type transcriptional regulator sarR OS=Staphylococcus aureus (strain bovine RF122 / ET3-1) GN=sarR PE=3 SV=3	338	5	1.00
ACCA_ STAAM	Acetyl-coenzyme A carboxylase carboxyl transferase subunit alpha OS=Staphylococcus aureus (strain Mu50 / ATCC 700699) GN=accA PE=1 SV=1	120	3	0.99
RNC_S TAAM	Ribonuclease 3 OS=Staphylococcus aureus (strain Mu50 / ATCC 700699) GN=rnc PE=3 SV=1	125	1	0.99

GLPK_ STA AW	Glycerol kinase OS=Staphylococcus aureus (strain MW2) GN=glpK PE=3 SV=1	1405	21	0.99
GLPD_ STA AC	Aerobic glycerol-3-phosphate dehydrogenase OS=Staphylococcus aureus (strain COL) GN=glpD PE=3 SV=1	543	9	0.99
DAAA_ STA AS	D-alanine aminotransferase OS=Staphylococcus aureus (strain MSSA476) GN=dat PE=3 SV=1	899	15	0.99
Y778_S TA AN	UPF0051 protein SA0778 OS=Staphylococcus aureus (strain N315) GN=SA0778 PE=1 SV=1	742	14	0.99
ODO1_ STA AN	2-oxoglutarate dehydrogenase E1 component OS=Staphylococcus aureus (strain N315) GN=odhA PE=1 SV=1	2427	41	0.99
SY Y_ ST AAC	Tyrosyl-tRNA synthetase OS=Staphylococcus aureus (strain COL) GN=tyrS PE=3 SV=1	119	3	0.99
GC SPA _ STA A M	Probable glycine dehydrogenase [decarboxylating] subunit 1 OS=Staphylococcus aureus (strain Mu50 / ATCC 700699) GN=gcvPA PE=1 SV=1	1391	18	0.99
APT_ ST AAB	Adenine phosphoribosyltransferase OS=Staphylococcus aureus (strain bovine RF122 / ET3-1) GN=apt PE=3 SV=1	49	1	0.99
PDX S_ TA AC	Pyridoxal biosynthesis lyase pdxS OS=Staphylococcus aureus (strain COL) GN=pdxS PE=3 SV=1	1517	24	0.99
RPO B_ STA AR	DNA-directed RNA polymerase subunit beta OS=Staphylococcus aureus (strain MRSA252) GN=rpoB PE=3 SV=1	1860	35	0.99
RPO D_ STA AN	RNA polymerase sigma factor rpoD OS=Staphylococcus aureus (strain N315) GN=rpoD PE=1 SV=1	151	3	0.98
BI KB_ TA AM	Putative 8-amino-7-oxononanoate synthase/2-amino-3- ketobutyrate coenzyme A ligase OS=Staphylococcus aureus (strain Mu50 / ATCC 700699) GN=SAV0550 PE=1 SV=1	1770	26	0.98
SE CA_ STA AB	Protein translocase subunit secA OS=Staphylococcus aureus (strain bovine RF122 / ET3-1) GN=secA PE=3 SV=1	773	13	0.98
SY C_ ST AAS	Cysteinyl-tRNA synthetase OS=Staphylococcus aureus (strain MSSA476) GN=cysS PE=3 SV=1	613	9	0.98
Y2196_ STA AS	Putative 2-hydroxyacid dehydrogenase SAS2196 OS=Staphylococcus aureus (strain MSSA476) GN=SAS2196 PE=3 SV=1	1221	17	0.98
MURE_ STA AS	UDP-N-acetylmuramoyl-L-alanyl-D-glutamate--L-lysine ligase OS=Staphylococcus aureus (strain MSSA476) GN=murE PE=3 SV=1	231	4	0.98

MNMA_ STAAM	tRNA-specific 2-thiouridylase <i>mnmA</i> OS=Staphylococcus aureus (strain Mu50 / ATCC 700699) GN= <i>mnmA</i> PE=1 SV=1	165	3	0.98
FTN_ ST AAB	Ferritin OS=Staphylococcus aureus (strain bovine RF122 / ET3-1) GN= <i>ftnA</i> PE=3 SV=1	640	11	0.98
EZRA_ S TAAB	Septation ring formation regulator <i>ezrA</i> OS=Staphylococcus aureus (strain bovine RF122 / ET3-1) GN= <i>ezrA</i> PE=3 SV=1	512	6	0.97
FABZ_ S TAAB	(3R)-hydroxymyristoyl-[acyl-carrier-protein] dehydratase OS=Staphylococcus aureus (strain bovine RF122 / ET3-1) GN= <i>fabZ</i> PE=3 SV=1	256	4	0.97
FOLB_ S TAAC	Dihydroneopterin aldolase OS=Staphylococcus aureus (strain COL) GN= <i>folB</i> PE=3 SV=1	75	1	0.97
PTA_ ST AAS	Phosphate acetyltransferase OS=Staphylococcus aureus (strain <i>MSSA476</i>) GN= <i>pta</i> PE=3 SV=1	1096	17	0.97
Y829_ S TAAN	Uncharacterized protein SA0829 OS=Staphylococcus aureus (strain N315) GN=SA0829 PE=1 SV=1	1549	23	0.97
PPAC_ STAAB	Probable manganese-dependent inorganic pyrophosphatase OS=Staphylococcus aureus (strain bovine RF122 / ET3-1) GN= <i>ppaC</i> PE=3 SV=1	965	14	0.97
TELL_ S TAAS	TelA-like protein SAS1347 OS=Staphylococcus aureus (strain <i>MSSA476</i>) GN=SAS1347 PE=3 SV=1	221	4	0.97
ENO_ S TAAB	Enolase OS=Staphylococcus aureus (strain bovine RF122 / ET3-1) GN= <i>eno</i> PE=3 SV=1	1939	29	0.96
DLDH_ STAAC	Dihydrolipoyl dehydrogenase OS=Staphylococcus aureus (strain COL) GN= <i>pdhD</i> PE=3 SV=1	1940	29	0.96
Y1302_ STA A3	Uncharacterized protein SAUSA300_1302 OS=Staphylococcus aureus (strain USA300) GN=SAUSA300_1302 PE=3 SV=1	202	5	0.96
Y593_ S TAAR	UPF0447 protein SAR0593 OS=Staphylococcus aureus (strain MRSA252) GN=SAR0593 PE=3 SV=1	390	5	0.96
LEP_ ST AAC	Signal peptidase IB OS=Staphylococcus aureus (strain COL) GN= <i>spsB</i> PE=3 SV=2	310	4	0.95
MENB_ STAAS	Naphthoate synthase OS=Staphylococcus aureus (strain <i>MSSA476</i>) GN= <i>menB</i> PE=3 SV=1	1293	22	0.95
RS21_ S TAA1	30S ribosomal protein S21 OS=Staphylococcus aureus (strain Mu3 / ATCC 700698) GN= <i>rpsU</i> PE=3 SV=1	123	2	0.95
SARA_ STAAB	Transcriptional regulator <i>sarA</i> OS=Staphylococcus aureus (strain bovine RF122 / ET3-1) GN= <i>sarA</i> PE=3 SV=1	470	7	0.95
ERA_ ST	GTP-binding protein era homolog OS=Staphylococcus aureus	352	8	0.95

AAB	(strain bovine RF122 / ET3-1) GN=era PE=3 SV=1			
RL25_S TAA3	50S ribosomal protein L25 OS=Staphylococcus aureus (strain USA300) GN=rpIY PE=3 SV=1	791	12	0.95
GYRB_ STAAC	DNA gyrase subunit B OS=Staphylococcus aureus (strain COL) GN=gyrB PE=3 SV=3	322	4	0.94
Y618_S TAAB	UPF0082 protein SAB0618 OS=Staphylococcus aureus (strain bovine RF122 / ET3-1) GN=SAB0618 PE=3 SV=1	469	6	0.94
ACKA_ STAAB	Acetate kinase OS=Staphylococcus aureus (strain bovine RF122 / ET3-1) GN=ackA PE=3 SV=1	831	15	0.94
MQO1_ STAAM	Probable malate:quinone oxidoreductase 1 OS=Staphylococcus aureus (strain Mu50 / ATCC 700699) GN=mqo1 PE=1 SV=1	266	6	0.94
CLS1_S TAAC	Cardiolipin synthase 1 OS=Staphylococcus aureus (strain COL) GN=cls1 PE=3 SV=1	92	2	0.94
CCPA_ STAAC	Probable catabolite control protein A OS=Staphylococcus aureus (strain COL) GN=ccpA PE=3 SV=1	616	10	0.94
PGCA_ STAAM	Phosphoglucomutase OS=Staphylococcus aureus (strain Mu50 / ATCC 700699) GN=pgcA PE=1 SV=2	205	4	0.94
TKT_ST AAC	Transketolase OS=Staphylococcus aureus (strain COL) GN=tkt PE=3 SV=1	1293	20	0.93
Y1195_ STAAN	Probable tautomerase SA1195.1 OS=Staphylococcus aureus (strain N315) GN=SA1195.1 PE=1 SV=2	232	4	0.93
KITH_S TAAM	Thymidine kinase OS=Staphylococcus aureus (strain Mu50 / ATCC 700699) GN=tdk PE=3 SV=1	118	3	0.93
DPO3B _STAA C	DNA polymerase III subunit beta OS=Staphylococcus aureus (strain COL) GN=dnaN PE=3 SV=1	485	11	0.93
IF2_ST AAS	Translation initiation factor IF-2 OS=Staphylococcus aureus (strain MSSA476) GN=infB PE=3 SV=1	993	13	0.93
MURB_ STAAR	UDP-N-acetylenolpyruvoylglucosamine reductase OS=Staphylococcus aureus (strain MRSA252) GN=murB PE=3 SV=1	236	5	0.93
Y1541_ STAAS	UPF0271 protein SAS1541 OS=Staphylococcus aureus (strain MSSA476) GN=SAS1541 PE=3 SV=1	85	1	0.93
TOP1_S TAAM	DNA topoisomerase 1 OS=Staphylococcus aureus (strain Mu50 / ATCC 700699) GN=topA PE=3 SV=1	192	4	0.93
HUTU_	Urocanate hydratase OS=Staphylococcus aureus (strain COL)	508	9	0.93

STAAC	GN=hutU PE=3 SV=1			
MSRB_ STAAE	Peptide methionine sulfoxide reductase msrB OS=Staphylococcus aureus (strain Newman) GN=msrB PE=3 SV=1	195	3	0.93
LEPA_S TAAC	GTP-binding protein lepA OS=Staphylococcus aureus (strain COL) GN=lepA PE=3 SV=1	471	9	0.92
RL10_S TAAS	50S ribosomal protein L10 OS=Staphylococcus aureus (strain MSSA476) GN=rplJ PE=3 SV=1	574	5	0.92
Y508_S TAAW	Uncharacterized epimerase/dehydratase MW0508 OS=Staphylococcus aureus (strain MW2) GN=MW0508 PE=3 SV=1	533	9	0.92
MTNN_ STAAB	5'-methylthioadenosine/S-adenosylhomocysteine nucleosidase OS=Staphylococcus aureus (strain bovine RF122 / ET3-1) GN=mtnN PE=3 SV=1	100	1	0.92
MURG_ STAAC	UDP-N-acetylglucosamine--N-acetylmuramyl-(pentapeptide) pyrophosphoryl-undecaprenol N-acetylglucosamine transferase OS=Staphylococcus aureus (strain COL) GN=murG PE=3 SV=1	458	8	0.92
ARGI_S TAAC	Arginase OS=Staphylococcus aureus (strain COL) GN=arg PE=3 SV=1	322	4	0.92
CYSK_ STAAC	Cysteine synthase OS=Staphylococcus aureus (strain COL) GN=cysK PE=3 SV=1	2191	28	0.92
ISPD2_ STAAC	2-C-methyl-D-erythritol 4-phosphate cytidyltransferase 2 OS=Staphylococcus aureus (strain COL) GN=ispD2 PE=3 SV=1	600	13	0.92
PYRF_S TAAC	Orotidine 5'-phosphate decarboxylase OS=Staphylococcus aureus (strain COL) GN=pyrF PE=3 SV=1	345	5	0.91
SYA_ST AAS	Alanyl-tRNA synthetase OS=Staphylococcus aureus (strain MSSA476) GN=alaS PE=3 SV=1	821	14	0.91
PEPVL_ STAAB	Putative dipeptidase SAB1611c OS=Staphylococcus aureus (strain bovine RF122 / ET3-1) GN=SAB1611c PE=3 SV=1	971	16	0.91
GCST_ STAAR	Aminomethyltransferase OS=Staphylococcus aureus (strain MRSA252) GN=gcvT PE=3 SV=1	1182	20	0.91
DNAJ_S TAAU	Chaperone protein dnaJ OS=Staphylococcus aureus GN=dnaJ PE=3 SV=1	70	1	0.91
GPMI_S TAAC	2,3-bisphosphoglycerate-independent phosphoglycerate mutase OS=Staphylococcus aureus (strain COL) GN=gpmI PE=3 SV=1	721	12	0.91

HSLO_ STAAM	33 kDa chaperonin OS=Staphylococcus aureus (strain Mu50 / ATCC 700699) GN=hsIO PE=1 SV=1	111	2	0.91
END4_ TAA3	Probable endonuclease 4 OS=Staphylococcus aureus (strain USA300) GN=nfo PE=3 SV=1	155	3	0.91
DHPS_ STAAR	Dihydropteroate synthase OS=Staphylococcus aureus (strain MRSA252) GN=folP PE=3 SV=1	63	1	0.91
Y1530_ STAAN	Uncharacterized peptidase SA1530 OS=Staphylococcus aureus (strain N315) GN=SA1530 PE=1 SV=2	225	5	0.91
CLPC_ TAA3	ATP-dependent Clp protease ATP-binding subunit clpC OS=Staphylococcus aureus (strain COL) GN=clpC PE=3 SV=1	678	13	0.91
Y704_ TAA3	Uncharacterized protein SAB0704 OS=Staphylococcus aureus (strain bovine RF122 / ET3-1) GN=SAB0704 PE=3 SV=1	760	10	0.91
DEOC2_ STAA C	Deoxyribose-phosphate aldolase 2 OS=Staphylococcus aureus (strain COL) GN=deoC2 PE=3 SV=1	575	7	0.91
ACCD_ STAAS	Acetyl-coenzyme A carboxylase carboxyl transferase subunit beta OS=Staphylococcus aureus (strain MSSA476) GN=accD PE=3 SV=1	116	2	0.90
SYN_ ST AAB	Asparaginyl-tRNA synthetase OS=Staphylococcus aureus (strain bovine RF122 / ET3-1) GN=asnS PE=3 SV=1	635	11	0.90
ODPA_ STAAC	Pyruvate dehydrogenase E1 component subunit alpha OS=Staphylococcus aureus (strain COL) GN=pdhA PE=3 SV=1	1603	27	0.90
ARGR_ STAAB	Arginine repressor OS=Staphylococcus aureus (strain bovine RF122 / ET3-1) GN=argR PE=3 SV=1	164	1	0.90
KPYK_ STAAC	Pyruvate kinase OS=Staphylococcus aureus (strain COL) GN=pyk PE=3 SV=1	1578	19	0.90
TGT_ ST AAB	Queuine tRNA-ribosyltransferase OS=Staphylococcus aureus (strain bovine RF122 / ET3-1) GN=tgt PE=3 SV=1	144	2	0.90
SYR_ ST AAR	Arginyl-tRNA synthetase OS=Staphylococcus aureus (strain MRSA252) GN=argS PE=3 SV=1	890	12	0.90
HPRK_ STAAB	HPr kinase/phosphorylase OS=Staphylococcus aureus (strain bovine RF122 / ET3-1) GN=hprK PE=3 SV=1	214	4	0.90
Y1727_ STAAN	UPF0316 protein SA1727 OS=Staphylococcus aureus (strain N315) GN=SA1727 PE=1 SV=1	97	2	0.89
ADDA_ STAAR	ATP-dependent helicase/nuclease subunit A OS=Staphylococcus aureus (strain MRSA252) GN=addA PE=3 SV=1	107	2	0.89

HEMH_ STAAR	Ferrochelatase OS=Staphylococcus aureus (strain MRSA252) GN=hemH PE=3 SV=1	145	4	0.89
TRMFO_ STAA2	Methylenetetrahydrofolate--tRNA-(uracil-5-)-methyltransferase trmFO OS=Staphylococcus aureus (strain JH1) GN=trmFO PE=3 SV=1	224	3	0.89
HEM3_ STAAB	Porphobilinogen deaminase OS=Staphylococcus aureus (strain bovine RF122 / ET3-1) GN=hemC PE=3 SV=1	111	2	0.89
DDL_ ST AAS	D-alanine--D-alanine ligase OS=Staphylococcus aureus (strain MSSA476) GN=ddl PE=3 SV=1	404	7	0.89
PTPA_ S TAAR	Low molecular weight protein-tyrosine-phosphatase ptpA OS=Staphylococcus aureus (strain MRSA252) GN=ptpA PE=3 SV=1	197	3	0.89
PANB_ STAAB	3-methyl-2-oxobutanoate hydroxymethyltransferase OS=Staphylococcus aureus (strain bovine RF122 / ET3-1) GN=panB PE=3 SV=1	289	4	0.89
PGK_ S TAAB	Phosphoglycerate kinase OS=Staphylococcus aureus (strain bovine RF122 / ET3-1) GN=pgk PE=3 SV=1	732	12	0.88
UREE_ STAAR	Urease accessory protein ureE OS=Staphylococcus aureus (strain MRSA252) GN=ureE PE=3 SV=1	44	1	0.88
HPRT_ S TAAC	Hypoxanthine-guanine phosphoribosyltransferase OS=Staphylococcus aureus (strain COL) GN=hpt PE=3 SV=1	362	5	0.88
PDXK_ STAAC	Putative pyridoxine kinase OS=Staphylococcus aureus (strain COL) GN=pdxK PE=3 SV=1	147	3	0.88
RS20_ S TAA1	30S ribosomal protein S20 OS=Staphylococcus aureus (strain Mu3 / ATCC 700698) GN=rpsT PE=3 SV=1	311	5	0.88
RISB_ S TAAB	6,7-dimethyl-8-ribityllumazine synthase OS=Staphylococcus aureus (strain bovine RF122 / ET3-1) GN=ribH PE=3 SV=1	181	3	0.88
RL9_ ST AA1	50S ribosomal protein L9 OS=Staphylococcus aureus (strain Mu3 / ATCC 700698) GN=rplI PE=3 SV=1	274	5	0.88
CDR_ S TAA8	Coenzyme A disulfide reductase OS=Staphylococcus aureus (strain NCTC 8325) GN=cdr PE=1 SV=3	315	4	0.88
NAGD_ STAAC	Protein nagD homolog OS=Staphylococcus aureus (strain COL) GN=nagD PE=3 SV=1	227	4	0.87
RSMA_ STAAE	Ribosomal RNA small subunit methyltransferase A OS=Staphylococcus aureus (strain Newman) GN=rsmA PE=3 SV=1	64	1	0.87
CATA_ STAAB	Catalase OS=Staphylococcus aureus (strain bovine RF122 / ET3-1) GN=kata PE=3 SV=2	1783	29	0.87

Y1560_ STAAN	UPF0478 protein SA1560 OS=Staphylococcus aureus (strain N315) GN=SA1560 PE=1 SV=1	852	10	0.87
RNJ2_ TAA3	Ribonuclease J 2 OS=Staphylococcus aureus (strain USA300) GN=SAUSA300_1168 PE=3 SV=2	269	3	0.87
SECY_ TAAC	Preprotein translocase subunit secY OS=Staphylococcus aureus (strain COL) GN=secY PE=3 SV=1	49	1	0.87
URE1_ TAAR	Urease subunit alpha OS=Staphylococcus aureus (strain MRSA252) GN=ureC PE=3 SV=1	100	2	0.86
FDHL_ TAAC	Putative formate dehydrogenase SACOL2301 OS=Staphylococcus aureus (strain COL) GN=SACOL2301 PE=3 SV=1	517	11	0.86
KPRS_ STAAC	Ribose-phosphate pyrophosphokinase OS=Staphylococcus aureus (strain COL) GN=prs PE=3 SV=1	640	8	0.86
YSI3_ TAAU	Putative phosphotransferase in Sigma70 operon OS=Staphylococcus aureus PE=3 SV=1	239	5	0.86
RSBW_ STAAS	Serine-protein kinase rsbW OS=Staphylococcus aureus (strain MSSA476) GN=rsbW PE=3 SV=1	87	1	0.86
ROCA_ STAAS	1-pyrroline-5-carboxylate dehydrogenase OS=Staphylococcus aureus (strain MSSA476) GN=rocA PE=3 SV=1	2715	42	0.86
DEOB_ STAAB	Phosphopentomutase OS=Staphylococcus aureus (strain bovine RF122 / ET3-1) GN=deoB PE=3 SV=1	493	9	0.86
KTHY_ TAAS	Thymidylate kinase OS=Staphylococcus aureus (strain MSSA476) GN=tmk PE=3 SV=1	85	2	0.86
NANA_ STAAC	N-acetylneuraminate lyase OS=Staphylococcus aureus (strain COL) GN=nanA PE=3 SV=1	212	4	0.86
GUAA_ STAAB	GMP synthase [glutamine-hydrolyzing] OS=Staphylococcus aureus (strain bovine RF122 / ET3-1) GN=guaA PE=3 SV=1	1249	19	0.86
PPNK_ STAAB	Probable inorganic polyphosphate/ATP-NAD kinase OS=Staphylococcus aureus (strain bovine RF122 / ET3-1) GN=ppnK PE=3 SV=1	46	1	0.86
THLA_ TAAC	Probable acetyl-CoA acyltransferase OS=Staphylococcus aureus (strain COL) GN=SACOL0426 PE=3 SV=1	708	10	0.85
SYM_ TAAS	Methionyl-tRNA synthetase OS=Staphylococcus aureus (strain MSSA476) GN=metG PE=3 SV=1	859	14	0.85
FEMA_ STAAC	Aminoacyltransferase femA OS=Staphylococcus aureus (strain COL) GN=femA PE=3 SV=2	414	5	0.85
DEF_ ST	Peptide deformylase OS=Staphylococcus aureus (strain Mu50 /	237	3	0.85

AAM	ATCC 700699) GN=def PE=1 SV=1			
Y941_S TAAN	UPF0356 protein SA0941 OS=Staphylococcus aureus (strain N315) GN=SA0941 PE=3 SV=2	504	8	0.84
Y1261_ STAAN	UPF0403 protein SA1261 OS=Staphylococcus aureus (strain N315) GN=SA1261 PE=1 SV=1	178	2	0.84
SYW_S TAAR	Tryptophanyl-tRNA synthetase OS=Staphylococcus aureus (strain MRSA252) GN=trpS PE=3 SV=1	284	5	0.84
Y724_S TAAB	Epimerase family protein SAB0724c OS=Staphylococcus aureus (strain bovine RF122 / ET3-1) GN=SAB0724c PE=3 SV=1	165	2	0.83
AHPC_ STAAB	Alkyl hydroperoxide reductase subunit C OS=Staphylococcus aureus (strain bovine RF122 / ET3-1) GN=ahpC PE=3 SV=1	1378	19	0.83
GCP_S TAAC	Probable O-sialoglycoprotein endopeptidase OS=Staphylococcus aureus (strain COL) GN=gcp PE=3 SV=1	59	1	0.83
RELA_S TAAR	GTP pyrophosphokinase OS=Staphylococcus aureus (strain MRSA252) GN=relA PE=3 SV=1	212	4	0.83
MGRA_ STAAC	HTH-type transcriptional regulator mgrA OS=Staphylococcus aureus (strain COL) GN=mgrA PE=3 SV=3	297	4	0.83
Y1592_ STAAR	UPF0403 protein SAR1592 OS=Staphylococcus aureus (strain MRSA252) GN=SAR1592 PE=3 SV=1	175	3	0.82
GTAB_ STAAC	UTP--glucose-1-phosphate uridylyltransferase OS=Staphylococcus aureus (strain COL) GN=gtaB PE=3 SV=1	202	4	0.82
Y1438_ STAAR	DegV domain-containing protein SAR1438 OS=Staphylococcus aureus (strain MRSA252) GN=SAR1438 PE=4 SV=1	377	4	0.82
PUTP_S TAAU	Sodium/proline symporter OS=Staphylococcus aureus GN=putP PE=3 SV=2	77	1	0.82
Y1532_ STAAN	Putative universal stress protein SA1532 OS=Staphylococcus aureus (strain N315) GN=SA1532 PE=1 SV=1	716	11	0.81
GSA1_S TAAB	Glutamate-1-semialdehyde 2,1-aminomutase 1 OS=Staphylococcus aureus (strain bovine RF122 / ET3-1) GN=hemL1 PE=3 SV=1	327	6	0.81
LUXS_S TAAC	S-ribosylhomocysteine lyase OS=Staphylococcus aureus (strain COL) GN=luxS PE=3 SV=1	168	3	0.81
RSMH_ STAAM	Ribosomal RNA small subunit methyltransferase H OS=Staphylococcus aureus (strain Mu50 / ATCC 700699) GN=rsmH PE=1 SV=1	269	4	0.81
METN2_ TAAC	Methionine import ATP-binding protein MetN 2 OS=Staphylococcus aureus (strain USA300) GN=metN2 PE=3 SV=1	76	2	0.81

STAA3	SV=1			
TPIS_S TAAC	Triosephosphate isomerase OS=Staphylococcus aureus (strain COL) GN=tpiA PE=3 SV=1	1154	18	0.80
URTF_S TAAM	Probable uridylyltransferase SAV2171 OS=Staphylococcus aureus (strain Mu50 / ATCC 700699) GN=SAV2171 PE=1 SV=1	199	4	0.80
PTGA_ STAAS	Glucose-specific phosphotransferase enzyme IIA component OS=Staphylococcus aureus (strain MSSA476) GN=crr PE=3 SV=1	313	5	0.80
AROC_ STAAS	Chorismate synthase OS=Staphylococcus aureus (strain MSSA476) GN=aroC PE=3 SV=1	231	4	0.80
PCRA_ STAAR	ATP-dependent DNA helicase pcrA OS=Staphylococcus aureus (strain MRSA252) GN=pcrA PE=3 SV=1	220	5	0.80
DNAA_ STAAR	Chromosomal replication initiator protein dnaA OS=Staphylococcus aureus (strain MRSA252) GN=dnaA PE=3 SV=1	139	3	0.80
G3P1_S TAAC	Glyceraldehyde-3-phosphate dehydrogenase 1 OS=Staphylococcus aureus (strain COL) GN=gapA1 PE=3 SV=1	2098	29	0.80
HIS8_S TAAR	Histidinol-phosphate aminotransferase OS=Staphylococcus aureus (strain MRSA252) GN=hisC PE=3 SV=1	77	1	0.79
SYFA_S TAAB	Phenylalanyl-tRNA synthetase alpha chain OS=Staphylococcus aureus (strain bovine RF122 / ET3-1) GN=pheS PE=3 SV=1	171	4	0.79
RECA_ STAAB	Protein recA OS=Staphylococcus aureus (strain bovine RF122 / ET3-1) GN=recA PE=3 SV=1	445	6	0.79
Y873_S TAAN	UPF0477 protein SA0873 OS=Staphylococcus aureus (strain N315) GN=SA0873 PE=1 SV=1	392	8	0.79
THIO_S TAAB	Thioredoxin OS=Staphylococcus aureus (strain bovine RF122 / ET3-1) GN=trxA PE=3 SV=1	1086	16	0.79
MNMG_ STAAM	tRNA uridine 5-carboxymethylaminomethyl modification enzyme mnmG OS=Staphylococcus aureus (strain Mu50 / ATCC 700699) GN=mnmG PE=1 SV=1	375	7	0.79
ODPB_ STAAM	Pyruvate dehydrogenase E1 component subunit beta OS=Staphylococcus aureus (strain Mu50 / ATCC 700699) GN=pdhB PE=1 SV=1	1634	23	0.79
ODO2_ STAA3	Dihydrolipoyllysine-residue succinyltransferase component of 2-oxoglutarate dehydrogenase complex OS=Staphylococcus aureus (strain USA300) GN=odhB PE=3 SV=1	1472	21	0.78!

RL7_ST AA1	50S ribosomal protein L7/L12 OS=Staphylococcus aureus (strain Mu3 / ATCC 700698) GN=rpL PE=3 SV=1	1014	10	0.78
GLMU_ STAAB	Bifunctional protein glmU OS=Staphylococcus aureus (strain bovine RF122 / ET3-1) GN=glmU PE=3 SV=2	188	3	0.77
K6PF_S TAA2	6-phosphofructokinase OS=Staphylococcus aureus (strain JH1) GN=pfkA PE=3 SV=1	555	8	0.77
CODY_ STAAB	GTP-sensing transcriptional pleiotropic repressor codY OS=Staphylococcus aureus (strain bovine RF122 / ET3-1) GN=codY PE=3 SV=1	480	7	0.77
RRF_ST AAB	Ribosome-recycling factor OS=Staphylococcus aureus (strain bovine RF122 / ET3-1) GN=frr PE=3 SV=1	406	9	0.77
ALD1_S TAAR	Putative aldehyde dehydrogenase SAR2210 OS=Staphylococcus aureus (strain MRSA252) GN=SAR2210 PE=3 SV=1	575	10	0.77
EBPS_S TAAS	Elastin-binding protein ebpS OS=Staphylococcus aureus (strain MSSA476) GN=ebpS PE=3 SV=3	303	3	0.77
PLSY_S TAAM	Glycerol-3-phosphate acyltransferase OS=Staphylococcus aureus (strain Mu50 / ATCC 700699) GN=plsY PE=3 SV=1	72	1	0.77
PTG3C_ STAAR	PTS system glucose-specific EIICBA component OS=Staphylococcus aureus (strain MRSA252) GN=ptsG PE=3 SV=1	147	3	0.77
TPX_ST AAC	Probable thiol peroxidase OS=Staphylococcus aureus (strain COL) GN=tpx PE=3 SV=1	609	8	0.77
OHRL_ STAAS	Organic hydroperoxide resistance protein-like OS=Staphylococcus aureus (strain MSSA476) GN=SAS0768 PE=3 SV=1	50	1	0.77
MOAC_ STAAM	Molybdenum cofactor biosynthesis protein C OS=Staphylococcus aureus (strain Mu50 / ATCC 700699) GN=moaC PE=3 SV=1	60	1	0.77
GSA2_S TAA1	Glutamate-1-semialdehyde 2,1-aminomutase 2 OS=Staphylococcus aureus (strain Mu3 / ATCC 700698) GN=hemL2 PE=3 SV=1	288	5	0.77
TRMHL _STAA M	Putative trmH family tRNA/rRNA methyltransferase OS=Staphylococcus aureus (strain Mu50 / ATCC 700699) GN=SAV0531 PE=1 SV=1	76	1	0.77
HSLU_S TAAC	ATP-dependent protease ATPase subunit HslU OS=Staphylococcus aureus (strain COL) GN=hslU PE=3 SV=1	303	5	0.76
Y197A_ STAAN	UPF0457 protein SA1975.1 OS=Staphylococcus aureus (strain N315) GN=SA1975.1 PE=1 SV=1	481	8	0.76

BSAA_ STAAC	Glutathione peroxidase homolog BsaA OS=Staphylococcus aureus (strain COL) GN=bsaA PE=3 SV=1	179	4	0.76
PPI1_S TAA3	Putative peptidyl-prolyl cis-trans isomerase OS=Staphylococcus aureus (strain USA300) GN=SAUSA300_0857 PE=3 SV=1	619	11	0.76
Y1445_ STAAB	UPF0365 protein SAB1445c OS=Staphylococcus aureus (strain bovine RF122 / ET3-1) GN=SAB1445c PE=3 SV=1	738	10	0.76
Y1019_ STAAN	Uncharacterized N-acetyltransferase SA1019 OS=Staphylococcus aureus (strain N315) GN=SA1019 PE=1 SV=1	276	4	0.75
HCHA_ STAAC	Chaperone protein hchA OS=Staphylococcus aureus (strain COL) GN=hchA PE=3 SV=1	613	9	0.75
Y2572_ STAAS	UPF0312 protein SAS2572 OS=Staphylococcus aureus (strain MSSA476) GN=SAS2572 PE=3 SV=1	247	1	0.74
Y361_S TAAW	Uncharacterized protein MW0361 OS=Staphylococcus aureus (strain MW2) GN=MW0361 PE=4 SV=1	501	7	0.74
PDP_ST AAC	Pyrimidine-nucleoside phosphorylase OS=Staphylococcus aureus (strain COL) GN=pdp PE=1 SV=1	903	12	0.74
RSBV_ STAAC	Anti-sigma-B factor antagonist OS=Staphylococcus aureus (strain COL) GN=rsbV PE=3 SV=2	118	2	0.73
Y1445_ STAAN	UPF0297 protein SA1445 OS=Staphylococcus aureus (strain N315) GN=SA1445 PE=1 SV=1	164	3	0.73
OAT2_S TAAC	Ornithine aminotransferase 2 OS=Staphylococcus aureus (strain COL) GN=rocD2 PE=3 SV=1	1228	18	0.73
NFRA_ STAAS	NADPH-dependent oxidoreductase OS=Staphylococcus aureus (strain MSSA476) GN=nfrA PE=3 SV=1	79	1	0.73
Y1508_ STAAS	Putative metalloprotease SAS1508 OS=Staphylococcus aureus (strain MSSA476) GN=SAS1508 PE=3 SV=1	102	2	0.70
FEMB_ STAAW	Aminoacyltransferase femB OS=Staphylococcus aureus (strain MW2) GN=femB PE=3 SV=1	125	1	0.70
ALF1_S TAAS	Fructose-bisphosphate aldolase class 1 OS=Staphylococcus aureus (strain MSSA476) GN=fda PE=3 SV=3	1406	19	0.70
GPSB_ STAAB	Cell cycle protein gpsB OS=Staphylococcus aureus (strain bovine RF122 / ET3-1) GN=gpsB PE=3 SV=1	305	5	0.70
DBH_S TAAC	DNA-binding protein HU OS=Staphylococcus aureus (strain COL) GN=hup PE=3 SV=1	1070	12	0.70
ROT_ST	HTH-type transcriptional regulator rot OS=Staphylococcus	267	4	0.70

AA8	aureus (strain NCTC 8325) GN=rot PE=3 SV=2			
ALDA_STAAS	Putative aldehyde dehydrogenase AldA OS=Staphylococcus aureus (strain MSSA476) GN=aldA PE=3 SV=1	2032	28	0.69
SODM2_STAA B	Superoxide dismutase [Mn/Fe] 2 OS=Staphylococcus aureus (strain bovine RF122 / ET3-1) GN=sodM PE=3 SV=1	101	2	0.69
rndY160_8_STAA 3	UPF0758 protein SAUSA300_1608 OS=Staphylococcus aureus (strain USA300) GN=SAUSA300_1608 PE=3 SV=1	45	1	0.69
CNA_S TAAU	Collagen adhesin OS=Staphylococcus aureus GN=cna PE=1 SV=1	165	3	0.68
P5CR_S TAAM	Pyrroline-5-carboxylate reductase OS=Staphylococcus aureus (strain Mu50 / ATCC 700699) GN=proC PE=1 SV=1	130	2	0.68
COAW_STAAM	Type II pantothenate kinase OS=Staphylococcus aureus (strain Mu50 / ATCC 700699) GN=coaW PE=1 SV=1	49	1	0.67
IMDH_S TAAW	Inosine-5'-monophosphate dehydrogenase OS=Staphylococcus aureus (strain MW2) GN=guaB PE=3 SV=1	2199	34	0.65
DLTC_S TAAB	D-alanine--poly(phosphoribitol) ligase subunit 2 OS=Staphylococcus aureus (strain bovine RF122 / ET3-1) GN=dlcC PE=3 SV=1	333	3	0.65
GATC_STAAB	Aspartyl/glutamyl-tRNA(Asn/Gln) amidotransferase subunit C OS=Staphylococcus aureus (strain bovine RF122 / ET3-1) GN=gatC PE=3 SV=1	248	4	0.65
SARS_STAAR	HTH-type transcriptional regulator sarS OS=Staphylococcus aureus (strain MRSA252) GN=sarS PE=3 SV=1	213	5	0.64
Y1566_STAAB	UPF0173 metal-dependent hydrolase SAB1566c OS=Staphylococcus aureus (strain bovine RF122 / ET3-1) GN=SAB1566c PE=3 SV=1	209	3	0.63
Y1186_STAAN	Uncharacterized protein SA1186 OS=Staphylococcus aureus (strain N315) GN=SA1186 PE=1 SV=1	75	2	0.61
GREA_STAAB	Transcription elongation factor greA OS=Staphylococcus aureus (strain bovine RF122 / ET3-1) GN=greA PE=3 SV=1	556	8	0.61
TYSY_S TAAM	Thymidylate synthase OS=Staphylococcus aureus (strain Mu50 / ATCC 700699) GN=thyA PE=1 SV=1	57	1	0.60
Y863_S TAAN	UPF0738 protein SA0863 OS=Staphylococcus aureus (strain N315) GN=SA0863 PE=3 SV=1	85	2	0.60
Y2548_	Uncharacterized protein MW2548 OS=Staphylococcus aureus	66	1	0.59

STA AW	(strain MW2) GN=MW2548 PE=4 SV=1			
CLPL_S TAAS	ATP-dependent Clp protease ATP-binding subunit clpL OS=Staphylococcus aureus (strain MSSA476) GN=clpL PE=3 SV=1	1099	17	0.58
AGRA_ STAAC	Accessory gene regulator A OS=Staphylococcus aureus (strain COL) GN=agrA PE=3 SV=1	123	2	0.57
PTHP_S TAAC	Phosphocarrier protein HPr OS=Staphylococcus aureus (strain COL) GN=ptsH PE=3 SV=1	170	1	0.57
NAGB_ STAAB	Glucosamine-6-phosphate deaminase OS=Staphylococcus aureus (strain bovine RF122 / ET3-1) GN=nagB PE=3 SV=1	44	1	0.57
RPOE_ STAAC	Probable DNA-directed RNA polymerase subunit delta OS=Staphylococcus aureus (strain COL) GN=rpoE PE=3 SV=1	655	8	0.55
Y1663_ STAAN	UPF0342 protein SA1663 OS=Staphylococcus aureus (strain N315) GN=SA1663 PE=1 SV=1	1170	14	0.55
Y2259_ STAAS	Uncharacterized lipoprotein SAS2259 OS=Staphylococcus aureus (strain MSSA476) GN=SAS2259 PE=4 SV=1	191	3	0.55
UP355_ STAAC	UPF0355 protein SACOL0457 OS=Staphylococcus aureus (strain COL) GN=SACOL0457 PE=3 SV=1	388	6	0.53
Y1692_ STAAN	Uncharacterized protein SA1692 OS=Staphylococcus aureus (strain N315) GN=SA1692 PE=3 SV=1	288	4	0.52
Y1696_ STAAN	UPF0435 protein SA1696 OS=Staphylococcus aureus (strain N315) GN=SA1696 PE=1 SV=1	279	3	0.51
XPT_ST AAC	Xanthine phosphoribosyltransferase OS=Staphylococcus aureus (strain COL) GN=xpt PE=3 SV=1	378	6	0.48
LTAS_S TAAB	Glycerol phosphate lipoteichoic acid synthase OS=Staphylococcus aureus (strain bovine RF122 / ET3-1) GN=ltaS PE=3 SV=1	122	2	0.48
SLE1_S TAA3	N-acetylmuramoyl-L-alanine amidase sle1 OS=Staphylococcus aureus (strain USA300) GN=sle1 PE=3 SV=1	207	4	0.47
ISAB_S TAAB	Immunodominant staphylococcal antigen B OS=Staphylococcus aureus (strain bovine RF122 / ET3-1) GN=isaB PE=3 SV=1	203	3	0.44
SBI_ST AAM	Immunoglobulin-binding protein sbi OS=Staphylococcus aureus (strain Mu50 / ATCC 700699) GN=sbi PE=1 SV=2	243	4	0.42
ACP_ST AAB	Acyl carrier protein OS=Staphylococcus aureus (strain bovine RF122 / ET3-1) GN=acpP PE=3 SV=1	347	4	0.40
SP5G_S	Putative septation protein spoVG OS=Staphylococcus aureus	157	3	0.40

TAA2	(strain JH1) GN=spoVG PE=3 SV=1			
HPS_ST AAR	3-hexulose-6-phosphate synthase OS=Staphylococcus aureus (strain MRSA252) GN=SAR0574 PE=3 SV=1	691	9	0.40
COPZ_ STAAC	Copper chaperone copZ OS=Staphylococcus aureus (strain COL) GN=copZ PE=3 SV=1	131	2	0.38
GCSH_ STAAM	Glycine cleavage system H protein OS=Staphylococcus aureus (strain Mu50 / ATCC 700699) GN=gcvH PE=3 SV=1	514	8	0.36
Y2467_ STAAS	Uncharacterized hydrolase SAS2467 OS=Staphylococcus aureus (strain MSSA476) GN=SAS2467 PE=3 SV=1	78	1	0.36
Y2370_ STAAS	Uncharacterized oxidoreductase SAS2370 OS=Staphylococcus aureus (strain MSSA476) GN=SAS2370 PE=3 SV=1	145	2	0.34
Y1443_ STAAN	UPF0473 protein SA1443 OS=Staphylococcus aureus (strain N315) GN=SA1443 PE=1 SV=1	246	4	0.33
ATL_ST AAS	Bifunctional autolysin OS=Staphylococcus aureus (strain MSSA476) GN=atl PE=3 SV=1	2879	43	0.32
ASP23_ STAA3	Alkaline shock protein 23 OS=Staphylococcus aureus (strain USA300) GN=asp23 PE=3 SV=1	1496	22	0.27
SSAA2_ STAAC	Staphylococcal secretory antigen ssaA2 OS=Staphylococcus aureus (strain COL) GN=ssaA2 PE=3 SV=1	1049	12	0.26
LIP2_ST AAC	Lipase 2 OS=Staphylococcus aureus (strain COL) GN=lip2 PE=3 SV=2	122	3	0.23
SDRE_ STAAS	Serine-aspartate repeat-containing protein E OS=Staphylococcus aureus (strain MSSA476) GN=sdrE PE=3 SV=1	66	1	0.20
ESXA_S TAAC	Virulence factor esxA OS=Staphylococcus aureus (strain COL) GN=esxA PE=3 SV=1	497	5	0.18
ISAA_S TAAC	Probable transglycosylase isaA OS=Staphylococcus aureus (strain COL) GN=isaA PE=1 SV=1	320	4	0.16
CSPA_ STAAB	Cold shock protein cspA OS=Staphylococcus aureus (strain bovine RF122 / ET3-1) GN=cspA PE=3 SV=1	290	4	0.16!
SPA_ST AA8	Immunoglobulin G-binding protein A OS=Staphylococcus aureus (strain NCTC 8325) GN=spa PE=1 SV=3	2521	34	0.14
CLFA_S TAAS	Clumping factor A OS=Staphylococcus aureus (strain MSSA476) GN=clfA PE=3 SV=1	83	1	0.12
Y772_S TAAN	UPF0337 protein SA0772 OS=Staphylococcus aureus (strain N315) GN=SA0772 PE=1 SV=1	267	4	0.10

ZDH1_S	Zinc-type alcohol dehydrogenase-like protein SACOL2177	50	1
TAAC	OS=Staphylococcus aureus (strain COL) GN=SACOL2177 PE=3 SV=1		

Table 8 : Nano LC-MALDI analysis data , presenting identified proteins, with their accession code, Nr of peptide hits with matching sequences and ratio of protein expression in ErCu to protein expression in *MSSA476*